

## Introduction to Remote Sensing

Summary related to University of Washington course ESS 421: Intro. to Remote Sensing  
taught Winter 2015 by Professor Stephen E. Wood (SEW)  
compiled by Michael C. McGoodwin (MCM). Content last updated 5/6/2020

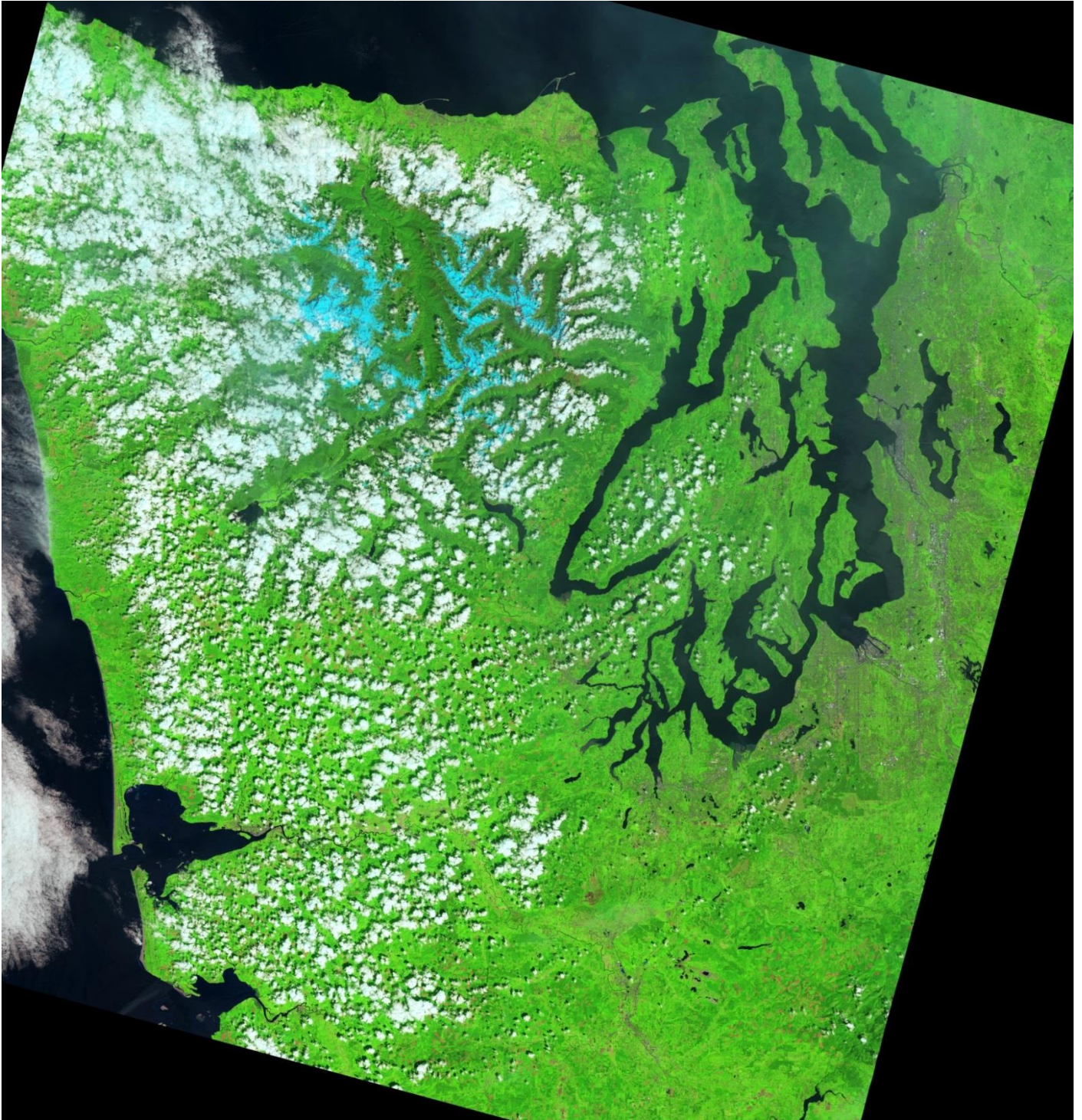


Image of Western WA including Seattle, taken June 11, 2014 by Landsat 8 OLI (Landsat 8 Operational Land Imager=OLI L1T, WRS-2 path=46 row=27); false color (USGS “natural color”): (band 6 SWIR 1.56 - 1.66  $\mu\text{m}$  as R, band 5 Near IR 0.845 - 0.885  $\mu\text{m}$  as G, and band 4 0.63 - 0.68  $\mu\text{m}$  as B) downsampled to 240 m resolution, cropped & contrast enhanced by MCM. Slanted image margins are due to sun synchronous orbit of spacecraft inclined at 98.1°.

# Table of Contents

|   |     |
|---|-----|
| Table of Contents .....   | 2   |
| Introduction.....   | 3   |
| Status of Assignments.....  | 4   |
| Websites for Remote Sensing Data & Imagery .....  | 6   |
| Electromagnetic Spectrum and Light Physics.....   | 8   |
| Diagrams of the EM Spectrum .....   | 8   |
| Nomenclature of Spectral Ranges .....   | 10  |
| EM Radiation Absorption and Transmission in the Atmosphere .....                              | 11  |
| Blackbody, Graybody, Planck’s Law, Stefan-Boltzmann’s law .....                               | 13  |
| Remote Sensing RS: Selected Concepts.....   | 14  |
| Resolution Types in RS .....  | 15  |
| Radiometry Concepts .....   | 18  |
| Surfaces and Their Interaction with Light: Reflection, Refraction, and Absorption .....       | 20  |
| Satellite Path Parameters .....   | 38  |
| Comparison of Satellite Orbits (Compared to Geosynchronous Earth Orbit GEO) .....             | 38  |
| Satellite Imaging Scanning Methods .....  | 39  |
| Multispectral Images.....   | 40  |
| Selected Earth RS Spacecraft, Aircraft, and Sensors .....                                     | 42  |
| Lists of Space Missions, Satellites, and Sensors.....   | 42  |
| Recent Spacecraft .....   | 43  |
| Advanced Land Imager (ALI, aboard Earth Observing-1 Mission EO-1) .....                       | 44  |
| Advanced Very High Resolution Radiometer (AVHRR) and Its Successor VIIRS .....                | 45  |
| Advanced Spaceborne Thermal Emission and Reflection Radiometer (ASTER, aboard Terra) .....    | 47  |
| Airborne Visible Infrared Imaging Spectrometer (AVIRIS) .....                                 | 50  |
| Cloud-Aerosol Lidar and Infrared Pathfinder Satellite Observation satellite (CALIPSO) .....   | 50  |
| Geostationary Operational Environmental Satellites (GOES, NOAA/NASA) .....                    | 51  |
| Gravity Recovery and Climate Experiment (GRACE).....  | 52  |
| Hyperion Grating Imaging Spectrometer (Hyperion, aboard Earth Observing-1 Mission EO-1) ..... | 53  |
| Landsat Multispectral Scanner (MSS, on Landsat 1-5) .....                                     | 53  |
| Landsat 4-7 Thematic Mappers (TM and ETM+).....   | 55  |
| Landsat 8: Operational Land Imager (OLI) and Thermal Infrared Sensor (TIRS) .....             | 56  |
| Moderate-resolution Imaging Spectroradiometer (MODIS) .....                                   | 56  |
| MODIS/ASTER Airborne Simulator (MASTER) — ARC=Ames Research Center .....                      | 57  |
| Polar Ionospheric X-ray Imaging Experiment (PIXIE).....                                       | 57  |
| Solar Terrestrial Relations Observatory (STEREO) spacecraft .....                             | 58  |
| Terra EOS Spacecraft .....  | 58  |
| WIND Spacecraft and WIND-WAVES .....  | 58  |
| Aerial Photography: Vantage Point, Cameras, Filters, and Film .....                           | 59  |
| Elements of Visual Image Interpretation .....   | 59  |
| Photogrammetry, Orthoimages, and Digital Elevation Models .....                               | 59  |
| Multispectral Remote Sensing Systems, Spectroscopy, and Spectroscopic Imaging .....           | 62  |
| Concept of Spectroscopy .....   | 62  |
| Sample Reflectance Spectra .....  | 67  |
| Thermal Infrared Remote Sensing.....  | 79  |
| Active and Passive Microwave (RADAR) Remote Sensing.....                                      | 86  |
| LiDAR Remote Sensing.....   | 92  |
| Remote Sensing of Vegetation.....   | 95  |
| Remote Sensing of Water.....  | 99  |
| Remote Sensing the Urban Landscape .....  | 99  |
| Remote Sensing of Soils, Minerals, and Geomorphology .....                                    | 100 |
| Glossary and Mini-Topics including Spacecraft Missions & Instruments.....                     | 101 |

## Introduction

This course zoomed by a fascinating huge body of knowledge and research, and my all too brief summary hits mostly highlights: items that seemed most fundamental or previously unclear to me, or that attracted my interest the most before I ran out of time. Familiar topics which I have previously reviewed in other summaries are generally not repeated unless I could improve on those earlier efforts.

**Syllabus:** <https://canvas.uw.edu/courses/947179/assignments/syllabus>

**HomePage** (for registered students): <https://canvas.uw.edu/courses/947179/pages/ess421-HomePage>

**Instructors:** Professor Stephen E. “Steve” Wood (SEW); TA: Batbaatar “Bataa” Jigjidsuren

**Sources:** Lecture notes, Assigned article PDFs, and assigned linked HTML articles from SEW; Textbook (below) and PPTs from textbook author (hereafter referred to as *JRJPPT*, some modified by SEW); Additional provided links; other web materials found by MCM. Many of the images and figures were initially presented in or prepared for the course laboratory exercises.

**Textbook:** *Remote Sensing Of The Environment* (2E 2007), by John R. Jensen. Powerpoints for this textbook (*JRJPPT*) are available only to instructors.<sup>1</sup> References to chapters are to this textbook.

**Acknowledgements, Copyrights, and Author Disclaimers:** I thank Professor Wood for allowing me to audit this very informative course and to join in the labs, and I thank his diligent and very helpful TA, Batbaatar Jigjidsuren. I am a retired physician and merely audited this class—although I am learning, I claim no expertise in this field.

---

<sup>1</sup> <http://www.pearsonhighered.com/educator/product/PowerPoints-Online-Remote-Sensing-of-the-Environment-An-Earth-Resource/9780136129134.page>

## Status of Assignments

The tables in this section are of value only to the author—it was used to organize my approach to the assignments and to assist in preparing this summary. However, the assigned course URL links would be of interest.

Lecture PDFs (authorship uncertain, some are possibly mixes of Jensen ± SEW)

| <b>Assignment</b>                   | <b>Status</b> |
|-------------------------------------|---------------|
| Lecture 1 Geological Remote Sensing | DONE, added   |
| Lecture 2 Satellites and Orbits     | DONE, added   |
| Lecture 3 Imaging & Resolution etc. | DONE, added   |
| Lecture 4 Light and Surfaces        | DONE, added   |
| Lecture 5 Atmospheric Scattering    | DONE, added   |
| Lecture 6: Spectroscopy             | DONE, added   |

In Jensen textbook Intro. to RSE (or in Powerpoints relating to the text)

| <b>Assignment</b>  | <b>Status</b>                    |
|--|----------------------------------|
| Ch.1: RSE  | All chap read, some added: DONE  |
| Jensen Chapter 1 (local file PDF)  | Read, some added, DONE           |
| Ch.2: EM Radiation   | All chap read, some added: DONE  |
| Jensen Chapter 2 (local file PDF 2a and 2b.)   | Read, some added, DONE           |
| Ch.3: Hx Aerial Photography & Platforms (no PPT available)   | All chap: DONE                   |
| Ch.4: Aerial Photography: Cameras, Film, etc. (no PPT available)   | All chap: DONE                   |
| Ch. 5: Visual Image Interpretation p. 127-145  | All read, min. added, DONE       |
| Jensen Ch. 5: Visual Image Interpretation (local file)   | Read, none added, DONE           |
| Ch. 6: Photogrammetry, 149-160 (skim only), 162-169 (read more closely): (no PPT available)  | All chap Read, some added, DONE  |
| Ch. 7: Multispectral RS Systems: pp. 193-211, 223-229, 231-232, 233-236, 237-240 (no PPT available)  | All read, some added, DONE       |
| Ch. 8: TIR RS: pp 249-265+. Also 261-265+, 269-272, 274-282. Focus esp. on pp. 274-276   | all chap. read, some added, DONE |
| Jensen Chapter 8 TIR (local file PPTX)   | Read, some added, DONE           |
| Ch. 9: Active & Passive Microwave/Radar: pp. 291-294, 330-332 (Passive Microwave); 294-302 (includes Range Resolution, but can skip Azimuth Resolution), 305-329 | Some added, DONE                 |
| Jensen Chapter 9 Radar (local file PPTX)   | Some added, DONE                 |
| Ch. 10: LIDAR RS: pp 335-345   | Minimal added, DONE              |
| Jensen Chapter 10 LIDAR (local file PPTX)  | Minimal added, DONE              |
| Ch. 11 RS of Vegetation: 355-370, 370-82; 382-393 (focus on SR, NDVI, NDMI, SAVI, REP)   | Read, Minimal added, DONE        |

|   |   |
|---|---|
| Jensen Chapter 11 Vegetation (local file PPTX)  | Read, Minimal added, DONE                   |
| Ch. 12: RS of Water: pp 409-419; 423-426; 486-437                                     | Read, none added, DONE                      |
| Jensen Chapter 12 Water (local file PPTX)   | Read, minimal added, DONE                   |
| Ch. 13: RA of Urban Landscape [not assigned]  | Read, not assigned, not added, DONE         |
| Ch. 14: RS of Soils, Minerals, and Geomorphology: pp. 507 - 521                       | Read, minimal added, DONE                   |
| Ch. 15: In Situ Reflectance Measurement: 569-579                                      | Read, minimal added, DONE                   |
| Color Plates: 2-1; 2-2; 4-2; [DONE]<br>4-4; 5-1,2,3; 7-4; 7-5; 7-7; 11 (all 6) [DONE] | All color plates in textbook reviewed; DONE |

Web Linked assignments (public source URL given where available, authorship give where known):

- [NASA Mission Science: Tour of the Electromagnetic Spectrum](#) DONE, no add
- [NASA Observatory: Catalog of Earth Satellite Orbits](#) DONE, added  
[Description of categories, not an actual catalog of spacecraft or instruments]
- [Aerial Photography during the Cuban Missile Crisis](#) DONE, no add  
[National Geospatial-Intelligence Agency NGIA]
- [Schowengerdt, Ch.1 Nature of RS,<sup>2</sup> Sect. 1.4.1 \(ONLY\) pp.16-30 \[pdf\]](#) DONE, added
- [Imaging geometries Broom- CalTech PDF](#) DONE, added
- J.N. Pelton, *Satellite Communications, 2012*, Chapter 2 “Orbits, Service, and Systems”<sup>3</sup> hereafter called “Pelton 2012” DONE, added
- [Microimages-RS-Tutorial Intro to RSE \[expanded fr. assigned\]](#) DONE, added
- Nicholas M. Short, Sr., Fed. Am. Scientists, [Remote Sensing Tutorial: General Principles for Recognizing Vegetation Principles of Spectroscopy Absorption Processes Factors that Modify or "Confound" Spectral Curves; Data Analysis AVIRIS and other Imaging Spectrometers](#) DONE, not added
- [Kirk Waters: Bathymetric Lidar](#) DONE, not added
- Josh Bandfield, LIDAR (local file: Banfield\_LiDAR.pdf) DONE, added
- Mellon et al. (2008)—Thermal Inertia of the Surface of Mars (local file: Mellon\_Thermal\_Inertia\_2008.pdf) Glanced at, DONE
- Cracknell Thermal Inertia (local file: Cracknell\_Thermal\_Inertia\_RSS\_1996.pdf) Glanced at, DONE
- Radar and Microwave Remote Sensing (local file unk. author possibly by SEW ± Jensen: Radar\_Microwave\_RS\_SEW.pdf) Glanced at, DONE
- Planetary Regolith versus Soil RS, Space weathering (local file unk. author prob. by SEW: Regolith\_Soil\_Planetary\_RS\_SEW.pdf) Glanced at, DONE
- Planetary Subsurface, Porosphere=Regolith, (local file unk. author UW Dept. Seminar 2013: Subsurface\_Planetary\_RS\_2013\_SEW.pdf) Glanced at, DONE
- Thermal IR Imaging RS: Surface Temp., Thermal Inertia, SST, Volcanos (local file unk. author possibly by SEW ± Jensen: ThermalIR\_SurfaceTemp\_RS\_SEWorJensen.pdf) Glanced at, DONE

<sup>2</sup> Robert A. Schowengerdt, *Remote Sensing (Third edition)*, Chapter 1: The Nature of Remote Sensing, 2007, Academic Press.

<sup>3</sup> Available as 17 pp PDF at

[http://www.springer.com/cda/content/document/cda\\_downloaddocument/9781461419938-c1.pdf](http://www.springer.com/cda/content/document/cda_downloaddocument/9781461419938-c1.pdf)

# Websites for Remote Sensing Data & Imagery

(Links & comments provided by SEW, edited & supplemented by MCM;  
some unlinked local files are listed for personal use)

## General RS, Spacecraft and Sensors, and Multiple Topics

- [UW Libraries Geospatial Resources Guide](#)
- [GLOVIS = the USGS Global Visualization Viewer](#)

This is the main data portal to USGS remote sensing data. You can search for data and download it for free. Requires Java and JavaScript to be enabled. It is, "An online search and order tool for selected satellite data. The viewer allows access to all available browse images from the Landsat 7 ETM+, Landsat 4/5 TM, Landsat 1-5 MSS, [Landsat 8 OLI, TIRS], EO-1 ALI, EO-1 Hyperion, MRLC, and Tri-Decadal data sets, as well as Aster TIR, Aster VNIR and MODIS browse images from the DAAC inventory. Through a graphic map display, the user can select any area of interest and immediately view all available browse images for the specified location." Useful sublinks include:

|                      |   |
|----------------------|---|
| Viewer               | <a href="http://glovis.usgs.gov">http://glovis.usgs.gov</a>   |
| Quick Start Guide:   | <a href="http://glovis.usgs.gov/QuickStart.shtml">http://glovis.usgs.gov/QuickStart.shtml</a>       |
| About Browse Images: | <a href="http://glovis.usgs.gov/AboutBrowse.shtml">http://glovis.usgs.gov/AboutBrowse.shtml</a>     |
| User Guide:          | <a href="http://glovis.usgs.gov/ImgViewerHelp.shtml">http://glovis.usgs.gov/ImgViewerHelp.shtml</a> |
- [USGS LandsatLook Viewer](#) "fast and easy viewing of 3 million Landsat images all around the globe with just a simple web browser". "Natural color" false color images only
- [NASA Goddard Remote Sensing Data Resource List \(extensive lists\)](#)
- [USGS National Map Viewer and Download Platform \(includes orthoimagery and Elevations\)](#)
- [ITC Database Of Satellites And Sensors](#) (ITC = Acronym for The International Institute for Geo-information Science and Earth Observation, University of Twente in Netherlands. Lists 225 satellites and 330 sensors, incl. status for planned or scheduled launches)
- [NASA LaRC Satellite Overpass Predictor](#) (not updated since 2007, does not list satellites launched after 2007)  
See also [NASA S'Cool](#) (sends results by email)
- [Landsat Science \(Summary of data resources from Landsat\)](#)
- [USGS Earth Explorer](#) (A complete search and order tool for aerial photos, elevation data and satellite products distributed by the USGS. Must login)
- [USGS Earth Resources Observation and Science \(EROS\) Center - Remote Sensing Section](#) (Landsat, Lidar, etc.)
- [ESA \(European Space Agency\) Landsat-8 Portal](#) [not Firefox, use Chrome] - Only has images of Europe, but is a good, simple map interface for images from the newest [Landsat 8 satellite](#) (launched in 2013). Can easily define area of interest and browse results, but need to register to download.
- [Microimages—Introduction to Remote Sensing](#) (local file: Smith\_MicroimagesIntroToRSE.pdf)
- [Physics Online Reference](#) (Physics-Help Info, for HS & college)
- [Basic of Visual Interpretation](#) (local file: Visual\_Image\_Interpretation\_UNIGIS.pdf)
- [Radiometry and Photometry—Shaw](#) (local file: Shaw\_Radiometry\_Photometry.pdf   DONE, added.
- [Image Interpretation Big 8—Smithsonian](#) (local file: Image\_Interpretation\_Smithsonian.pdf)
- [Planetary Society](#)
- Fed. Am. Scientists (Nicholas M. Short, Sr.): [Remote Sensing Tutorial: General Principles for Recognizing Vegetation](#)  
[Principles of Spectroscopy](#)  
[Absorption Processes](#)  
[Factors that Modify or "Confound" Spectral Curves; Data Analysis](#)  
[AVIRIS and other Imaging Spectrometers](#)
- [ImageJ](#): Freeware NIH Java-based image processing software, including stacks & mathematical manipulation: <http://imagej.nih.gov/ij/index.html>
- [Stanford CS 178 - Digital Photography](#)

## Mathematics and Excel

- [Geometry of Radiation: Solid angles for RS](#) (local files: [GeometrySolidAngleForRS.pdf](#) and [Steradian.ppt](#))
- [Significant Figures in Numbers—Morgan](#) (also, see local file: [Crowell\\_Significant\\_Figures.pdf](#))
- [Excel 2002 formulas—Walkenbach](#) (local file on K: [Excel2002Formulas\\_Walkenbach.pdf](#))
- [Excel 2010 Tutorial—Goodwin College](#) (local file on K: [Excel\\_2010\\_Tutorial\\_GoodwinCollege.pdf](#))
- [Excel 2010 Tutorials—MS](#)

## Thermal Radiation and Planck Function

- [Planck Function Computing—Smith](#) (local file: [Smith\\_Computing\\_The\\_Planck\\_Function.pdf](#))  
see also local file: [Black\\_body\\_radiation\\_calculator\\_Union\\_College.xls](#)

## Spectroscopy and ENVI (Exelis Visual Information Solutions)

- [USGS Spectroscopy Lab \(USGS\)](#)
- [Spectroscopy of Rocks and Minerals, and Principles of Spectroscopy: Roger Clark, USGS](#)
- [ENVI Tutorial—WWU](#) (local file: [ENVI\\_4.5\\_Tutorial\\_WWU.pdf](#))  
see also local file: [ENVI\\_5.0\\_Tutorial\\_Cornell.pdf](#)
- [ENVI 5.2 documentation](#)

## Radar and Microwave Data and Images

- [JPL Imaging Radar site:](#)
- [Spaceborne Imaging Radar-C/X-band Synthetic Aperture Radar \(SIR-C/X-SAR\)](#) . To obtain data, use the [USGS Earth Explorer tool](#)
- [Canada's Radarsat1 and Radarsat2 data portal](#) . A pretty good interface but you have to register even just to get any search results.
- [TerraSAR radar satellite](#)
- [Imaging with Passive Microwave](#)
- [Passive Microwave Sensing \(Cornell\)](#)

## LIDAR Data and Images

- [OpenTopography](#) EXCELLENT place to start, great interfaces, tools and documentation (may need to register to use some features)
- [United States Interagency Elevation Inventory USIEI](#). According to the Wikipedia article about the National Lidar Dataset, this is "currently, the best source for nationwide LiDAR availability from public sources...". [Note: The USIEI link doesn't seem to work using Chrome on a Windows 7 machine, but it did using Chrome on a Mac, and using Internet Explorer on the Windows 7 machine...]
- [Puget Sound Lidar Consortium](#) Recommended for local (W Washington) Lidar data and information, associated with several UW-ESS people. (Need to register to use most things)
- [Lidar Portal](#) by Red Arrow Maps - SEW: "I haven't tried this one yet, but it looks really good"
- [Lidar Links for Mappers](#) - A good list of links (including most of the ones above), also maintained by Red Arrow Maps

## GIS and USGS Resources

- [UNIGIS International Association](#)  
"world's premier distance education initiative ... in Geographical Information Science and Systems (GISc). See local file [Elements of Visual Image Interpretation](#)
- [US Topo GeoPDFs](#) (computer generated contour "quadrangles" USA maps in GeoPDF format)

# Electromagnetic Spectrum and Light Physics

See also Jensen Chapter 2. Electromagnetic Radiation Principles

Light is a wave-like electromagnetic radiation (EM radiation), having mutually perpendicular magnetic and electric fields, both of which oscillate perpendicular to the direction of propagation), and is also particle-like.

The relationship of light *wavelength* to *frequency* in vacuum is

$$c = \nu\lambda$$

where  $c$  = speed of light in vacuum  $\approx 3 \times 10^8 \text{ m s}^{-1}$  (defined as exactly 299,792,458  $\text{m s}^{-1}$ )  
 $\lambda$  = wavelength (m are SI units, but usually expressed in nm,  $\mu\text{m}$  or cm in RS)  
 $\nu$  = frequency (Hz or  $\text{s}^{-1}$ )

Therefore

$$\nu = \frac{c}{\lambda} \text{ and } \lambda = \frac{c}{\nu}$$

Photons are the particles or wave packets that make up bulk light. The energy of one photon depends solely on the frequency:

$$E = h\nu = \frac{hc}{\lambda}$$

where  $E$  = energy (Joules)  
 $\nu$  = frequency (Hz or  $\text{s}^{-1}$ )  
 $h$  = Planck constant (or Planck's constant) =  $6.62606957 \times 10^{-34} \text{ J s}$  (i.e.,  $\text{m}^2 \text{ kg} / \text{s}$ )

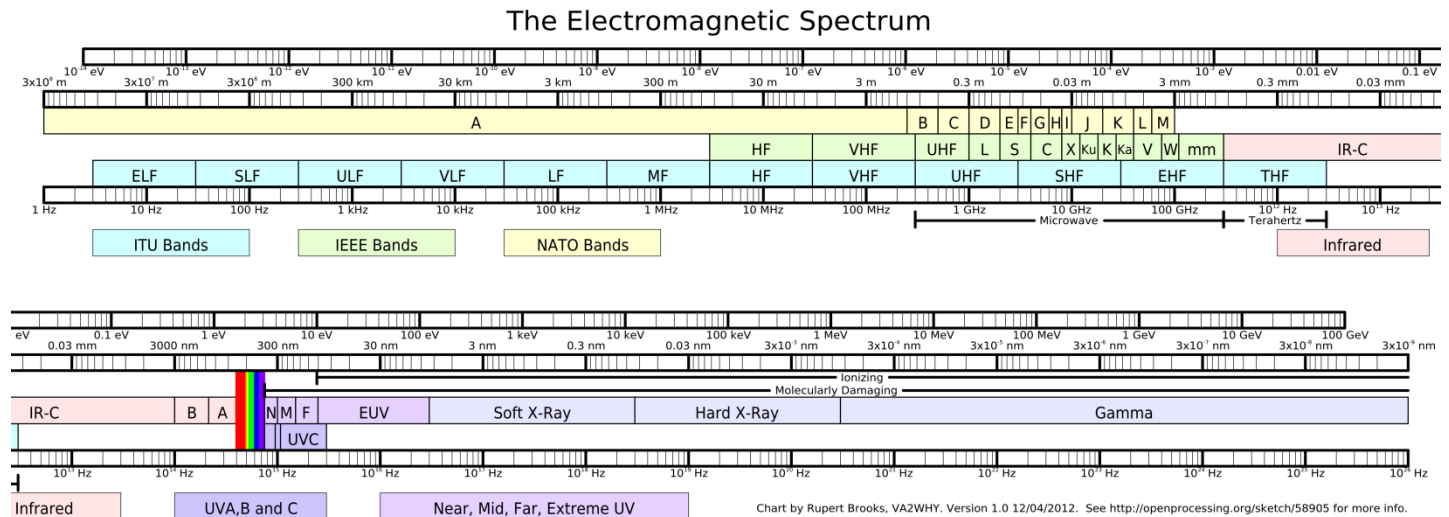
Photons carry *momentum* with magnitude  $|\vec{p}| = h/\lambda$  and hence exert pressure (expressed in  $\text{N m}^{-2}$  or Pa).

A little more about light physics may be found [here](#).

## Diagrams of the EM Spectrum

A very detailed and informative EM Spectrum poster is found [here](#).<sup>4</sup>

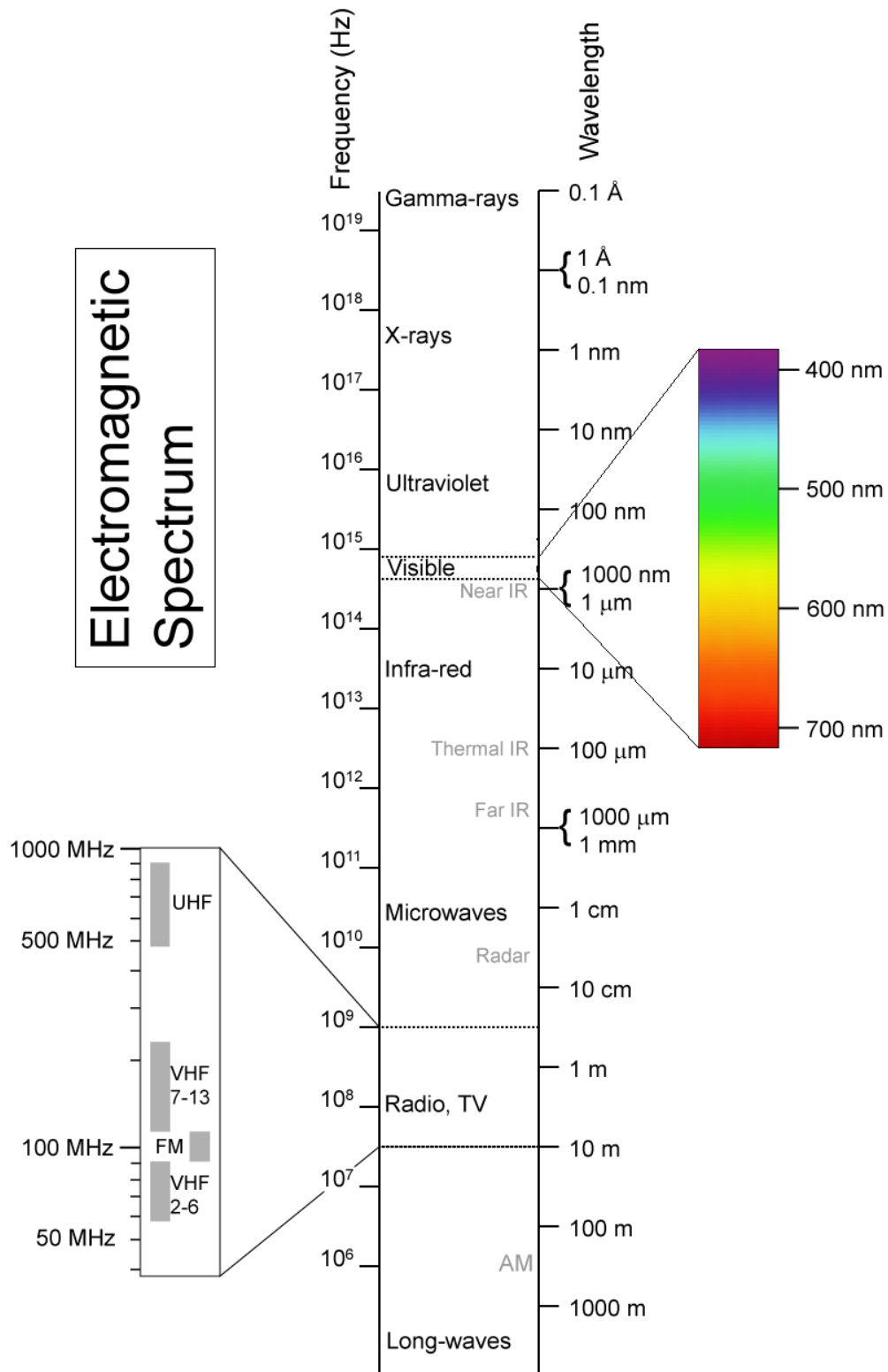
A less detailed example of the EM spectrum follows:<sup>5</sup>



<sup>4</sup> [http://unihedron.com/projects/spectrum/downloads/spectrum\\_20090210.pdf](http://unihedron.com/projects/spectrum/downloads/spectrum_20090210.pdf)

<sup>5</sup> <http://www.itsrainingelephants.com/blog-archives-foulab/2012/04/electromagnetic-spectrum-chart/index.html> , Rupert Brooks, modified MCM

The following is from Wikipedia (and was provided by SEW):<sup>6</sup>



<sup>6</sup> <http://upload.wikimedia.org/wikipedia/commons/8/8a/Electromagnetic-Spectrum.png>

## Nomenclature of Spectral Ranges

There are a number of classifications of infrared IR:

ASTER uses the following:

|                                  |                  |                          |
|----------------------------------|------------------|--------------------------|
| VNIR = visible light and near-IR | 400 to 1400 nm   | 0.4 to 1.4 $\mu\text{m}$ |
| SWIR = Shortwave Infrared        | 1400 to 3000 nm  | 1.4 to 3 $\mu\text{m}$   |
| TIR = Thermal Infrared           | 8000 to 15000 nm | 8 to 15 $\mu\text{m}$    |

Astronomers typically divide the infrared spectrum as follows:<sup>7</sup>

| Designation   | Abbreviation | Wavelength                           |
|---------------|--------------|--------------------------------------|
| Near-Infrared | NIR          | (0.7–1) to 5 $\mu\text{m}$           |
| Mid-Infrared  | MIR          | 5 to (25–40) $\mu\text{m}$           |
| Far-Infrared  | FIR          | (25–40) to (200–350) $\mu\text{m}$ . |

Note that SW IR and Near IR are combined here.

A 2007 listing of Remote Sensing uses the following broad spectral regions:<sup>8</sup>

TABLE 1-3. The primary spectral regions used in earth remote sensing. The boundaries of some atmospheric windows are not distinct and one will find small variations in these values in different references.

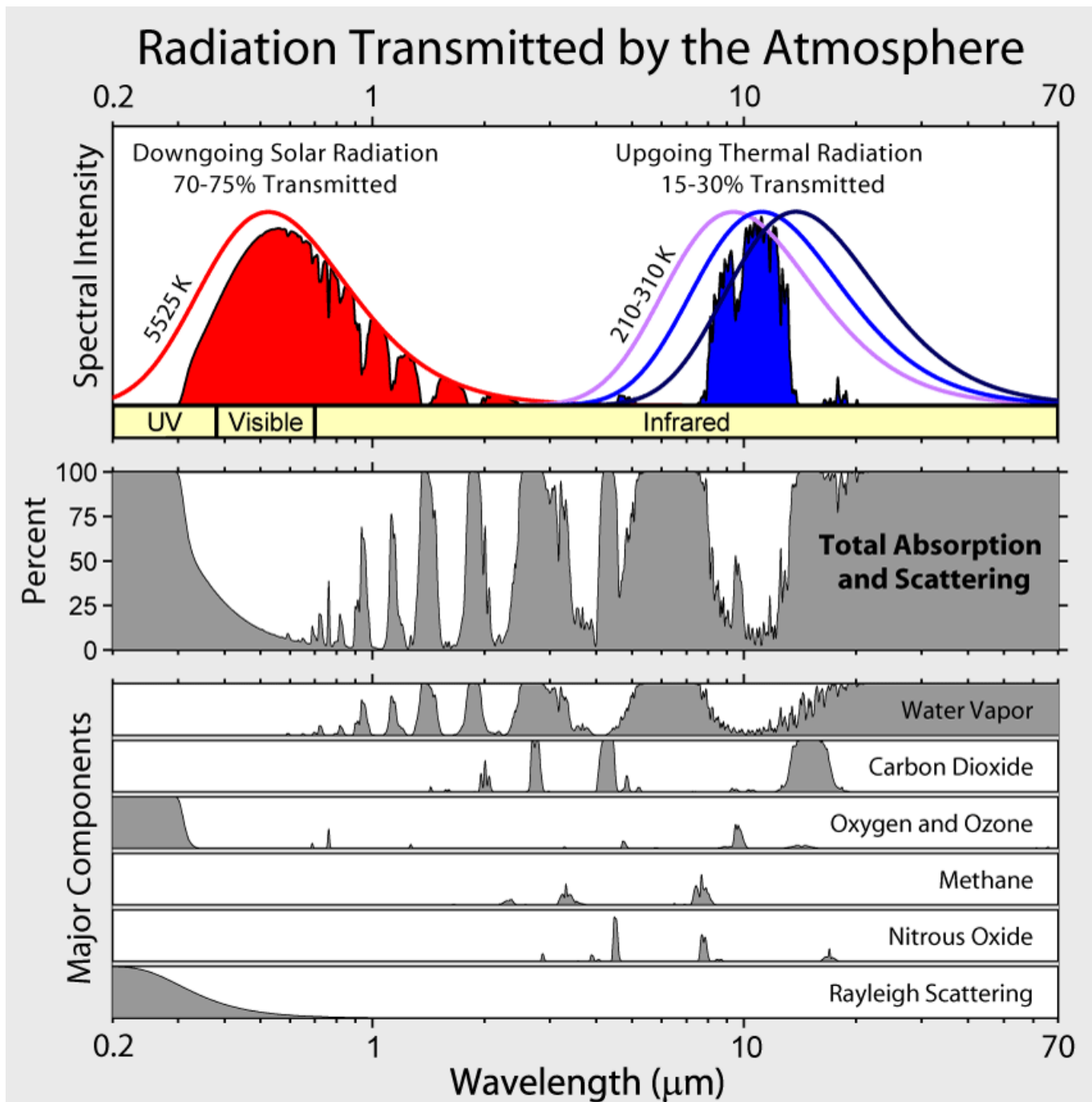
| name                                       | wavelength range   | radiation source                       | surface property of interest              |
|--|--|--|---|
| Visible (V)                                | 0.4–0.7 $\mu\text{m}$  | solar                                  | reflectance                               |
| Near InfraRed (NIR)                        | 0.7–1.1 $\mu\text{m}$  | solar                                  | reflectance                               |
| Short Wave InfraRed (SWIR)                 | 1.1–1.35 $\mu\text{m}$<br>1.4–1.8 $\mu\text{m}$<br>2–2.5 $\mu\text{m}$ | solar                                  | reflectance                               |
| MidWave InfraRed (MWIR)                    | 3–4 $\mu\text{m}$<br>4.5–5 $\mu\text{m}$                               | solar, thermal                         | reflectance, temperature                  |
| Thermal or LongWave InfraRed (TIR or LWIR) | 8–9.5 $\mu\text{m}$<br>10–14 $\mu\text{m}$                             | thermal                                | temperature                               |
| microwave, radar                           | 1 mm–1 m   | thermal (passive), artificial (active) | temperature (passive), roughness (active) |

<sup>7</sup> <http://www.ipac.caltech.edu/outreach/Edu/Regions/irregions.html>

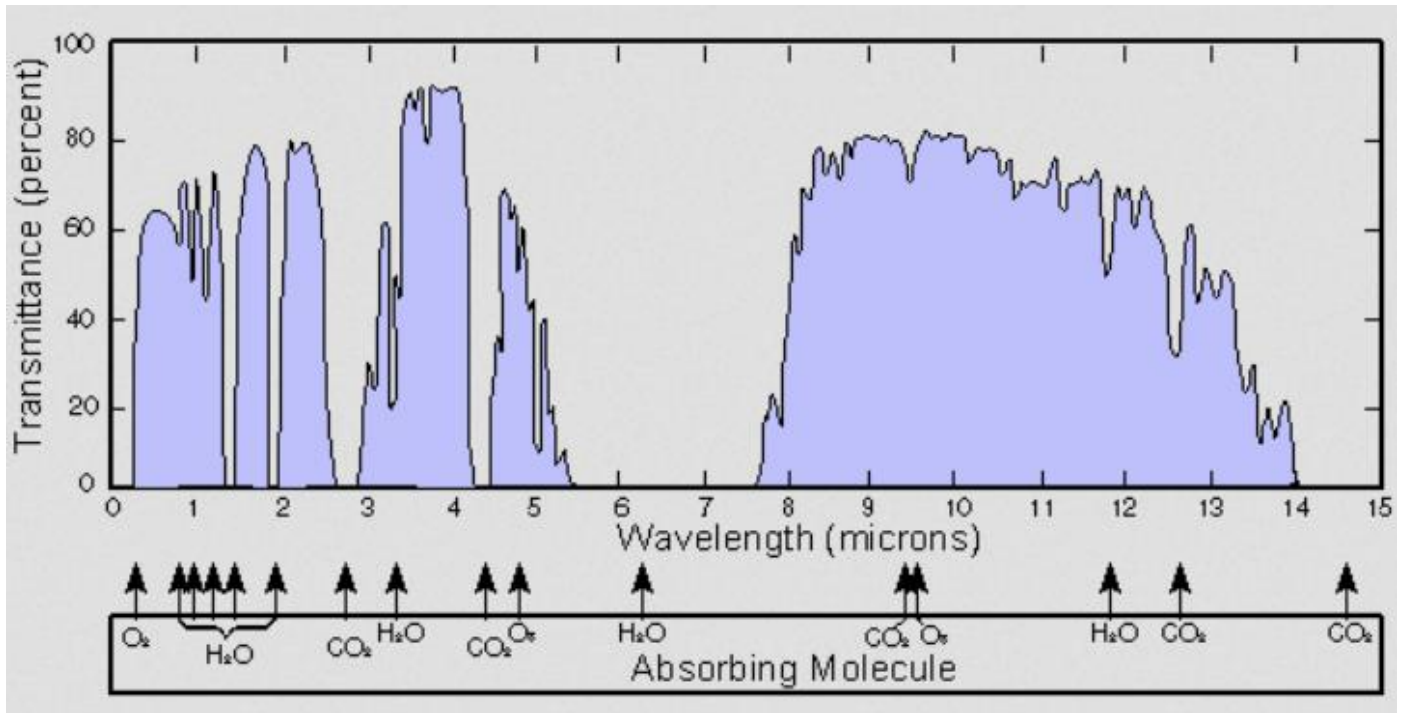
<sup>8</sup> Schowengerdt op. cit.

## EM Radiation Absorption and Transmission in the Atmosphere<sup>9</sup>

The transmission of IR through the atmosphere is strong for the IR window at 8 to 14  $\mu\text{m}$  (in TIR or MIR). Smaller and more fragmented IR windows are found in 0.7 to 5.5  $\mu\text{m}$  (in NIR). The following graphs depict these windows, along with the visible light window.



<sup>9</sup> Image from SEW lecture notes, unk. origin



Transmission of EM radiation by Earth atmosphere.<sup>10</sup>

<sup>10</sup> <http://en.wikipedia.org/wiki/Infrared>

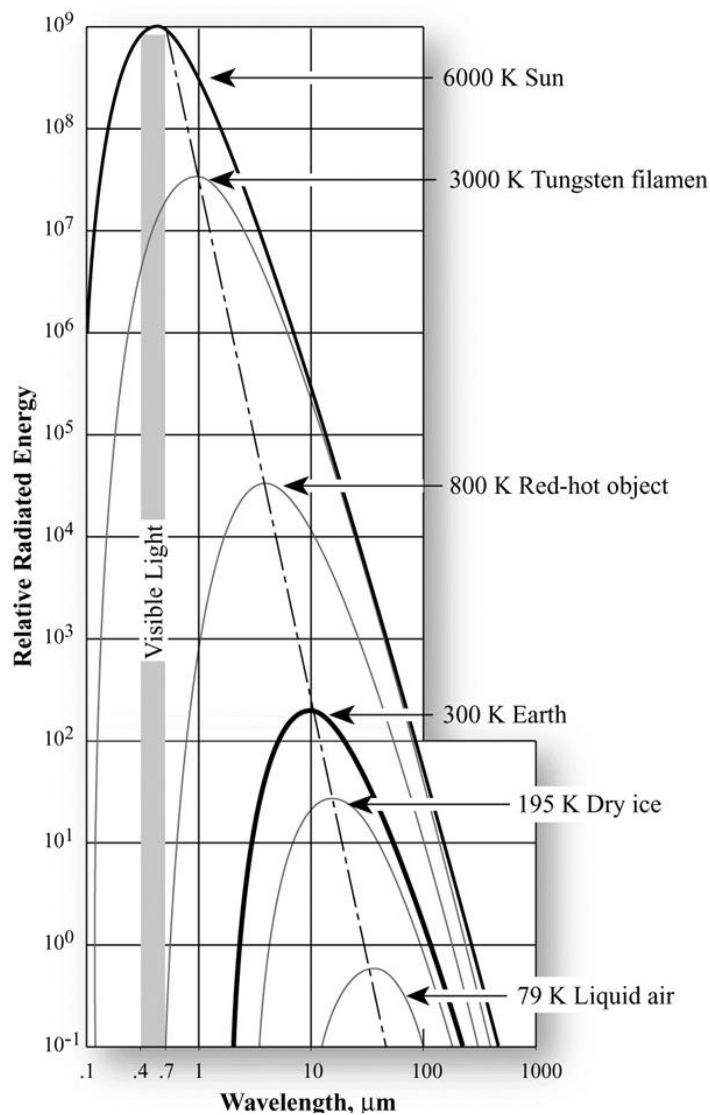
## Blackbody, Graybody, Planck's Law, Stefan-Boltzmann's law

I have reviewed Stefan-Boltzmann's law and Planck's blackbody law in other summaries.

Natural materials differ in emissivity. Their emission curve (spectral radiant exitance) may deviate substantially from that of a blackbody, and such materials are sometimes called graybodies. Two different rocks with the same kinetic temperature but with different emissivities can appear to have different temperatures when sensed by a thermal radiometer.

The following figure illustrates blackbody radiation from radiators with a wide range of temperatures. The Earth is like a ~300 K blackbody, a red-hot object is like a 800 K blackbody, and the Sun appears as a 6000 K blackbody:<sup>11</sup> The "relative radiated energy" given off by a hotter blackbody is always greater for all wavelengths than by a colder blackbody (provided emissivities are close to 1). However, the following is not a contradiction: "Thermal or longwave infrared (TIR or LWIR) light includes wavelengths between 8,000 and 15,000 nanometers. Most of the energy in this part of the spectrum is emitted (not reflected) by the Earth as heat, so it can be observed both day and night."<sup>12</sup>

The following are representative blackbody spectral radiances:



<sup>11</sup> JRJPPT on Electromagnetic Radiation Principles 2009, provided by SEW.

<sup>12</sup> <http://earthobservatory.nasa.gov/Features/FalseColor/page5.php>

# Remote Sensing RS: Selected Concepts

See also intro. in Jensen Chapter 1. Remote Sensing of the Environment. This is a strongly multi-disciplinary complex field—I will not attempt to summarize many of the fundamental but straightforward or well-known principles that are presented throughout this textbook.

## Definition of RS

RS is (according to the ASPRS which combines photogrammetry and RS), “the art, science, and technology of obtaining reliable information about physical objects and the environment, through the process of recording, measuring and interpreting imagery and digital representations of energy patterns derived from noncontact sensor systems”<sup>13</sup> RS is a multidisciplinary science (and an art) employing mathematics and logic as well as many branches of science and technology:

- physical—physics, chemistry, earth and space sciences, GIS, surveying, cartography
- biological—botany, zoology, ecology, wildlife management
- social sciences—geography, sociology, anthropology

It is also an art, especially in the realm of image interpretation, where real-world analyst experience is often essential.

## Correlation with In Situ Ground Reference Data

Remotely sensed data must be correlated with and calibrated using In Situ measurements. RS often measures and/or images *surrogates* for the actual physical property of interest. Ground based fieldwork is often needed to assess biophysical and cultural characteristics apparent only at ground level. For instance, the determination of in situ vegetation Leaf Area Index LAI, or use of an in situ spectroradiometer to determine a crop’s spectral reflectance can be used to calibrate RS information. Ground reference data may have its own inaccuracies, such as sampling error or faulty calibration of instruments, so a detailed understanding of local and RS limitations is needed.

Ground observers often also use Global Positioning System GPS for precise location correlation.

## Uses of RS

Remote Sensing is good for:

- Coverage of large and/or inaccessible areas
- Mapping of “hidden” properties not visible by eye (or smell or touch or etc...)
- Systematic and automated data collection and analysis

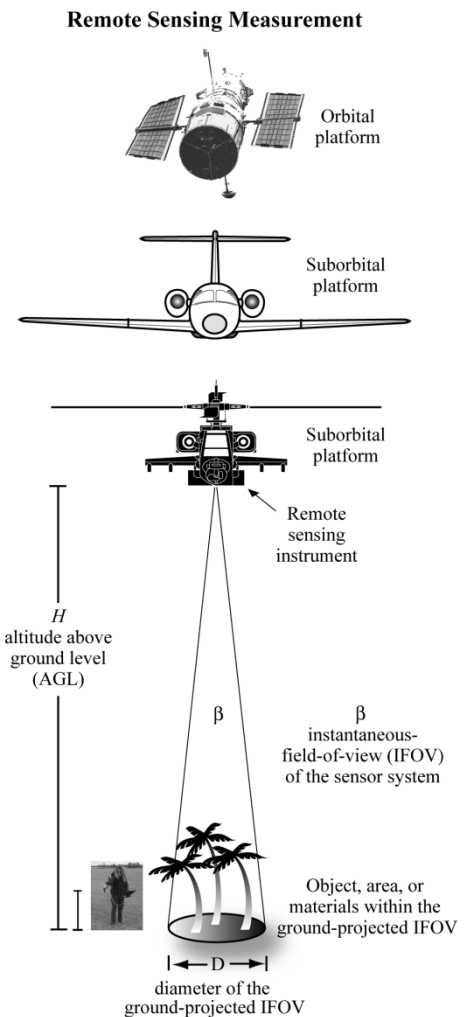
Remote Sensing is not good for:

- Easy magical solutions (When somebody enhances an image in the movies...)
- A substitute for field observations

Knowledge of capabilities and limitations of remote sensing data and techniques is essential for making it useful! [SEW]

*Remote sensing* is a collection of observational techniques to acquire data, including geospatial data.

*Geographical Information Systems (GIS)* are software tools and databases for combining and manipulating multiple geospatial datasets (using a common geographic grid).



<sup>13</sup> ASPRS = American Society of Photogrammetry and Remote Sensing, quoted by SEW.

*Geospatial analysis* is the processing, analysis, and interpretation of spatial information.

This class will focus on remote sensing and (to some degree) geospatial analysis

*Spectral Datasets*: Only three wavelengths can be shown in a single [RGB] image but all wavelengths can be shown in a spectrum.

### Geometric Acquisition Parameters

The following general Image concepts are important, but usage varies from aerial analog photography and digital RS (so a diagram specific to the circumstances can be helpful):<sup>14</sup>

H AGL (Height Above Ground Level)

$\beta$  = Angle that the full sensor or camera views (FOV or IFOV).

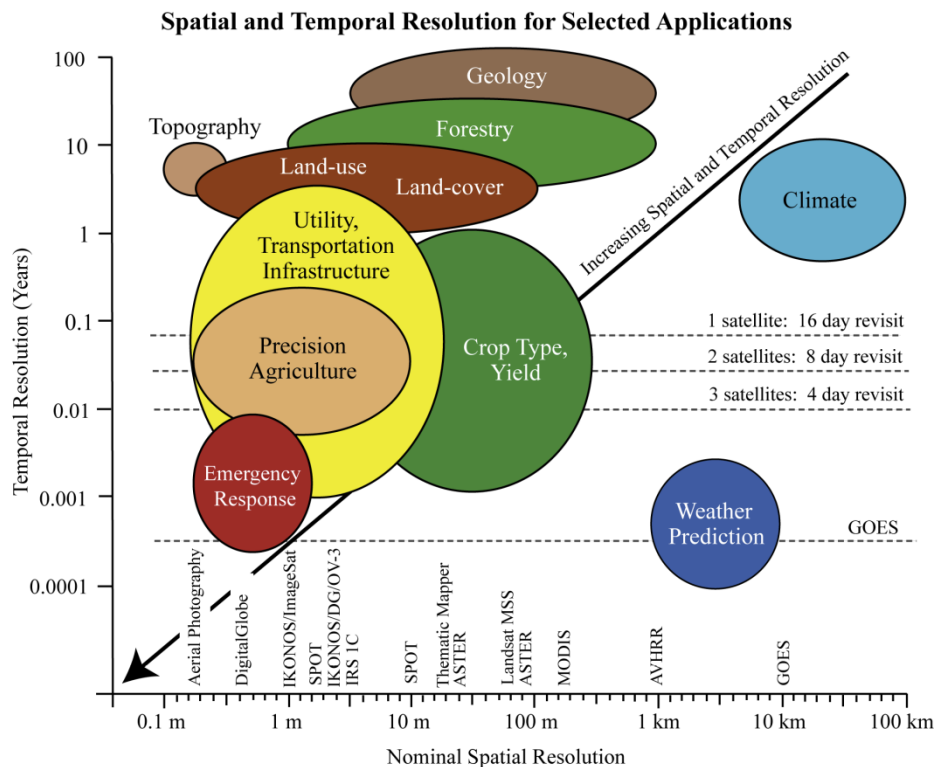
IFOV = Ground-projected Instantaneous Field of View aka GIFOV. For film aerial photography, IFOV may apply to the full camera or sensor. For digital RS, the term is usually applied to the view of a single detector/pixel/cell (per SEW), expressed as radians<sup>2</sup> or sr or degrees<sup>2</sup> for small angles (1 sr =  $(180/\pi)^2$  square degree).

D = Diameter of ground projected FOV or IFOV

f = focal length of imaging lens

GSI = Ground-Projected Sample Interval. (The Ground sample distance GSD is the distance between pixel centers measured on the ground).

### Resolution Types in RS



Current Typical Spatial versus Temporal Resolution by Mission Type<sup>15</sup>

<sup>14</sup> Image is from John R. Jensen JRJPPT 2007 titled "Geography 551: Principles of Remote Sensing", 2007. Definitions modified in accord with SEW lecture notes.

<sup>15</sup> Jensen JRJPPT 2007.

## I. Spatial Resolution

The size of the field of view of a single pixel/detector element/cell, e.g., 10 x 10m. It may be said to be the size of the smallest possible object that can be detected. SR may be expressed as the FWHM of a point spread function PSF or line spread function LSF. However, different systems may have the same FWHM yet differ in MTF (modulation transfer function). For digital systems, spatial resolution is most commonly expressed as the ground dimensions of an image cell [aka pixel/detector element = single detector in detector array]. This resolution is also called *Ground Sample Distance (GSD)*—it is the distance between pixel centers measured on the ground.<sup>16</sup> Cell sizes for Landsats are 15 to 30 m, IKONOS RGB has cell size of 4 meters, QuickBird is 0.65 m, WorldView-1 and -2 have 0.46 m, GeoEye-1 2008 has 0.41 m, GeoEye-2 has 0.31 m.<sup>17</sup>

“Shape is one visual factor that we can use to recognize and identify objects in an image. Shape is usually discernible only if the object dimensions are several times larger than the cell dimensions. On the other hand, objects smaller than the image cell size may be detectable in an image. If such an object is sufficiently brighter or darker than its surroundings, it will dominate the averaged brightness of the image cell it falls within, and that cell will contrast in brightness with the adjacent cells. We may not be able to identify what the object is, but we can see that something is present that is different from its surroundings, especially if the “background” area is relatively uniform.”<sup>18</sup>

Resolution depends on *Signal to Noise SNR*. “High SNR requires collection of as many photons as possible. But there is a finite # of photons to collect. You can increase the number of photons your detector collects, and thus increase your signal-to-noise, if you:

Look at a larger area (resulting in a poorer spatial resolution), or

Stare at an area for longer time (*dwell time*). This is limited by the motion of the spacecraft.”

Increasing spatial resolution decreases photons to work with per pixel, may need to reduce number of spectral bands and thus spectral resolution.<sup>19</sup>

In optical systems with aperture diameter  $D$  and wavelength  $\lambda$ , the Rayleigh criterion for diffraction limit of angular resolution is given by  $\theta \approx 1.22 (\lambda/D)$ , which is the angular distance from the center to the first null or dark circular ring of the Airy disk, the diffraction-limited point spread function.<sup>20</sup> Two points may be resolved from each other (with ideal optics) when separated by at least the radius of the Airy disk.

### Johnson Criteria for Spatial Resolution:

“The minimum required resolution according to Johnson's criteria are expressed in terms of line pairs of image resolution across a target, in terms of several tasks...: <sup>21</sup>

- Detection, an object is present (1.0 +/- 0.25 line pairs) [4 pixels/m]
- Orientation, symmetrical, asymmetric, horizontal, or vertical (1.4 +/- 0.35 line pairs)
- Recognition, the type object can be discerned, a person versus a car (4 +/- 0.8 line pairs); [16 pixels per m]
- Identification, a specific object can be discerned, a woman versus a man, the specific car (6.4 +/- 1.5 line pairs); [26 pixels /m] ”

The following depicts resolution capabilities for various military objects of interest:<sup>22</sup>

---

<sup>16</sup> Also called *Ground-Projected Sample Interval (GSI)* or *Ground-Projected Instantaneous Field Of View (GIFOV)*.  
[http://en.wikipedia.org/wiki/Ground\\_sample\\_distance](http://en.wikipedia.org/wiki/Ground_sample_distance)

<sup>17</sup> <http://www.satimagingcorp.com/satellite-sensors/worldview-1/>

<sup>18</sup> Microimages—Introduction to Remote Sensing:

<http://www.microimages.com/documentation/Tutorials/introrse.pdf>

<sup>19</sup> Lecture notes SEW

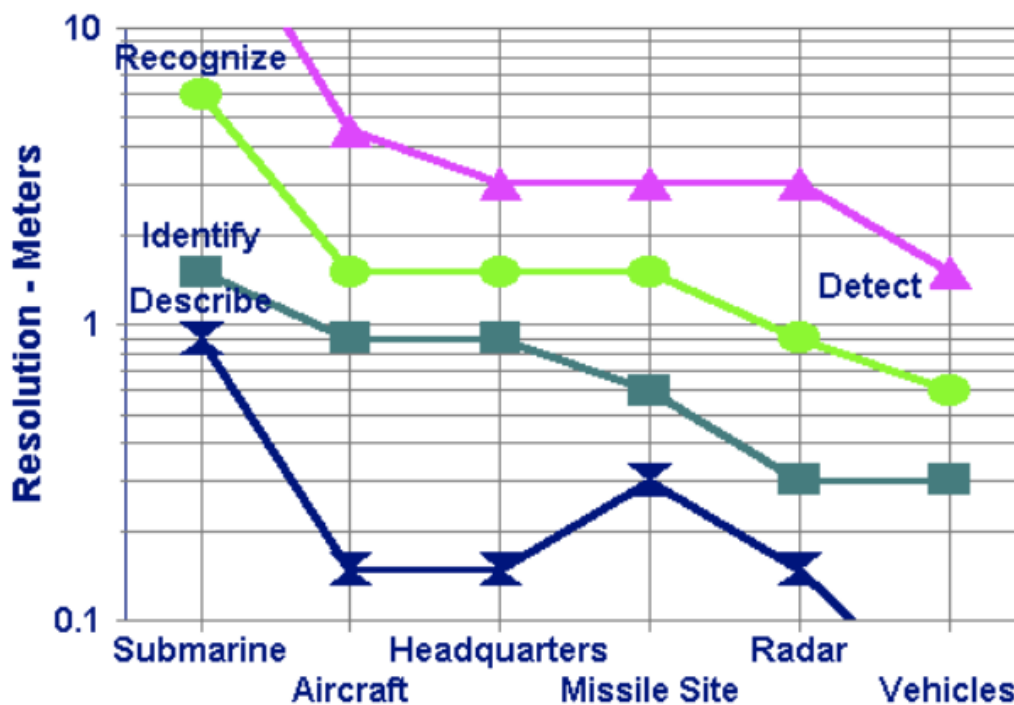
<sup>20</sup> [http://en.wikipedia.org/wiki/Diffraction-limited\\_system](http://en.wikipedia.org/wiki/Diffraction-limited_system)

<sup>21</sup> [http://en.wikipedia.org/wiki/Johnson%27s\\_criteria](http://en.wikipedia.org/wiki/Johnson%27s_criteria) and SEW lecture notes

also, <http://aissecuritysolutions.com/white-paper-on-long-range-surveillance-cameras.pdf>

<sup>22</sup> <http://www.globalsecurity.org/intell/library/imint/resolve1.htm>

## Resolution Capabilities



Johnson Criteria for Spatial Resolution

### II. Spectral Resolution

The number and size of spectral regions the sensor records data in, e.g., blue, green, red, NIR, TIR, microwave, etc. This is often quantitated as the FWHM in wavelength, although the bandpass is not necessarily Gaussian in shape. The upper and lower FWHM wavelengths determine the bandwidth. “In order to provide increased spectral discrimination, remote sensing systems designed to monitor the surface environment employ a multispectral design: parallel sensor arrays detecting radiation in a small number of broad wavelength bands. Most satellite systems use from three to six spectral bands in the visible to middle infrared wavelength region. Some systems also employ one or more thermal infrared bands. Bands in the infrared range are limited in width to avoid atmospheric water vapor absorption effects that significantly degrade the signal in certain wavelength intervals... These broad-band multispectral systems allow discrimination of different types of vegetation, rocks and soils, clear and turbid water, and some man-made materials... To provide even greater spectral resolution, so-called *hyperspectral sensors* make measurements in dozens to hundreds of adjacent, narrow wavelength bands (as little as 0.1  $\mu\text{m}$  in width).” Interpretation of single band images is aided by use of histograms showing the distribution of brightness levels. Images plotting band ratios may also be useful.<sup>23</sup> For hyperspectral sensors, the cross-track and in-track location data is combined with a 3rd axis, wavelength, to yield an “image cube” of cells.

### III. Temporal Resolution

How frequently the sensor acquires data from a particular region (e.g., every 30 days, as might apply to a satellite)

### IV. Radiometric Resolution

The ability of sensors to distinguish small differences in EM energy. This is typically characterized by the number of quantization (“gray” or brightness or digital number DN) levels available, typically  $2^7$  (0-127) to  $2^{12}$  (0 to 4095, as with ASTER), as determined by the number of bits available for data storage.<sup>24</sup> “Radiometric

<sup>23</sup> *ibid.*

<sup>24</sup> <http://www.nrcan.gc.ca/earth-sciences/geomatics/satellite-imagery-air-photos/satellite-imagery-products/educational-resources/9379>

resolution refers to the number of divisions of bit depth (for example, 255 for 8-bit, 65,536 for 16-bit, and so on) in data collected by a sensor.”<sup>25</sup>

## Radiometry Concepts

The following table presents a set of standardized names, symbols, and units for key quantities in *radiometry* (as opposed to photometry, per the excellent summary given by Joseph A. Shaw):<sup>26</sup>

## Radiometric quantities

Radiometry is the science that allows us to answer “how much light is there?”

| <u>Quantity</u> | <u>Symbol</u> | <u>Units</u>            |   |   |
|-----------------|---------------|-------------------------|---|---|
| Energy          | Q             | J                       |   |   |
| Power (flux)    | P, $\phi$     | W                       |   | $\frac{\partial Q}{\partial t}$                   |
| Intensity       | I             | W / sr                  |   | $\frac{\partial P}{\partial \Omega}$              |
| Irradiance      | E             | W / m <sup>2</sup>      | } | $\frac{\partial P}{\partial A}$                   |
| Exitance        | M             | W / m <sup>2</sup>      |   |   |
|                 |               |                         |   | exiting   |
| <b>Radiance</b> | L             | W / (m <sup>2</sup> sr) |   | $\frac{\partial^2 P}{\partial A \partial \Omega}$ |

Radiance is the most fundamental radiometric quantity

“spectral” anything = per unit wavelength or frequency  
 ex. “spectral radiance” W / (m<sup>2</sup> sr nm)

3

Energy Q here is Radiant Energy in J. Power P is the same as Radiant Flux and is given in W. Note the unexpected definition for radiometric (radiant) Intensity I as W/sr (in contrast to photometry where it is expressed as W/m<sup>2</sup>).<sup>27</sup> Irradiance E and Exitance M are closely related, are given as W/m<sup>2</sup>, and do not involve a solid angle. Radiance L adds a solid angle for the target or receiver, and is given as W/(m<sup>2</sup> sr).

### Solid Angles

The *solid angle*  $\omega$ , as measured on a sphere, is expressed in steradians (sr) as  $\omega = A/R^2$ , where A is the curving area subtended by the solid angle  $\omega$ , and R is the radius of the sphere. A full sphere has  $4\pi$  sr. (This is analogous to the planar angle  $\theta$ , which is expressed in radians as  $\theta = s/R$ , where s = arc of curving length the angle  $\theta$  subtends on a circle, and R is the radius. A full circle has  $2\pi$  radians.)

*Projected Solid Angle*  $\Omega$ : A spherical solid angle projected onto a planar surface  $A_p$  (where the surface normal may be partly or entirely oblique to the incident rays) is given in sr as the integral of

$$d\Omega = \frac{dA_p}{R^2} = dA \cos(\theta)/R^2 = d\omega \cos(\theta)$$

where for each element of projected solid angle  $d\Omega$ , the incident ray forms angle of incidence with respect to the surface normal of  $\theta$ .

<sup>25</sup> <http://support.esri.com/en/knowledgebase/GISDictionary/term/radiometric%20resolution>

<sup>26</sup> [http://www.coe.montana.edu/ee/jshaw/classes/EOSystems/F09/ClassResources/EE482\\_F09\\_RadiometryOverview\\_2pp.pdf](http://www.coe.montana.edu/ee/jshaw/classes/EOSystems/F09/ClassResources/EE482_F09_RadiometryOverview_2pp.pdf)

<sup>27</sup> [http://en.wikipedia.org/wiki/Intensity\\_%28physics%29](http://en.wikipedia.org/wiki/Intensity_%28physics%29)

A non-projected solid angle is used for a point source, such as a distant star, for which incoming light intensity  $I = P/\omega$ . By this definition,  $I$  for a particular  $\omega$  is invariant with distance (ignoring absorption).

We use a *projected solid angle* when some of a source or receiver area is not oriented normal to the incident light rays. In this case, one must obtain the projected solid angle by integrating over the target area  $A$  with  $\cos \theta$  (the angle of incidence):

$$d\Omega = dA \cos(\theta)/R^2$$

When one integrates a solid angle subtended by a circular cone having half-angle  $\Theta$  over an entire hemisphere (i.e., for azimuth  $0 < \varphi < 2\pi$  and zenith angle  $0 < \theta < \pi$ ), the solid angle subtended is  $2\pi$  steradians. In brief, a hemisphere subtends a solid angle of  $2\pi$ .

But when one integrates a projected solid angle subtended by a circular cone having half-angle  $\Theta$  over an entire hemisphere (again, for azimuth  $0 < \varphi < 2\pi$  and zenith angle  $0 < \theta < \pi$ ), the integrand includes an added  $\cos \theta$  term and the projected solid angle subtended is  $\pi$  sr rather than  $2\pi$  sr.

For a point source radiating power  $P$  in  $W$  isotropically, the irradiance  $E$  is falling on a spherical surface area that increases with distance, so that irradiance ( $W/m^2$ ) is given by  $E = P/4\pi R^2$ . Thus irradiance ( $W/m^2$ ) decreases as the inverse square of the distance.

## Lambertian Radiation and Surface

A surface that is a diffuse emitter or reflector is Lambertian if it has equal radiance  $L(\theta, \varphi)$  (expressed as  $W/(m^2 \text{ sr})$ ) in all directions. This does *not* mean that the intensity of light ( $W/\text{sr}$ ) is the same in all directions. The intensity in fact varies as the  $\cos \theta$ , where  $\theta$  is the angle of the emitted/reflected ray with respect to the surface normal. Because the projected solid angle of a hemisphere is  $\pi$  rather than  $2\pi$ , the irradiance into a hemisphere from a Lambertian surface is  $E = \pi L$ . A Lambertian surface is an ideal construct which is approximated by flat or matte finishes, but definitely not by specular surfaces.<sup>28</sup>

“A Lambertian surface is a surface of perfectly matte properties, which means that it adheres to Lambert’s cosine law. Lambert’s cosine law states that the reflected or transmitted luminous intensity in any direction from an element of a perfectly diffusing surface varies as the cosine of the angle between that direction and the normal vector of the surface. As a consequence, the luminance of that surface is the same regardless of the viewing angle.”<sup>29</sup> For example, a snowy landscape tends to have nearly the same apparent brightness in all emitted light directions.

“A surface which obeys Lambert’s law is said to be Lambertian, and exhibits Lambertian reflectance. Such a surface has the *same radiance when viewed from any angle*. This means, for example, that to the human eye it has the *same apparent brightness (or luminance)*. It has the same radiance because, although the emitted power from a given area element is reduced by the cosine of the emission angle, the apparent size (solid angle) of the observed area, as seen by a viewer, is decreased by a corresponding amount. Therefore, its radiance (power per unit solid angle per unit projected source area) is the same...”

When an area element is radiating as a result of being illuminated by a [localized] external source, the irradiance (energy or photons/time/area) landing on that area element will be proportional to the cosine of the angle between the illuminating source and the normal. A Lambertian scatterer will then scatter this light according to the same cosine law as a Lambertian emitter. This means that *although the radiance of the surface depends on the angle from the normal to the illuminating source, it will not depend on the angle from the normal to the observer*. For example, if the moon were a Lambertian scatterer, one would expect to see its scattered brightness appreciably diminish towards the terminator due to the increased angle at which sunlight hit the surface. The fact that it does not diminish illustrates that the moon is not a Lambertian scatterer, and in fact tends to scatter more light into the oblique angles than would a Lambertian scatterer.

The emission of a Lambertian radiator does not depend upon the amount of incident radiation, but rather from radiation originating in the emitting body itself. For example, if the sun were a Lambertian radiator, one would expect to see a constant brightness across the entire solar disc. The fact that the sun exhibits limb darkening in the visible region illustrates that it is not a Lambertian radiator. A black body is an example of a Lambertian radiator.”<sup>30</sup>

---

<sup>28</sup> [http://www.coe.montana.edu/ee/jshaw/classes/EOSystems/F09/ClassResources/EE482\\_F09\\_RadiometryOverview\\_2pp.pdf](http://www.coe.montana.edu/ee/jshaw/classes/EOSystems/F09/ClassResources/EE482_F09_RadiometryOverview_2pp.pdf)

<sup>29</sup> <http://www.schorsch.com/en/kbase/glossary/lambertian-surface.html>

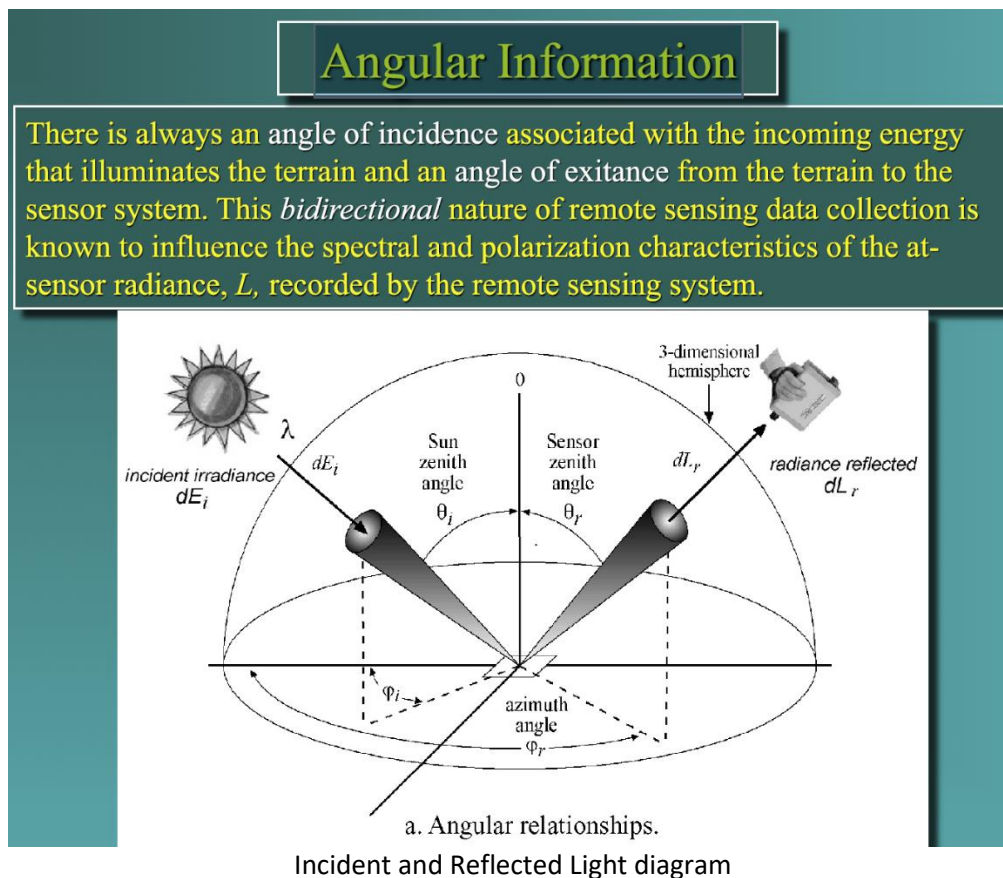
<sup>30</sup> [http://en.wikipedia.org/wiki/Lambert%27s\\_cosine\\_law](http://en.wikipedia.org/wiki/Lambert%27s_cosine_law)

## Light Gathering Capacity

In optical systems such as cameras, telescopes, and the human eye, the amount of light gathered is given by the product of source radiance and optical throughput. If source radiance is isotropic,  $P = L(A\Omega)$ , where  $P$  is power of light gathered,  $A$  is the area of the pupil or lens aperture, and  $L$  is the radiance. To increase light gathering, one may increase the aperture area  $A$ , the field of view  $\Omega$ , or the source brightness  $L$ . Radiance is invariant in a lossless optical system.<sup>31</sup>

## Surfaces and Their Interaction with Light: Reflection, Refraction, and Absorption

These are the angles of Sun vs. target and sensor vs. target:<sup>32</sup> Note the use of “bidirectional” does not refer to 2-way (forward/reverse) propagation, but rather to the directions of incident and reflected light.



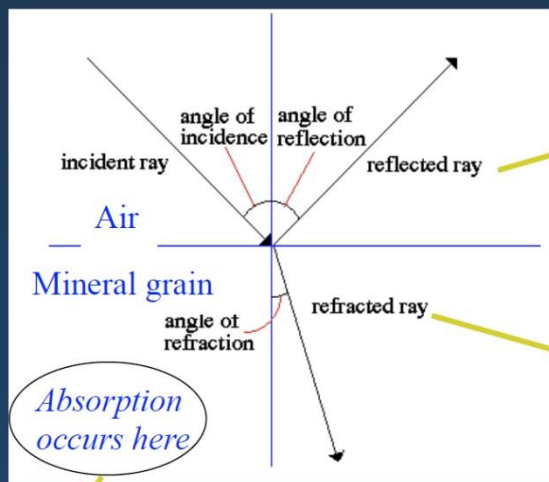
<sup>31</sup> [http://www.coe.montana.edu/ee/jshaw/classes/EOSystems/F09/ClassResources/EE482\\_F09\\_RadiometryOverview\\_2pp.pdf](http://www.coe.montana.edu/ee/jshaw/classes/EOSystems/F09/ClassResources/EE482_F09_RadiometryOverview_2pp.pdf)

<sup>32</sup> Image is from John R. Jensen JRJPPT 2007 titled “Geography 551: Principles of Remote Sensing”, 2007.



Sunlight specular reflection from liquid methane + ethane Jingpo Lacus lake on surface of Saturn's moon Titan  
 (NASA Cassini Visual and Infrared Mapping Spectrometer VIMS instrument in the 5 μm range taken on July 8, 2009 at a distance of about 200,000 km)<sup>33</sup>

## Light is reflected, absorbed, or transmitted (RAT Laws)



### Fresnel's law:

$$r_s = \frac{(n-1)^2 + K^2}{(n+1)^2 + K^2}$$

$n$  = refractive index  
 $K$  = extinction coefficient for the solid  
 $r_s$  = fraction of light reflected from the surface

The amount of specular (smooth surface) reflection is given by Fresnel's Law

### Beer's law:

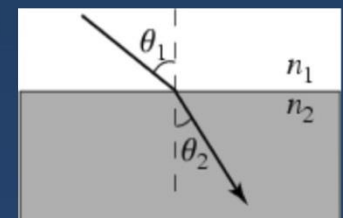
$$(L = L_0 e^{-kz})$$

$z$  = thickness of absorbing material  
 $k$  = absorption coefficient for the solid  
 $L_0$  = incoming directional radiance  
 $L$  = outgoing radiance

### Snell's law:

$$n_1 \cdot \sin\theta_1 = n_2 \cdot \sin\theta_2$$

Light passing from one medium to another is refracted according to Snell's Law



Slide from ESS 421 lecture 4 materials, showing laws governing Reflection, Absorption, and Refraction

<sup>33</sup> <http://photojournal.jpl.nasa.gov/Help/PIADetQuery.html>, search on PIA12481; and [http://solarsystem.nasa.gov/planets/profile.cfm?Object=Sat\\_Titan&Display=OverviewLong](http://solarsystem.nasa.gov/planets/profile.cfm?Object=Sat_Titan&Display=OverviewLong)  
 Page 21 of 110 RemoteSensing\_ESS421\_MCM\_Winter2015.docx

## Complex Index of Refraction $m = n^* = n + iK$

This is represented by  $n$ , the real component, and  $K$  the imaginary component, (also called the Extinction Coefficient). Thus, index of refraction  $m = n^* = n + iK$  (in complex number notation). "The complex index of refraction in Figure 4a [below] shows important properties of materials. As one moves to longer wavelengths (left to right in Figure 4a), the index of refraction decreases to a minimum just before a sharp rise (e.g. at 8.5 and 12.6  $\mu\text{m}$  in Figure 4a). The minimum is often near or even below  $n = 1$  [where  $n$  is the real part of the index]. The wavelength where  $n = 1$  is called the Christensen frequency and usually results in a minimum in reflected light because of the small (to zero) difference in the index of refraction compared to the surrounding medium (e.g. air or vacuum). The location of the observed reflectance minimum is also controlled by the extinction coefficient... Note that the Christensen frequency sometimes occurs at a wavelength shorter than the maximum in the extinction coefficient (e.g. Figure 4a). This maximum is called the restrahlen [actually, Reststrahlen] band: the location of fundamental vibrational stretching modes in the near and mid-infrared. The combination of  $n$  and  $K$  at these wavelengths often results in high reflectance."<sup>34</sup>

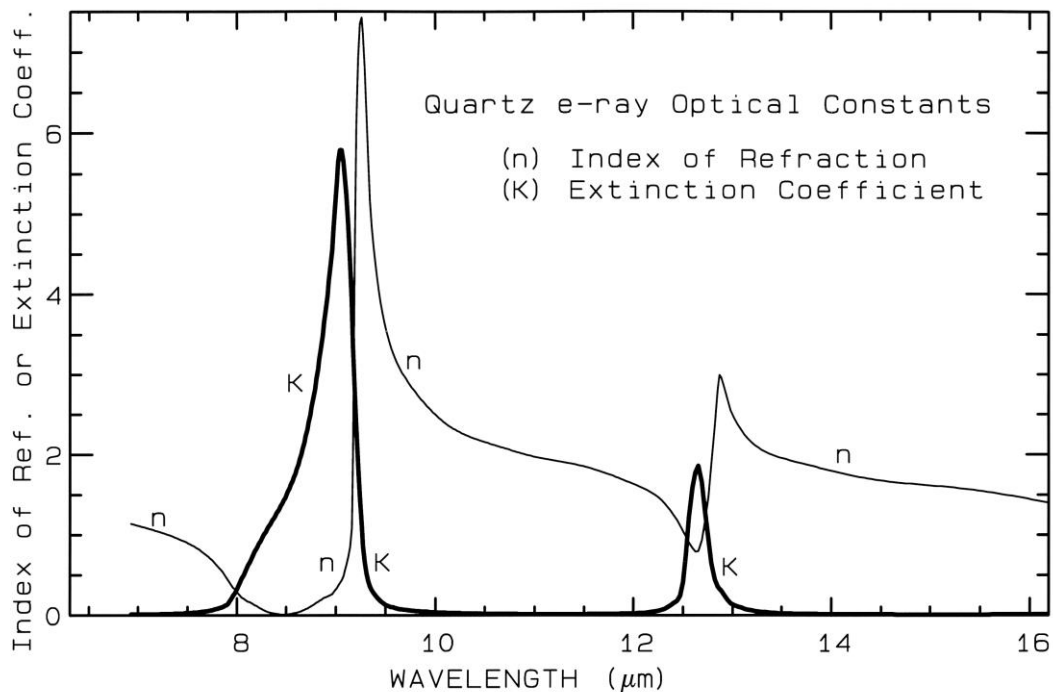
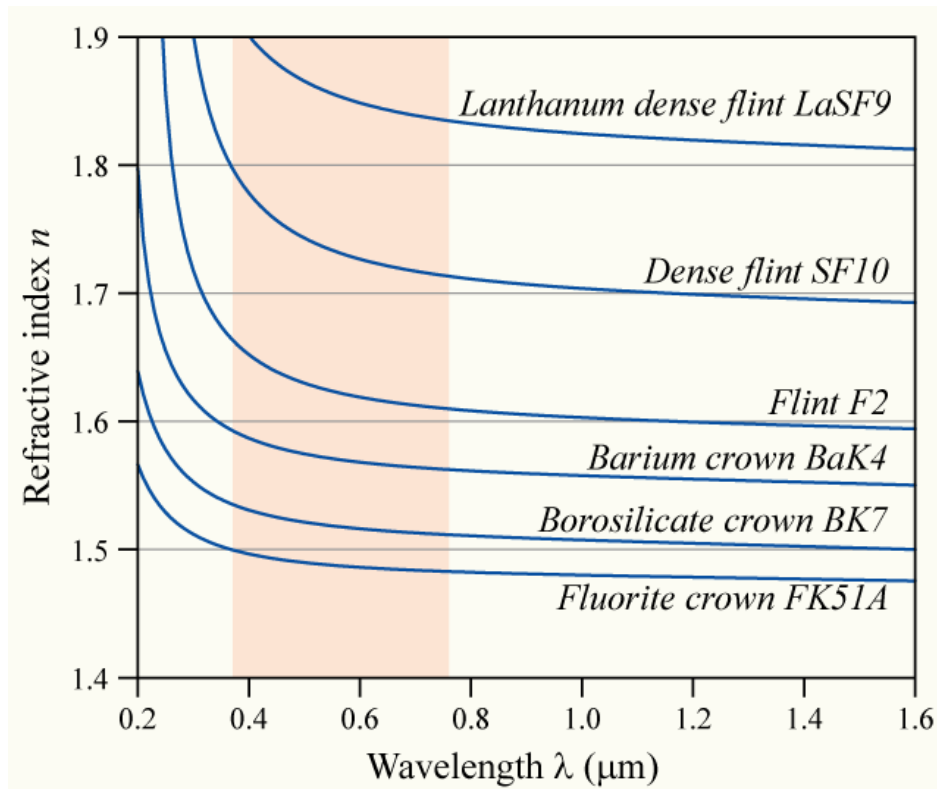


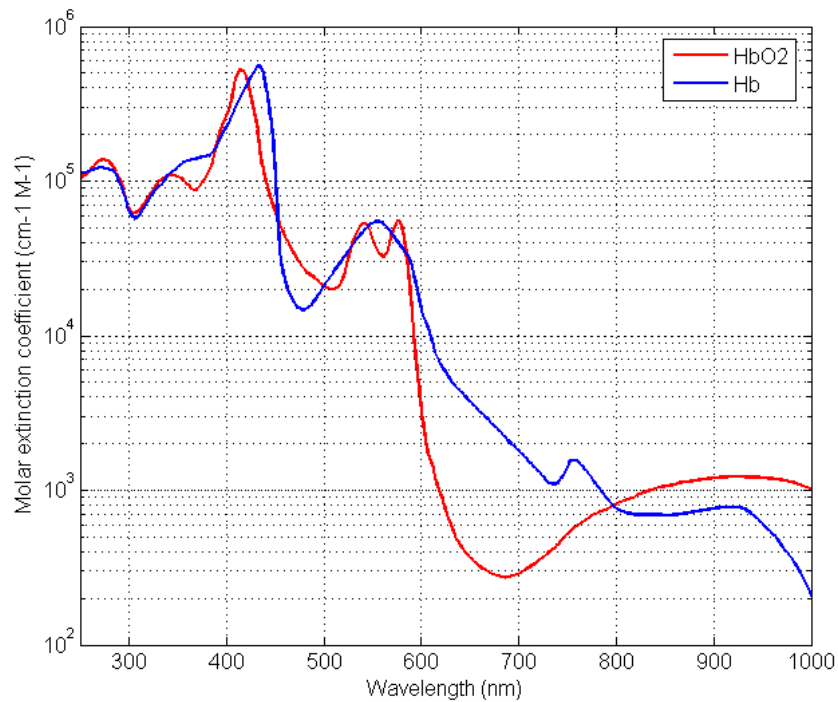
Figure 4a, Optical constants  $n$  and  $K$  for quartz,  $\text{SiO}_2$   
(this graph is repeated under Spectroscopy)

<sup>34</sup> <http://speclab.cr.usgs.gov/PAPERS.refl-mrs/refl4.html#section2.1> (text and following image)  
Page 22 of 110

The real part  $n$  of refractive index varies with wavelength, and so does the imaginary part (the Extinction Coefficient):



Variation in real Refractive Index  $n$  with Wavelength  
(here for representative solid glasses)<sup>35</sup>



Variation in molar Extinction Coefficient with wavelength  
(shown here for solutions of Hemoglobin  $\text{Hb}$  and Oxyhemoglobin  $\text{HbO}_2$ )<sup>36</sup>

<sup>35</sup> [http://en.wikipedia.org/wiki/Refractive\\_index#mediaviewer/File:Dispersion-curve.png](http://en.wikipedia.org/wiki/Refractive_index#mediaviewer/File:Dispersion-curve.png)  
Page 23 of 110

## Beer's law (Beer-Lambert Law) for Absorption

This expresses the exponentially decreasing transmission (increasing attenuation or absorption) of light passing through an absorbing medium, given by

$$L = L_0 e^{-kz}$$

where  $L_0$  = incoming directional radiance

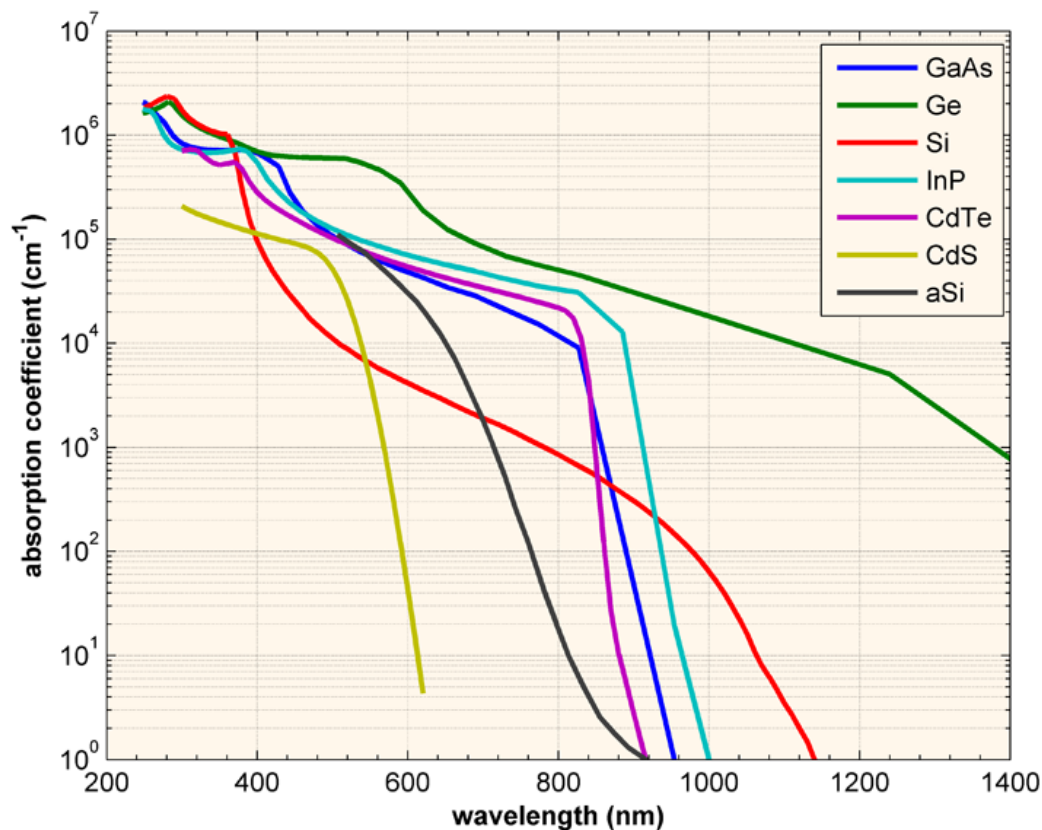
$L$  = outgoing radiance

$k$  = absorption coefficient

$z$  = thickness of material traversed

The rapidity of absorption with depth increases as absorption coefficient  $k$  increases. Note that the absorption coefficient  $k = 4\pi K/\lambda$ , and is therefore wavelength dependent.<sup>37</sup> The amount of light entering the material (i.e., not being reflected) and its internal path after refraction would vary with angle of incidence (direction), but once light has entered the material, the absorption as it traverses the medium would presumably not be further affected by angle of incidence (other than one might say that final path length varies with angle).

It would appear that  $k$  would decrease as wavelength increases, unless  $K$  happened to increase:



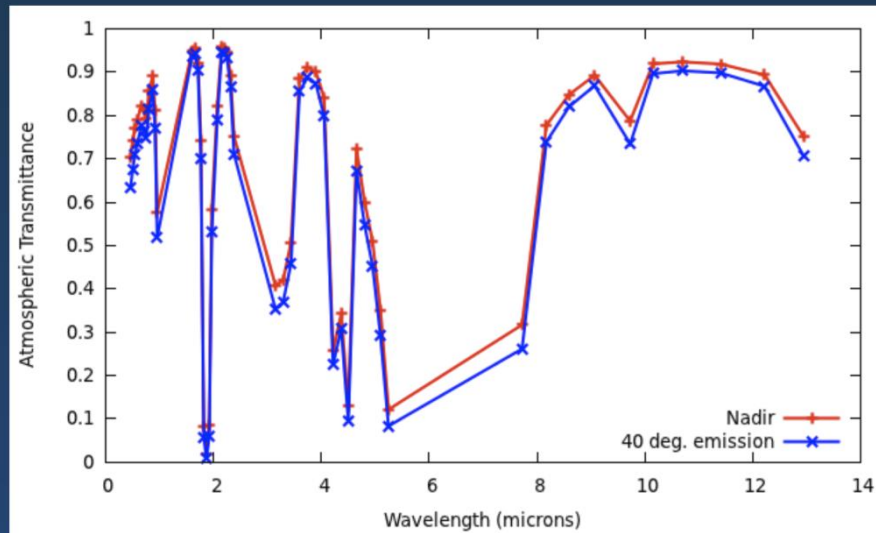
Decreasing  $k$  as  $\lambda$  increases in some solid substances<sup>38</sup>

<sup>36</sup> [http://en.wikipedia.org/wiki/Near-infrared\\_window\\_in\\_biological\\_tissue](http://en.wikipedia.org/wiki/Near-infrared_window_in_biological_tissue)

<sup>37</sup> <http://speclab.cr.usgs.gov/PAPERS.refl-mrs/refl4.html#section2.1>

<sup>38</sup> <http://www.pveducation.org/pvc/drom/pn-junction/absorption-coefficient>

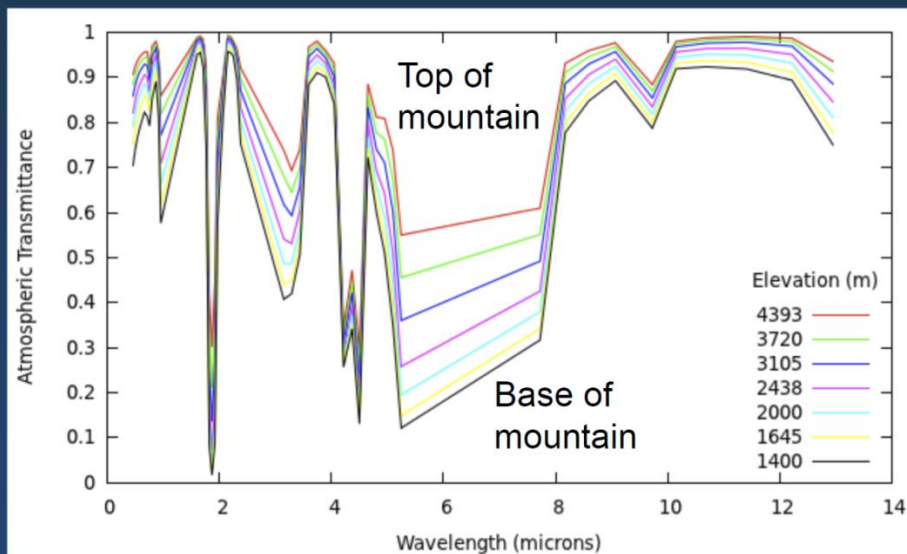
## Transmissivity decreases with atmospheric path length



An increase in emission angle increases the atmospheric path length

Transmissivity is affected by scattering and is a function of wavelength and path length (as determined here by emission angles, higher transmission for nadir vs. 40°; source unk.)

## Transmissivity increases with ground elevation

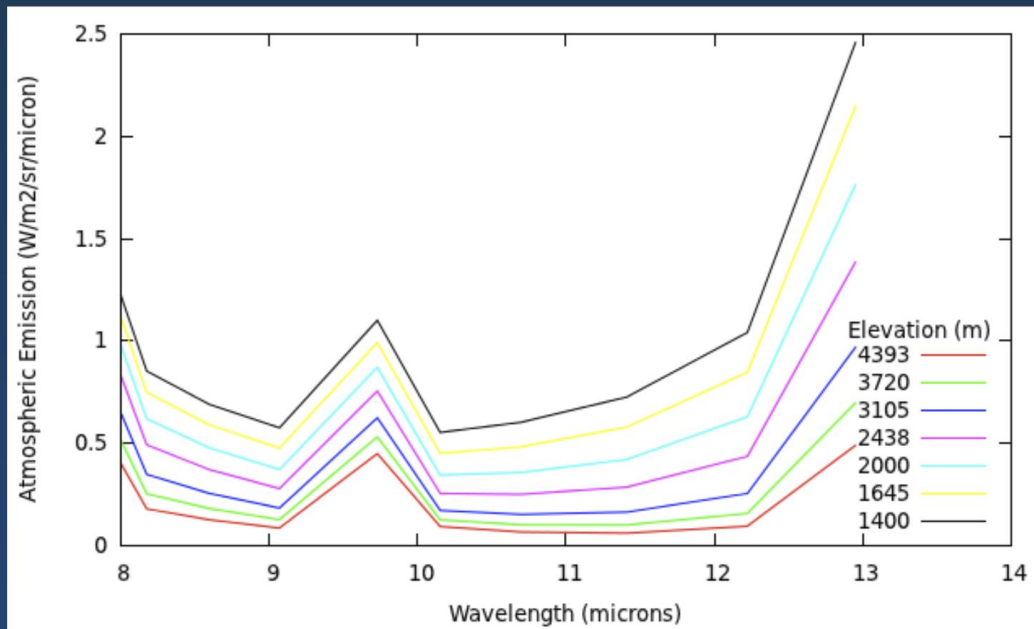


An increase in elevation decreases the atmospheric path length

Transmissivity is affected by scattering and is a function of wavelength and path length (as determined here by ground elevation at nadir). It increases with higher ground elevation (less atmospheric absorption between Sun and target) and decreases with lower ground elevation. (source unknown)

# Path spectral radiance $L_{s\uparrow}(\lambda)$ increases with atmospheric path length

Mt. Rainier - TIR MASTER data



A decrease in elevation increases the atmospheric path length

In addition to effects of scattering on transmissivity, upwelling path spectral radiance  $L_{\uparrow}(\lambda)$  is also affected by atmospheric emission. Atmospheric emission increases with atmospheric path length and therefore increases with lower ground elevation.  
(all 3 images are from Lecture 5 PDF, source unknown)

## Fresnel's Law

This expresses the *specular* reflection of light at a smooth surface interface between two media with differing index of refraction  $n$ . The angles of incidence and reflection (measured with respect to the Normal) are equal. It is given [approximately] by

$$R_s = \frac{(n - 1)^2 + K^2}{(n + 1)^2 + K^2}$$

where  $R_s$  = Specular Reflection (unitless fraction)

$n$  = real component of Refractive Index

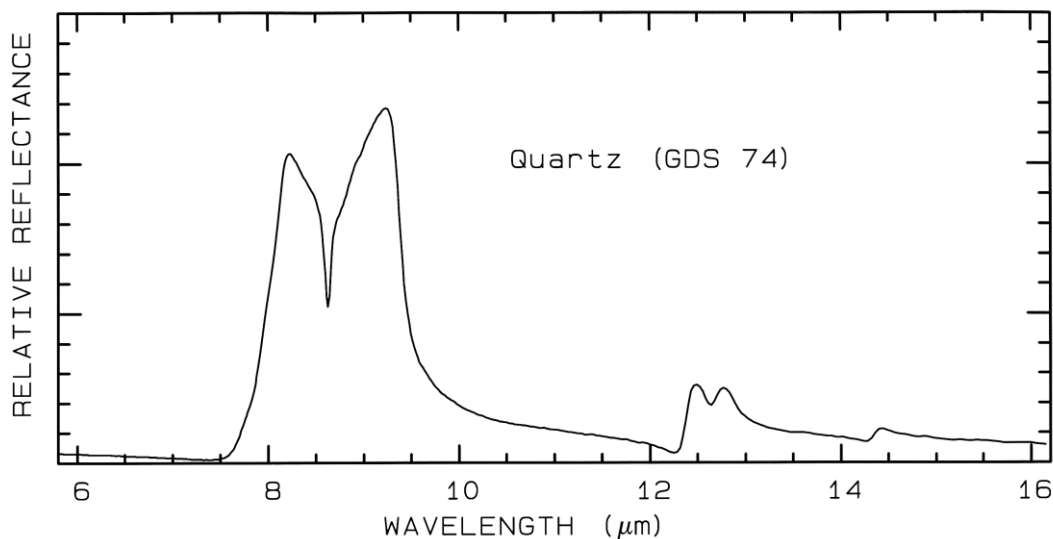
$K$  = complex component (Extinction coefficient) of Refractive Index

“At angles other than normal, the reflectance is a complex trigonometric function involving the polarization direction of the incident beam... The reflection from quartz grains as measured on a laboratory spectrometer is shown in Figure 4b [the following image]. While the spectrum is of a particulate surface, first surface reflection dominates all wavelengths, and so is similar to the spectrum of a slab of quartz.”<sup>39</sup>

The full formulation accounts for variation in angles  $i$  [of incidence] and  $e$  [of emergence] and polarization.

## Specular Reflection

This arises from surfaces that are glassy smooth relative to the wavelength. The incident angle  $i$  = emergence angle  $e$  for a perfect specular reflection. If the surface is a near perfect specular reflector (“glossy” but not mirror-like), most of the exitance is at the expected specular angle  $e$ , with some diffuse exitance as well. If the incoming beam has irradiance  $E$  ( $\text{W m}^{-2}$ ), the



Reflectance for quartz  $\text{SiO}_2$  by wavelength.

(The high reflectance from 8 to 10 is presumably due in the reststrahlen band mentioned above.)

“Specular reflection from a dielectric such as water can affect polarization and at Brewster's angle reflected light is completely linearly polarized parallel to the interface... Waves other than visible light can also exhibit specular reflection. This includes other electromagnetic waves, as well as non-electromagnetic waves. Examples include ionospheric reflection of radiowaves, reflection of radio- or microwave radar signals by flying objects, acoustic mirrors, which reflect sound, and atomic mirrors, which reflect neutral atoms.”<sup>40</sup>

## Snell's Law

This governs refraction when light crosses an interface between two media of differing refractive index ( $n_1$  and  $n_2$ ). The real part of Index of Refraction  $n$  = Speed of light in medium / Speed of light in Vacuum =  $v/c$ . When light enters a medium with greater  $n$ , the speed  $v$  is slower, the wavelength  $\lambda$  is shorter, but the

<sup>39</sup> <http://speclab.cr.usgs.gov/PAPERS.refl-mrs/refl4.html#section2.1>

<sup>40</sup> [http://en.wikipedia.org/wiki/Specular\\_reflection](http://en.wikipedia.org/wiki/Specular_reflection)

frequency  $\nu$  remains the same. In fact,  $\lambda = \lambda_0 / n$  where  $\lambda_0 =$  wavelength in vacuum. When light passes from a medium 1 with index of refraction  $n_1$  across an interface into a medium with index of refraction  $n_2$ , Snell's law is observed regarding the angles with respect to the Normal:

$$\frac{\sin \theta_1}{\sin \theta_2} = \frac{v_1}{v_2} = \frac{n_2}{n_1}$$

(Going from a lower to a higher refractive index causes bending toward the normal, thus a smaller angle  $\theta_2$  with respect to the Normal, because

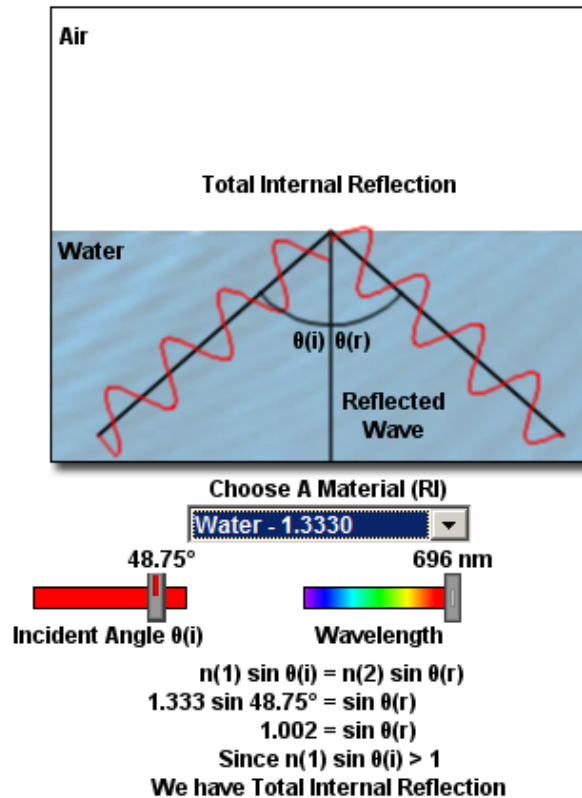
$$\sin \theta_2 = \frac{n_1}{n_2} \sin \theta_1$$

### Critical Angle (Total Internal) Reflection

“Upon passing through a medium of higher refractive index into a medium of lower refractive index, the path taken by light waves is determined by the incident angle with respect to the boundary between the two media... At the critical angle for the material through which the incident light ray propagates (48.75 degrees for ... water), the light will be totally internally reflected at the interface back into the material without passing through and undergoing refraction.”<sup>41</sup> This is a special type of reflection which occurs when Snell's law would otherwise require  $\sin \theta_2 > 1$ , which is impossible. The angle  $\theta_{\text{critical}}$  (with respect to the Normal) at which and beyond which total internal reflection occurs is given when  $\theta_{\text{critical}}$  is the value of  $\theta_1$  for which  $\theta_2$  equals  $90^\circ$ , so that (because  $\sin 90^\circ = 1$ ):

$$\theta_{\text{critical}} = \arcsin\left(\frac{n_2}{n_1} \sin \theta_2\right) = \arcsin \frac{n_2}{n_1}$$

For a water/air interface, this angle is about  $48.6^\circ$ . The following is from an excellent Java demo referenced just above.

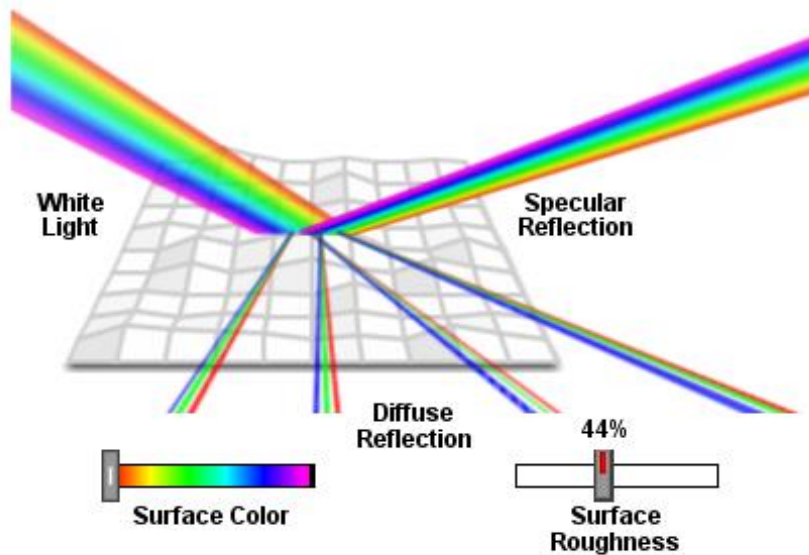


<sup>41</sup> <http://www.olympusmicro.com/primer/java/refraction/criticalangle/index.html> (includes Java demo)

## Specular vs. Diffuse Reflection

The topic of Lambertian diffuse reflection is discussed above.

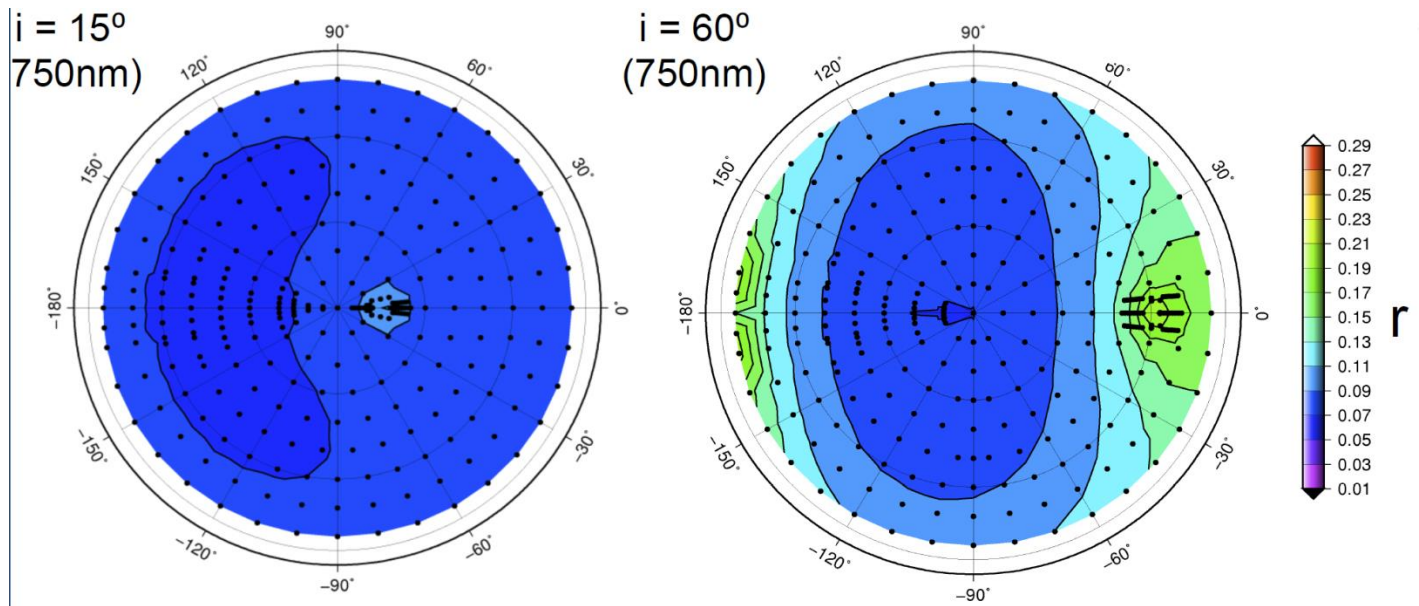
“The amount of light reflected by an object, and how it is reflected, is highly dependent upon the smoothness or texture of the surface. When surface imperfections are smaller than the wavelength of the incident light (as in the case of a mirror), virtually all of the light is reflected equally. However, in the real world most objects have convoluted surfaces that exhibit a diffuse reflection, with the incident light being reflected in all directions.”<sup>42</sup> The following image was created with settings chosen on the demo website, namely for white light and a somewhat rough surface:



A surface may exhibit back reflection, forward reflection, diffuse (Lambertian) reflection, specular reflection, or a combination thereof. Surfaces that are relatively smooth with respect to wavelength typically exhibit specular or forward reflection. Rough surfaces such as sand or conifers may be diffuse reflectors. More complex surfaces having for instance facets may back-reflect. The “envelope” of vectors comprising the pattern of reflected light (scattering envelopes) are also termed “phase functions.”

Irregular topography can have the effect of substantially changing angle of incidence with respect to the normal and angle to the sensor with respect to the normal, and of course can create shadowed areas of low reflectance. *Shadowed* areas are where direct illumination by the sun is blocked. More subtle *shaded* surfaces exhibit varying degrees of reduced reflection due to illumination geometry.

Polar phase diagrams may be created showing amount of reflectance as a function of azimuth source azimuth angle  $\phi$  and zenith angle  $\theta$ . The following example was included in our course Lecture 4 on Light and Surfaces. It depicts BUG Bidirectional Reflection Distribution Function (BRDF) measurements (i.e., of reflectance) for two different angles of incidence  $i$ , for a representative Apollo lunar sample, using a 100 W quartz halogen bulb as the light source. Here, the colors represent “lambert albedo,” scale bar is from 0.01-0.29.<sup>43</sup> It appears that light source (polygonal graphic) is positioned at the azimuth angle position marked 0°, but the diagram is a little confusing.



### Effect of Grain Size on Diffuse Reflection

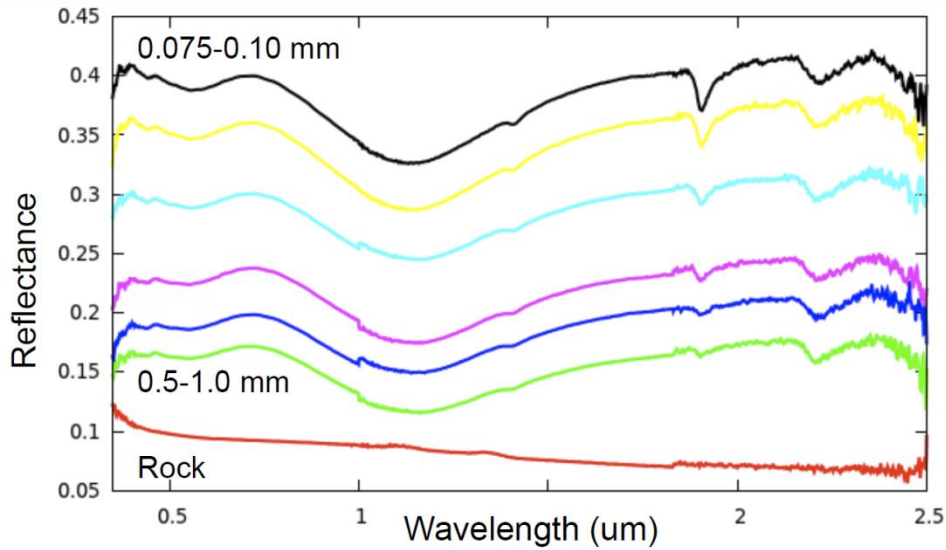
The reflectance by particulate materials tends to increase as particle size decreases. ““The amount of light scattered and absorbed by a grain is dependent on grain size... A larger grain has a greater internal path where photons may be absorbed according to Beers Law. It is the reflection from the surfaces and internal imperfections that control scattering. In a smaller grain there are proportionally more surface reflections compared to internal photon path lengths, or in other words, the surface-to-volume ratio is a function of grain size. If multiple scattering dominates, as is usually the case in the visible and near- infrared, the reflectance decreases as the grain size increases... However, in the mid-infrared, where absorption coefficients are much higher and the index of refraction varies strongly at the Christensen frequencies..., first surface reflection is a larger or even dominant component of the scattered signal. In these cases, the grain size effects are much more complex, even reversing trends commonly seen at shorter wavelengths ... [so that reflectance increases with increasing grain size].”<sup>44</sup>

This is illustrated in the Obsidian Spectra to follow:

<sup>43</sup> <http://meetingorganizer.copernicus.org/EPSC-DPS2011/EPSC-DPS2011-329-5.pdf>

<sup>44</sup> <http://speclab.cr.usgs.gov/PAPERS.refl-mrs/refl4.html#section4.3>

# Obsidian Spectra



Reflectance goes up as particle size decreases  
(image from course notes lecture 5, source unknown)

## Effect of Wet vs. Dry Grains on Diffuse Reflection

Wet sand is less reflective than dry sand, due to smaller scattering angles between sand [silica]/water interfaces (for which  $n = 1.33$  and  $1.46$ , respectively) compared to sand vs. air ( $n=1.33$  vs.  $1.0$ ), and thus greater path lengths are traversed within the sand. "It is commonly observed that natural multiple-scattering media such as sand and soils become noticeably darker when wet. The primary reason for this is that changing the medium surrounding the particles from air to water [or to benzene, as is also illustrated in their paper] decreases their relative refractive index [i.e., the difference in refractive index], hence increases the average degree of forwardness of scattering as determined by the asymmetry parameter (mean cosine of the scattering angle). [MCM Clarification: the scattering angle is the angle of deviation from the original path at the interface. The authors show that this mean angle increases (cosine decreases from 1) as the ratio of refractive indexes rises from 1 for identical substances.] As a consequence, incident photons have to be scattered more times before reemerging from the medium and are, therefore, exposed to a greater probability of being absorbed..."<sup>45</sup>

A diagram from this paper (right) shows how the asymmetry parameter  $g = \cos \theta$  (where  $\theta$  is the scattering angle) decreases from 1.0 (no scattering) as the ratio of the refractive indexes rises from 1.0, whether for Mie or geometic optics. The ratios are given by the index of refraction of the particle  $n$  divided by the index of refraction of the surrounding medium, for instance  $n_{\text{sand}}/n_{\text{air}}$  versus  $n_{\text{sand}}/n_{\text{water}}$ .

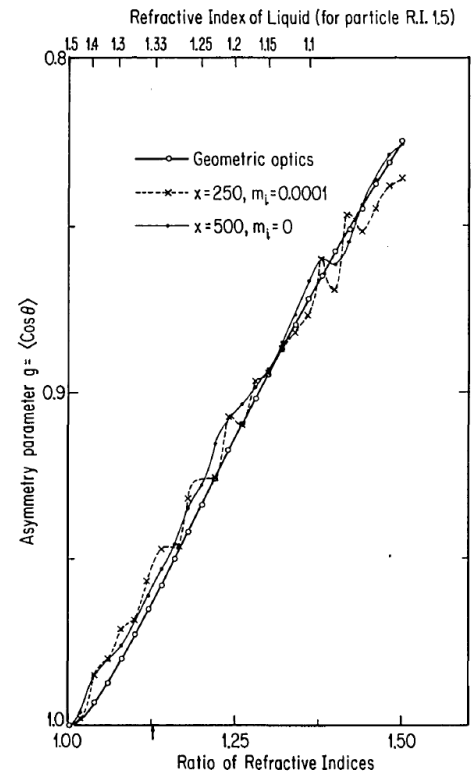


Fig. 1. Dependence of the mean cosine of the angle of scattering by a sphere (asymmetry parameter) on the refractive index (real part) relative to that of the surrounding medium. These calculations were made using both Mie theory and geometrical optics. The size parameter  $x$  is the sphere circumference divided by the wavelength, and  $m_i$  is the imaginary part of its refractive index.

<sup>45</sup> Sean A. Twomey et al, "Reflectance and albedo differences between wet and dry surfaces", *Applied Optics*, Vol. 25, Issue 3, pp. 431-437 (1986) /

## Spectral Reflectance and the Color of Water, Snow, and Ice

“Snow is highly reflective in the visible, where the solar spectrum’s maximum is located. Then albedo  $r$  is close to 1. However, the albedo decreases in the UV and IR spectral regions. The decrease in albedo is the most pronounced in the near-IR spectral region, with values of  $r$  close to zero at 1.5, 2.0, and 2.5  $\mu\text{m}$ , where ice absorption maxima are located. Snow is essentially black then [i.e., at those IR wavelengths].”<sup>46</sup>

The bright color of the undersurface of a ski can be seen to reemerge from nearby snow due to multiple scattering reflections.

“What causes the blue color that sometimes appears in snow and ice? As with water, this color is caused by the absorption of both red and yellow light (leaving light at the blue end of the visible light spectrum) [see Fig. 8 to the right]. The absorption spectrum of ice is similar to that of water, except that hydrogen bonding causes all peaks to shift to lower energy—making the color greener. This effect is augmented by scattering within snow, which causes the light to travel an indirect path, providing more opportunity for absorption... From the surface, snow and ice present a uniformly white face. This is because almost all of the visible light striking the snow or ice surface is reflected back, without any preference for a single color within the visible spectrum... The situation is different for light that is not reflected, but penetrates or is transmitted into the snow. As this light travels into the snow or ice, the ice grains scatter a large amount of light. If the light is to travel over any distance it must survive many such scattering events. In other words, it must keep scattering and not be absorbed. We usually see the light coming back from the near surface layers (less than 1 cm) after it has been scattered or bounced off other snow grains only a few times, and it still appears white. In simplest of terms, think of the ice or snow layer as a filter. If it is only a centimeter thick, all the light makes it through; if it is a meter thick, mostly blue light makes it through. This is similar to the way coffee often appears light when poured, but much darker when it is in a cup... Deeper in the snow, the preferential absorption of red begins to become noticeable. Just as with water, more red light is absorbed compared to blue. Not much more, but enough that over a considerable distance, say a meter or more, photons emerging from the snow layer tend to be made up of more blue light than red light. This is typically seen when poking a hole in the snow and looking down into the hole to see blue light, or in the blue color associated with the depths of crevasses in glaciers. In each case the blue light is the product of a relatively long travel path through the snow or ice. This spectral selection is related to absorption, and not to reflection.”<sup>47</sup>

“Ice is blue for the same reason water is blue: it is a result of an overtone of an oxygen-hydrogen (O-H) bond stretch in water which absorbs light at the red end of the visible spectrum.”<sup>48</sup> [explained in greater detail further below]

“...Because the absorption which gives water its color is in the red end of the visible spectrum, one sees blue, the complementary color of red, when observing light that has passed through several meters of water. This color of water can also be seen in snow and ice as an intense blue color scattered back from deep holes in fresh snow. Blue to bluegreen hues are also scattered back when light deeply penetrates frozen waterfalls and glaciers... Water is unique among the molecules of nature in its high concentration of OH bonds and in its plentiful supply. Most important, the OH symmetric ( $\nu_1$ ) and antisymmetric ( $\nu_3$ ) vibrational stretching fundamentals are at high enough energy [ $3650\text{ cm}^{-1}$  and  $3755\text{ cm}^{-1}$ , respectively] so that a four quantum

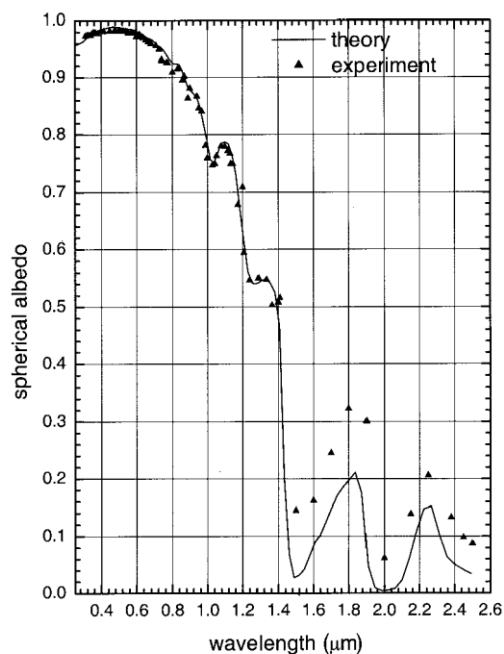


Fig. 8. Dependence of spherical albedo on wavelength according to measurements<sup>42</sup> and calculations made with Eq. (44) at  $b = 3.6$  and  $d = 0.22\text{ mm}$ .

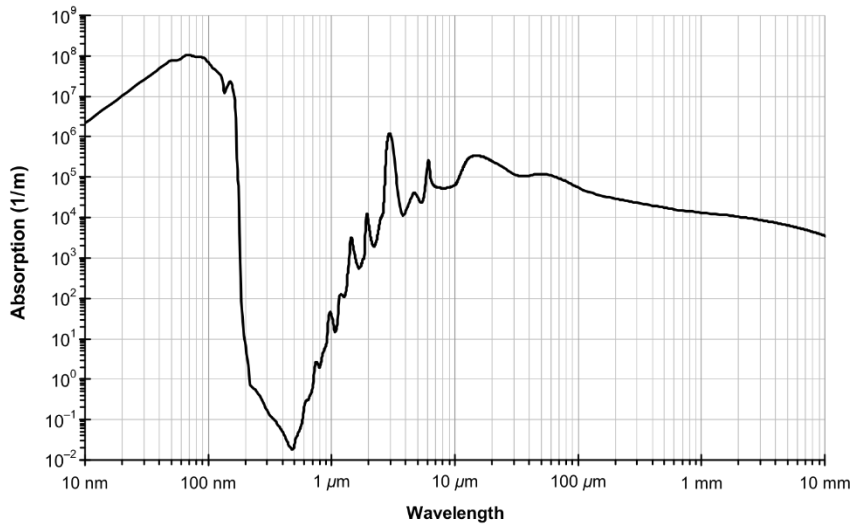
<sup>46</sup> Alexander A. Kokhanovsky and Eleonora P. Zege, “Scattering optics of snow”, *Applied Optics*, Vol. 43, Issue 7, pp. 1589-1602 (2004) (source of quote and of diagram “Fig. 8”)

<sup>47</sup> <http://www.webexhibits.org/causesofcolor/5C.html>

<sup>48</sup> [http://en.wikipedia.org/wiki/Blue\\_ice\\_%28glacial%29](http://en.wikipedia.org/wiki/Blue_ice_%28glacial%29)

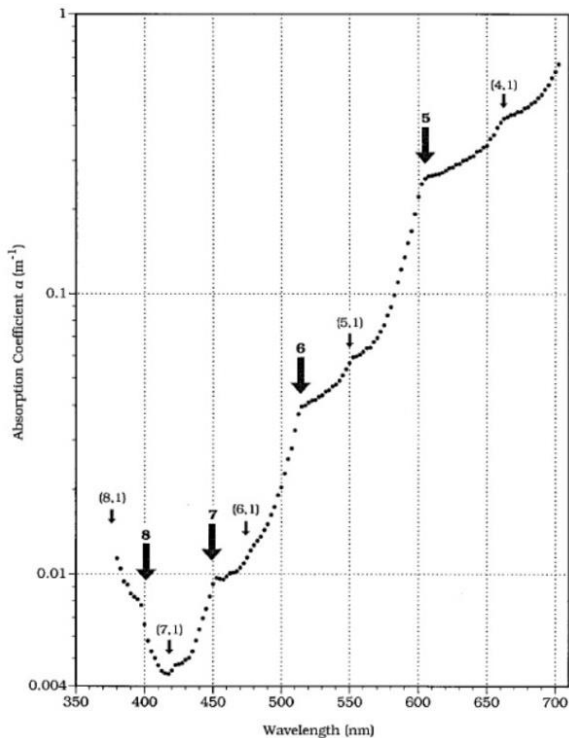
overtone transition ... at  $14,318.77 \text{ cm}^{-1}$  (698 nm), just at the red edge of the visible spectrum.”<sup>49</sup>

The following graphs help to clarify why water is blue.



“The absorption band at 698 nm ( $14,300 \text{ cm}^{-1}$ ) is a 3rd overtone ( $n=4$ ) [of the stretching vibrational mode  $\nu_1 + \nu_3$ ]. It tails off onto the visible region and is responsible for the intrinsic blue color of water.”<sup>50</sup>

This graph shows the position of visible light at 400 to 700 nm, and the rising absorption of wavelengths in the near IR. Absorption is minimal at blue wavelengths.



This graph depicts high resolution empirical (logarithmic) absorption coefficients for pure liquid water from near-UV at 380 nm to the near IR at 700+ nm. The transparency of water is greatest for blue light at about 420 nm.

According to the authors Robin M. Pope and Edward S. Fry, a nearby shoulder marked (7,1) arises from the computed 7th harmonic of the OH stretch modes ( $\nu_1 + \nu_3$ , apparently considered together) along with the fundamental = first harmonic = 1 of the scissoring bend ( $\nu_2$ ) (see below). The bolder arrows designate the location of harmonics solely of the OH stretch modes  $\nu_1 + \nu_3$ .

The  $(\nu_1 + \nu_3, \nu_2) = (4,1)$  mode is at 662 nm. Not shown on this graph are the peaks or shoulders at even higher levels of absorption in the near IR wavelengths from  $(\nu_1 + \nu_3, \nu_2) = (4,0)$  at 742 nm,<sup>51</sup> etc.

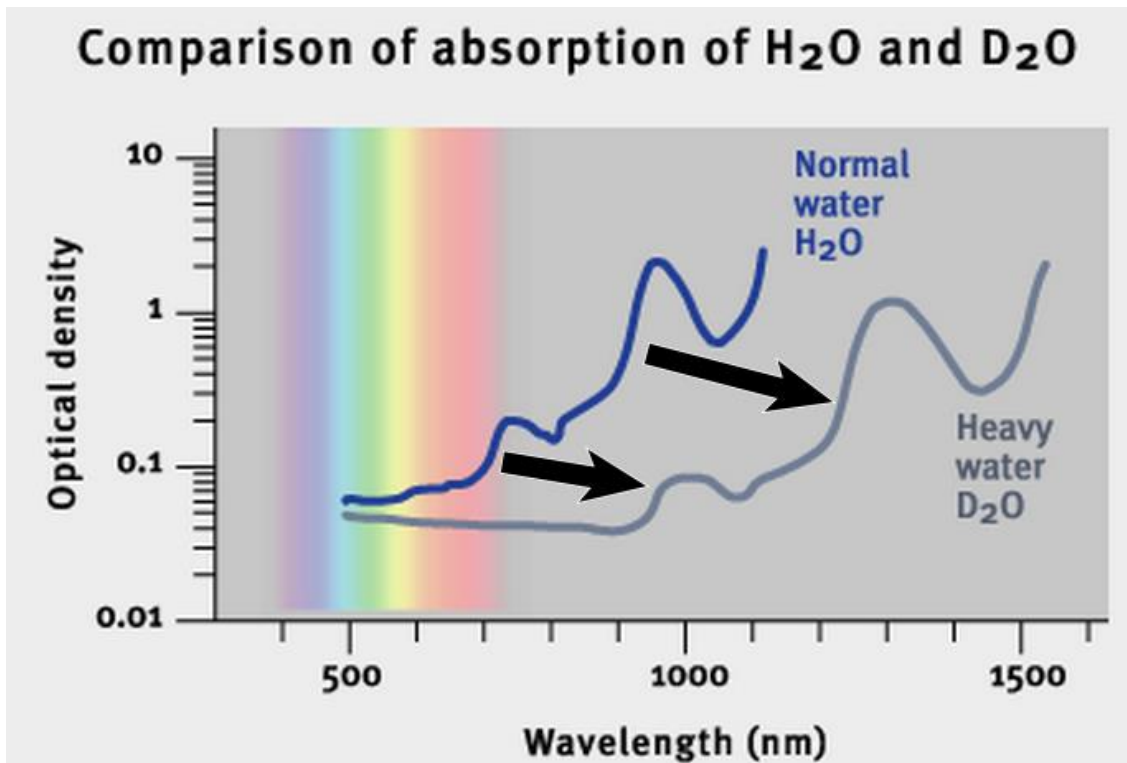
Fig. 12. Present results for the absorption of pure water. A large arrow with a boldface integer  $n$  indicates the predicted position of a shoulder that is due to the  $n$ th harmonic of the O–H stretch; the small arrows with mode assignments  $(j, 1)$  indicate the predicted position of a combination of the  $j$ th harmonic of the O–H stretch with the fundamental of the scissors mode.

<sup>49</sup> formerly <http://www.dartmouth.edu/~etrnsfer/water.htm>, no longer available

see also Charles L. Braun and Sergei N. Smirnov, “Why is water blue?”, *J. Chem. Educ.*, 1993, 70 (8), p 612.

<sup>50</sup> [https://en.wikipedia.org/wiki/Electromagnetic\\_absorption\\_by\\_water](https://en.wikipedia.org/wiki/Electromagnetic_absorption_by_water)

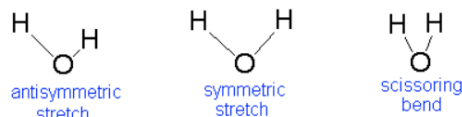
<sup>51</sup> [https://en.wikipedia.org/wiki/Electromagnetic\\_absorption\\_by\\_water](https://en.wikipedia.org/wiki/Electromagnetic_absorption_by_water) ibid.



Spectrophotometer semi-quantitative graphs for liquid H<sub>2</sub>O at room T (curve on left, with peak at 760 nm) and D<sub>2</sub>O (curve more to the right, with corresponding peak shifted to ~1000 nm) [note arrow added by MCM]. These graphs illustrate why water (H<sub>2</sub>O) is blue, while "heavy" water (D<sub>2</sub>O) is colorless. The graph gives the visible and near-IR spectrum of H<sub>2</sub>O and D<sub>2</sub>O at room temperature. The absorption below 700 nm in wavelength contributes to the color of pure water (the blue graph). This absorption consists of the short wavelength tail of [an absorption] band centered at 760 nm, and two weaker bands at 660 nm and 605 nm. The vibrational origin of this visible absorption of H<sub>2</sub>O is demonstrated by comparison with the spectrum of heavy water, D<sub>2</sub>O (the gray graph). Heavy water is chemically the same as regular (light) water, but with the two hydrogen atoms (as in H<sub>2</sub>O) replaced with deuterium atoms... The extra neutrons make 'heavy' water about 10% heavier. Heavy water is colorless because all of its corresponding vibrational transitions are shifted to lower energy (higher wavelength) by the increase in hydrogen isotope mass [shift highlighted with arrows added by MCM]. For example, the H<sub>2</sub>O band at 760 nm (the red end of the spectrum) is shifted to approximately 1000 nm in D<sub>2</sub>O. This is outside the spectrum of visible light, so heavy water has no color.<sup>52</sup>

The OH symmetric stretch ( $\nu_1$ ) and antisymmetric stretch ( $\nu_3$ ) fundamental vibrational stretching modes mentioned above are illustrated in the diagram to the right. [This is from a different source, and wavenumbers are slightly different.]<sup>53</sup> The OH scissoring bend ( $\nu_2$ ) mode is also shown, but its absorption peak is further into the mid-infrared at 5305 nm and is less relevant to the visible color of water.

#### Example 1: Consider Water



1. The Symmetric Stretch (Example shown is an H<sub>2</sub>O molecule at 3685 cm<sup>-1</sup>)
2. The Asymmetric Stretch (Example shown is an H<sub>2</sub>O molecule at 3506 cm<sup>-1</sup>)
3. Bend (Example shown is an H<sub>2</sub>O molecule at 1885 cm<sup>-1</sup>)

<sup>52</sup> <http://www.webexhibits.org/causesofcolor/5B.html> with annotations by MCM

<sup>53</sup> [http://chemwiki.ucdavis.edu/Physical\\_Chemistry/Spectroscopy/Vibrational\\_Spectroscopy/Vibrational\\_Modes](http://chemwiki.ucdavis.edu/Physical_Chemistry/Spectroscopy/Vibrational_Spectroscopy/Vibrational_Modes)

## Albedo

Also called *reflection coefficient*, derived from Latin albedo meaning "whiteness"..., is the diffuse reflectivity or reflecting power of a surface. It is the ratio of reflected radiation from the surface to incident radiation upon it. It is dimensionless and can be expressed as a percentage or on a scale from zero for a black surface with no reflection to 1 for perfect reflection of a white surface. "Albedo is the fraction of solar energy (shortwave radiation) reflected from the Earth back into space [as shortwave radiation]."<sup>54</sup> "Albedo depends on the frequency of the radiation. When quoted unqualified, it usually refers to some appropriate average across the spectrum of *visible light*. In general, the albedo depends on the directional distribution of incident radiation, except for Lambertian surfaces... which have an albedo that is independent of the incident distribution. In practice, a bidirectional reflectance distribution function (BRDF) may be required to accurately characterize the scattering properties of a surface, but albedo is very useful as a first approximation... The albedo is an important concept in climatology, astronomy, and calculating reflectivity of surfaces in ... buildings. The average overall albedo of Earth, its planetary albedo, is 30 to 35% because of cloud cover, but widely varies locally across the surface because of different geological and environmental features. The term was introduced into optics by Johann Heinrich Lambert in his 1760 work *Photometria*..." Albedos of typical materials in visible light range from 80% to 95% for fresh snow, 50% to 60% for ocean ice, 40% for desert sand, 10% to 25% for crops and grasslands, 8 to 20% for forests, 10% to 60% for water bodies (depending on angles), 20% to 40% for bricks and stones, and 4% for charcoal and fresh asphalt. [ , summer conifer forest is 0.08, bare soil is 0.17.]... Solar system orbiting objects have albedos ranging from 99% for Enceladus to 12% for the moon, and as low as 5% for certain asteroids.<sup>55</sup>

## Scattering

This will be only partially reviewed. Scattering is fundamental to radiative transfer and RS. Scattering direction (at least for a given photon) is unpredictable, unlike reflection. Scattering may be backward (backscattering), forward, or to the side. The *particle size parameter*  $x$  is defined as  $x = 2\pi r/\lambda$ , where  $r$  is the spherical particle radius. The regimes of scattering for spherical particles are defined in terms of  $x$  as follows:

- For  $x < 0.002$ , there is negligible scattering.
- Rayleigh or molecular scattering (for particles that are much smaller than the wavelength of light, e.g., molecules  $\sim 10^{-4}$   $\mu\text{m}$  typically of  $\text{O}_2$  or  $\text{N}_2$ ). Here  $0.002 < x < 0.2$ . Rayleigh accounts for the preferential scattering of blue light making the sky appear blue and sunsets red. The Rayleigh scattering cross section  $\tau_m$  is highly wavelength dependent, and proportional to  $\lambda^{-4}$ , thus much stronger for blue than red light. (It is even stronger for violet than blue light, but the eye is less sensitive for violet light.) Scattering at right angles is 1/2 the intensity of forward scattering. However, Rayleigh scattering dominates over Mie scattering at right angles because Mie is predominantly forward. It is related to polarizability of molecules. (Rayleigh scattering is named after Lord Rayleigh, John William Strutt, 1842-1919).
- Mie or non-molecular aerosol particle scattering (particles are comparable in size to the wavelength of light, e.g., smoke, dust, haze, pollution). Here  $0.2 < x < 2000$ . This is stronger than Rayleigh scattering, and it is less wavelength dependent. If large particles are present, Mie scattering dominates in the forward direction, and we see a white glare around the sun. Aerosols are important determinants of radiative balance and climate. Mie scattering is named after Gustav Mie (1869-1957).
- Non-selective or Geometric scattering (particles are much larger than the wavelength (e.g., water droplets forming clouds, ice crystals, hail). Here,  $x > 2000$ . It affects all wavelengths equally, thus appearing white

The *phase function* for scattering expresses the envelope of the scattering probabilities of radiance (light), vectors with magnitudes giving the relative probability that light will scatter in a particular direction  $\theta$ . The forward direction is defined as  $0^\circ$ . The shape of phase functions depends on the  $x$  regime:

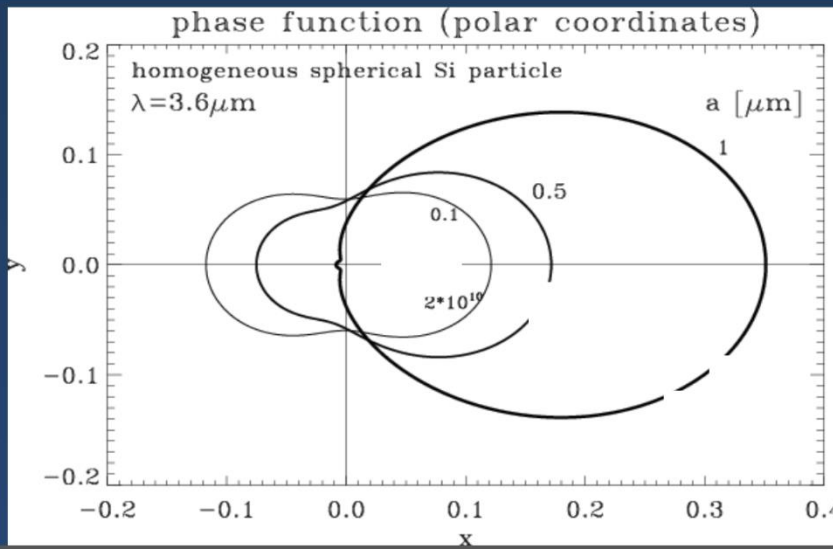
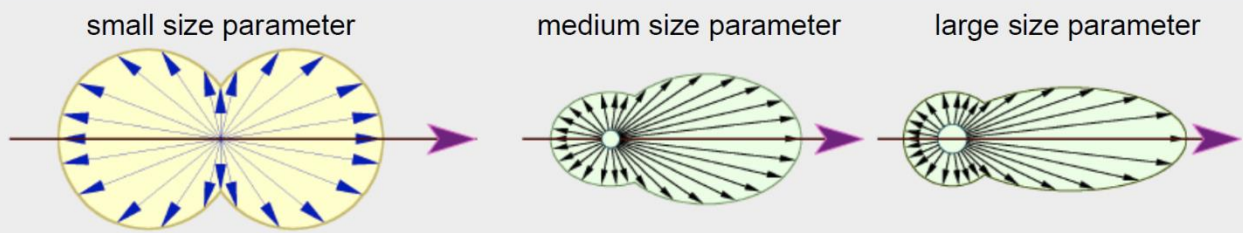
---

<sup>54</sup> <http://www.esr.org/outreach/glossary/albedo.html>

<sup>55</sup> Paraphrased and quoted from <http://en.wikipedia.org/wiki/Albedo>

# Phase Function

- Describes the directions that radiance (light) is scattered by particles

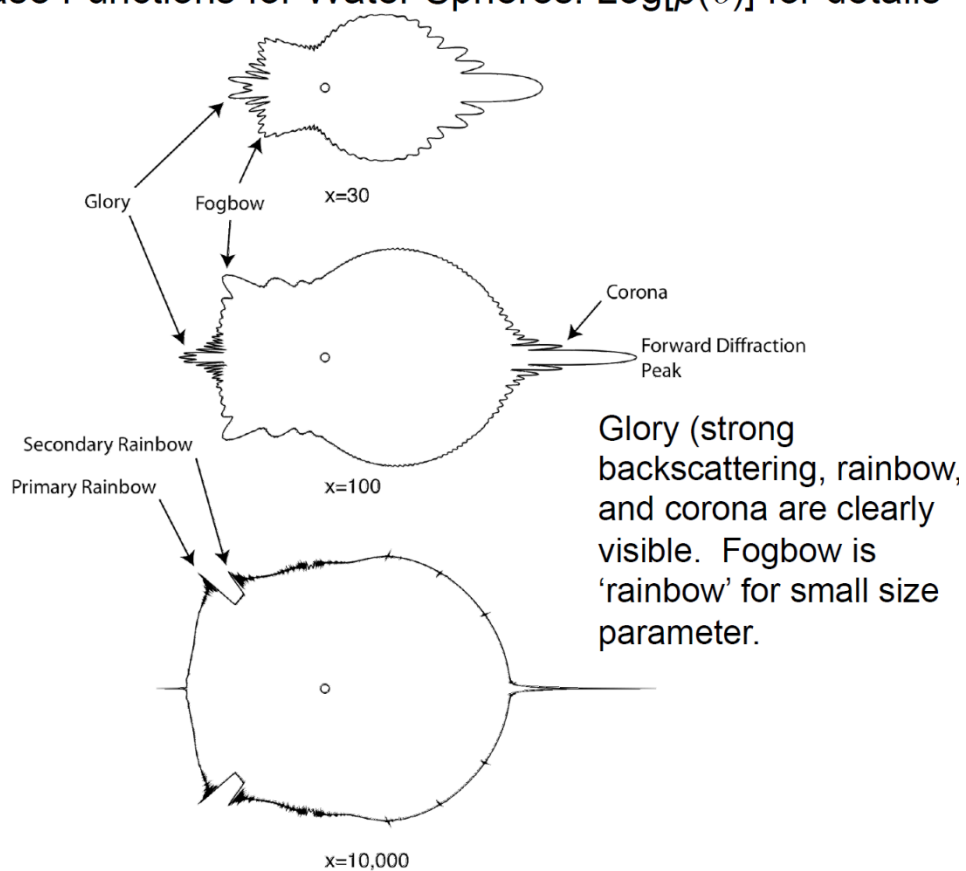


Scattering ?quasi-polar ?Cartesian phase diagrams plotting probability envelopes in fixed IR wavelength as a function apparently of particle diameter  $a$  in  $\mu\text{m}$  (i.e., not size parameter  $x$ )  
 (taken from lecture 5 PDF, of unk. source)

For small  $a = 0.5$ , Mie scattering is about the same forward and backward, but reduced to the sides. For  $a=3$ , scattering is predominantly forward. For  $a = 10$ , it is markedly forward.

Phase functions can be quite complicated. The following plot, in polar coordinates, the log of the probability vs. scattering angle. These show patterns that produce the primary and secondary rainbow, the fogbow, and the glory, all hydrometeor phenomena.

## Mie Phase Functions for Water Spheres: $\text{Log}[p(\theta)]$ for details



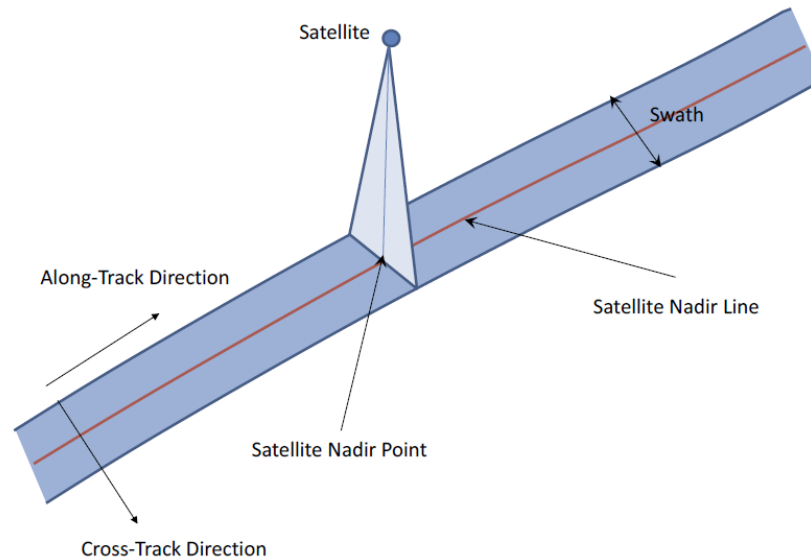
Polar plots of  $\text{Log } P(\theta)$  for hydrometeors. To the right is the forward direction for light source ( $\theta=0$ ).  
(taken from lecture 5 PDF, of unk. source)

## Satellite Path Parameters

These are as follows:

The nadir point path, or nadir line, is a line traced on the ground of points directly beneath an aircraft or satellite. The nadir at a given point is the local vertical direction pointing in the direction of the force of gravity at that location.<sup>56</sup>

“As the remote sensing instrument is carried along the satellite orbit, it typically images a strip on the surface along the *orbit track*. The width of this strip is known as the *swath* imaged by the camera. The direction along the satellite track is known as the *along-track direction*, and the direction orthogonal to the satellite track is known as the *cross-track direction*. The figure below defines these and some other imaging parameters.”<sup>57</sup>



## Comparison of Satellite Orbits (Compared to Geosynchronous Earth Orbit GEO)

### “Advantages of Low-Earth Orbit Systems

- Low latency or transmission delay
- Higher look angle (especially in high-latitude regions)
- Less path loss or beam spreading
- Easier to achieve high levels of frequency re-use
- Easier to operate to low-power/low-gain ground antennas

### Disadvantages of Low-Earth Orbit Systems

- Larger number of satellites to build and operate
- Coverage of areas of minimal traffic (oceans, deserts, jungles, and polar caps)
- Higher launch costs
- More complicated to deploy and operate – also more expensive TTC&M [Tracking, Telemetry Command & Monitoring]
- Much shorter in-orbit lifetime due to orbital degradation

### Advantages of Medium-Earth Orbit Systems

- Less latency and delay than GEO (but greater than LEO)
- Improved look angle to ground receivers
- Improved opportunity for frequency re-use as compared to GEO (but less than LEO)

<sup>56</sup> <http://en.wikipedia.org/wiki/Nadir>

<sup>57</sup> [http://www.its.caltech.edu/~ee157/lecture\\_note/Imaging%20geometries.pdf](http://www.its.caltech.edu/~ee157/lecture_note/Imaging%20geometries.pdf)

- Fewer satellites to deploy and operate and cheaper TTC&M systems than LEO (but more expensive than with GEO systems)
- Longer in-orbit lifetime than LEO systems
- Increased exposure to Van Allen Belt radiation

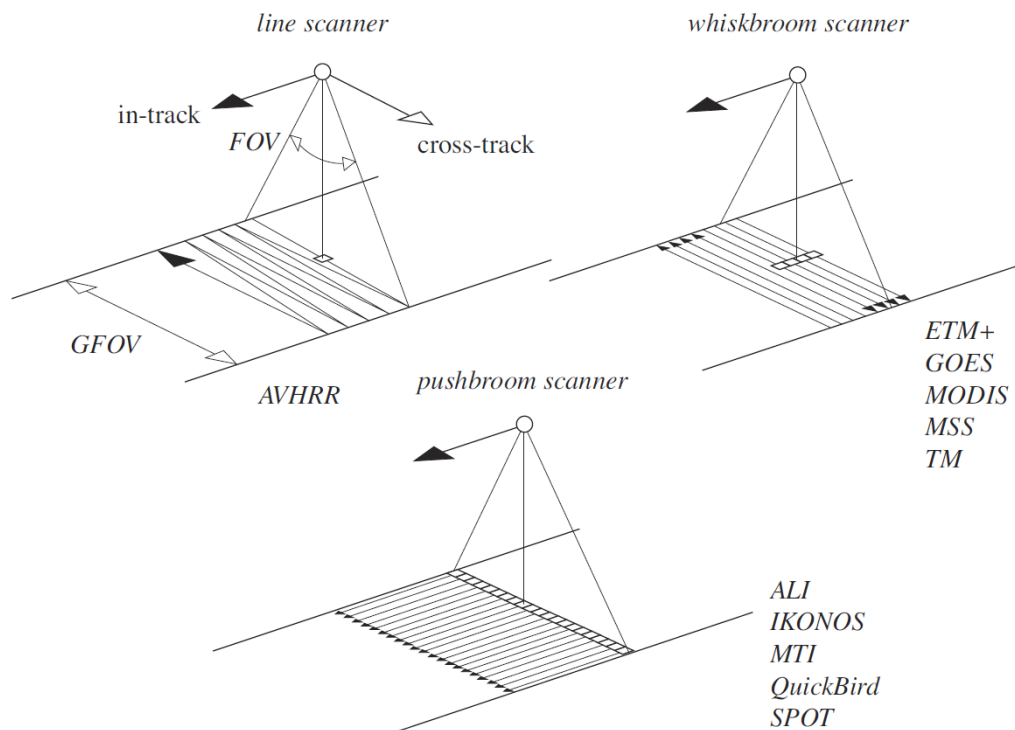
### Disadvantages of Medium-Earth Orbit Systems

- More satellites to deploy than GEO
- More expensive launch costs than GEO
- Ground antennas are generally more expensive and complex than with true LEO systems
- Coverage of low traffic areas (i.e., oceans deserts, jungles, etc.)” [Pelton 2012]

### Satellite Imaging Scanning Methods

These include the following:

- Traditional Analog or Digital Frame or Framing Camera (can capture images in R,G,B,NIR) “Staring”  
Good for simultaneous sampling of large area, good geometric control. Not suited to high spectral resolution.
- Line Scanner (such as AVHRR, typically with rotating scanning mirror)
- Whiskbroom Scanner (such as ETM+, GOES, MODIS, MSS, TM). “In a whisk broom sensor, a mirror scans across the satellite’s path, reflecting light into a single detector which collects data one pixel at a time. The moving parts make this type of sensor expensive and more prone to wearing out.”<sup>58</sup> Dwell time is low.
- Pushbroom Scanner (such as ALI on EO-1, IKONOS, MTI, QuickBird, and SPOT). “A ‘pushbroom’ (along track) sensor like ALI consists of a line of sensors arranged perpendicular to the flight direction of the spacecraft. Different areas of the surface are imaged as the spacecraft flies forward. Pushbroom sensors are generally lighter and less expensive than their whisk broom counterparts, and can gather more light because they look at a particular area for a longer time, like a long exposure on a camera [longer dwell time]. No moving parts. One drawback of pushbroom sensors is the varying sensitivity of the individual detectors.”<sup>59</sup>



<sup>58</sup> Robert A. Schowengerdt, Remote Sensing, (Third Edition), Chapter 1 - “The nature of remote sensing”, 2006

<sup>59</sup> Schowengerdt, op. cit.

Pushbroom is supplanting Whiskbroom or line scanner and has fewer moving parts.<sup>60</sup> “A pixel is created whenever the sensor system electronically samples the continuous data stream provided by the scanning. A line scanner uses a single detector element to scan the entire scene. Whiskbroom scanners, such as the Landsat TM, use several detector elements, aligned in-track, to achieve parallel scanning during each cycle of the scan mirror. A related type of scanner is the paddlebroom, exemplified by AVHRR and MODIS, with a two-sided mirror that rotates 360°, scanning continuously cross-track. A significant difference between paddlebroom and whiskbroom scanners is that the paddlebroom always scans in the same direction, while the whiskbroom reverses direction for each scan. Pushbroom scanners, such as SPOT, have a linear array of thousands of detector elements, aligned cross-track, which scan the full width of the collected data in parallel as the platform moves. For all types of scanners, the full cross-track angular coverage is called the *Field Of View (FOV)* and the corresponding ground coverage is called the *Ground-projected Field Of View (GFOV)*.”<sup>61</sup>

## Multispectral Images

“A three-band sensor with green, red, and near infrared bands is effective at discriminating vegetated and nonvegetated areas. The HRV sensor aboard the French SPOT (Système Probatoire d’Observation de la Terre) 1, 2, and 3 satellites (20 meter spatial resolution) has this design. Color-infrared film used in some aerial photography provides similar spectral coverage, with the red emulsion recording near infrared, the green emulsion recording red light, and the blue emulsion recording green light. The IKONOS satellite from Space Imaging (4-meter resolution) and the LISS II sensor on the Indian Research Satellites IRS-1A and 1B (36-meter resolution) add a blue band to provide complete coverage of the visible light range, and allow natural-color band composite images to be created. The Landsat Thematic Mapper (Landsat 4 and 5) and Enhanced Thematic Mapper Plus (Landsat 7) sensors add two bands in the middle infrared (MIR). Landsat TM band 5 (1.55 to 1.75  $\mu\text{m}$ ) and band 7 (2.08 to 2.35  $\mu\text{m}$ ) are sensitive to variations in the moisture content of vegetation and soils. Band 7 also covers a range that includes spectral absorption features found in several important types of minerals. An additional TM band (band 6) records part of the thermal infrared wavelength range (10.4 to 12.5  $\mu\text{m}$ ). (Bands 6 and 7 are not in wavelength order because band 7 was added late in the sensor design process.)”<sup>62</sup>

A list of the 36 multispectral bands for a representative multispectral imager, the EOS MODIS system (Earth Observing System: Moderate-resolution Imaging Spectroradiometer, launched with Terra in 1999) and the common uses for each band:<sup>63</sup>

---

<sup>60</sup> [http://earthobservatory.nasa.gov/Features/EO1/eo1\\_2.php](http://earthobservatory.nasa.gov/Features/EO1/eo1_2.php)

<sup>61</sup> Schowengerdt, op. cit.

<sup>62</sup> <http://www.microimages.com/documentation/Tutorials/intorse.pdf>

<sup>63</sup> Schowengerdt, op. cit.

TABLE 1-2. Primary geophysical variables measurable with each spectral band of the EOS MODIS system (Salomonson et al., 1995). Note the units of spectral range are nanometers (nm) for bands 1–19 and micrometers ( $\mu\text{m}$ ) for bands 20–36.

| geophysical variables           |                                 | band          | spectral range          | GSI (m) |
|---------------------------------|---------------------------------|---------------|-------------------------|---------|
| general                         | specific                        |               |                         |         |
| land/cloud boundaries           | vegetation chlorophyll          | 1             | 620–670 nm              | 250     |
|                                 | cloud and vegetation            | 2             | 841–876                 |         |
| land/cloud properties           | soil, vegetation differences    | 3             | 459–479                 | 500     |
|                                 | green vegetation                | 4             | 545–565                 |         |
|                                 | leaf/canopy properties          | 5             | 1230–1250               |         |
|                                 | snow/cloud differences          | 6             | 1628–1652               |         |
|                                 | land and cloud properties       | 7             | 2105–2155               |         |
| ocean color                     | chlorophyll observations        | 8             | 405–420                 | 1000    |
|                                 | chlorophyll observations        | 9             | 438–448                 |         |
|                                 | chlorophyll observations        | 10            | 483–493                 |         |
|                                 | chlorophyll observations        | 11            | 526–536                 |         |
|                                 | sediments                       | 12            | 546–556                 |         |
|                                 | sediments, atmosphere           | 13            | 662–672                 |         |
|                                 | chlorophyll fluorescence        | 14            | 673–683                 |         |
|                                 | aerosol properties              | 15            | 743–753                 |         |
| aerosol/atmosphere properties   | 16                              | 862–877       |                         |         |
| atmosphere/ clouds              | cloud/atmosphere properties     | 17            | 890–920                 | 1000    |
|                                 | cloud/atmosphere properties     | 18            | 931–941                 |         |
|                                 | cloud/atmosphere properties     | 19            | 915–965                 |         |
| thermal properties              | sea surface temperatures        | 20            | 3.66–3.84 $\mu\text{m}$ | 1000    |
|                                 | forest fires/volcanoes          | 21            | 3.929–3.989             |         |
|                                 | cloud/surface temperature       | 22            | 3.929–3.989             |         |
|                                 | cloud/ surface temperature      | 23            | 4.02–4.08               |         |
|                                 | troposphere temp/cloud fraction | 24            | 4.433–4.498             |         |
| troposphere temp/cloud fraction | 25                              | 4.482–4.549   |                         |         |
| atmosphere/ clouds              | cirrus clouds                   | 26            | 1.36–1.39               | 1000    |
| thermal properties              | mid-troposphere humidity        | 27            | 6.535–6.895             | 1000    |
|                                 | upper-troposphere humidity      | 28            | 7.175–7.475             |         |
|                                 | surface temperature             | 29            | 8.4–8.7                 |         |
|                                 | total ozone                     | 30            | 9.58–9.88               |         |
|                                 | cloud/surface temperature       | 31            | 10.78–11.28             |         |
|                                 | cloud/surface temperature       | 32            | 11.77–12.27             |         |
|                                 | cloud height and fraction       | 33            | 13.185–13.485           |         |
|                                 | cloud height and fraction       | 34            | 13.485–13.785           |         |
| cloud height and fraction       | 35                              | 13.785–14.085 |                         |         |
| cloud height and fraction       | 36                              | 14.085–14.385 |                         |         |

## Selected Earth RS Spacecraft, Aircraft, and Sensors

See also Jensen Chapter 3 History of Aerial Photography and Aerial Platforms

The term *satellite* is derived from Galileo's use of the Latin word *satelles*, meaning *servant*—he “concluded that somehow a planet ‘commanded’ its moons to remain in their constant orbits just as a master or mistress commanded the actions.”<sup>64</sup> Isaac Newton first conceived that objects could be shot into Earth orbit.

### Lists of Space Missions, Satellites, and Sensors

#### Upcoming American Space Missions

“AmericaSpace was founded in 2009 by two former aerospace engineers. Since then, this site has been dedicated to reporting on the state of America's space and aerospace efforts, which for many have been, and remain, synonymous of America's willingness, indeed enthusiasm, to reach new horizons... America is a nation that explores.”<sup>65</sup>

#### National Space Science Data Center NSSDC Master Catalog

“NASA Space Science Data Coordinated Archive serves as the permanent archive for NASA space science mission data. "Space science" means astronomy and astrophysics, solar and space plasma physics, and planetary and lunar science. As permanent archive, NSSDCA teams with NASA's discipline-specific space science "active archives" which provide access to data to researchers and, in some cases, to the general public... NSSDCA also serves as NASA's permanent archive for space physics mission data. It provides access to several geophysical models and to data from some non-NASA mission data... In addition to supporting active space physics and astrophysics researchers, NSSDCA also supports the general public both via several public-interest web-based services (e.g., the Photo Gallery) and via the offline mailing of CD-ROMs, photoprints, and other items... NSSDCA provides on-line information bases about NASA and non-NASA data as well as spacecraft and experiments that generate NASA space science data. NSSDCA also provides information and support relative to data management standards and technologies...”<sup>66</sup>

#### SATCAT Boxscore

Tabulation of missions by country<sup>67</sup>

#### Solar System probes

Wikipedia compilation: “This is a list of all space probes that have left Earth orbit (or were launched with that intention but failed), organised by their planned destination. It includes planetary probes, solar probes, and probes to asteroids and comets, but excludes lunar probes (listed separately at List of lunar probes). Flybys (such as gravity assists) that were incidental to the main purpose of the mission are also included. Confirmed future probes are included, but missions that are still at the concept stage, or which never progressed beyond the concept stage, are not.”<sup>68</sup>

---

<sup>64</sup> Joseph Pelton, “Orbits, Services and Systems, Chapter 2”, *Satellite Communications*, 2012 Edition available at [http://www.springer.com/cda/content/document/cda\\_downloaddocument/9781461419938-c1.pdf](http://www.springer.com/cda/content/document/cda_downloaddocument/9781461419938-c1.pdf)

<sup>65</sup> [www.americaspace.com](http://www.americaspace.com)

<sup>66</sup> <http://nssdc.gsfc.nasa.gov/nmc/>

<sup>67</sup> <http://celestrak.net/satcat/boxscore.asp>

<sup>68</sup> [http://en.wikipedia.org/wiki/List\\_of\\_Solar\\_System\\_probes](http://en.wikipedia.org/wiki/List_of_Solar_System_probes)

## Recent Spacecraft<sup>69</sup>

These are plotted by Number of Spectral Bands and by Ground-projected Sample Interval (GSI). Note that ETM+ and MSS are aboard Landsats.

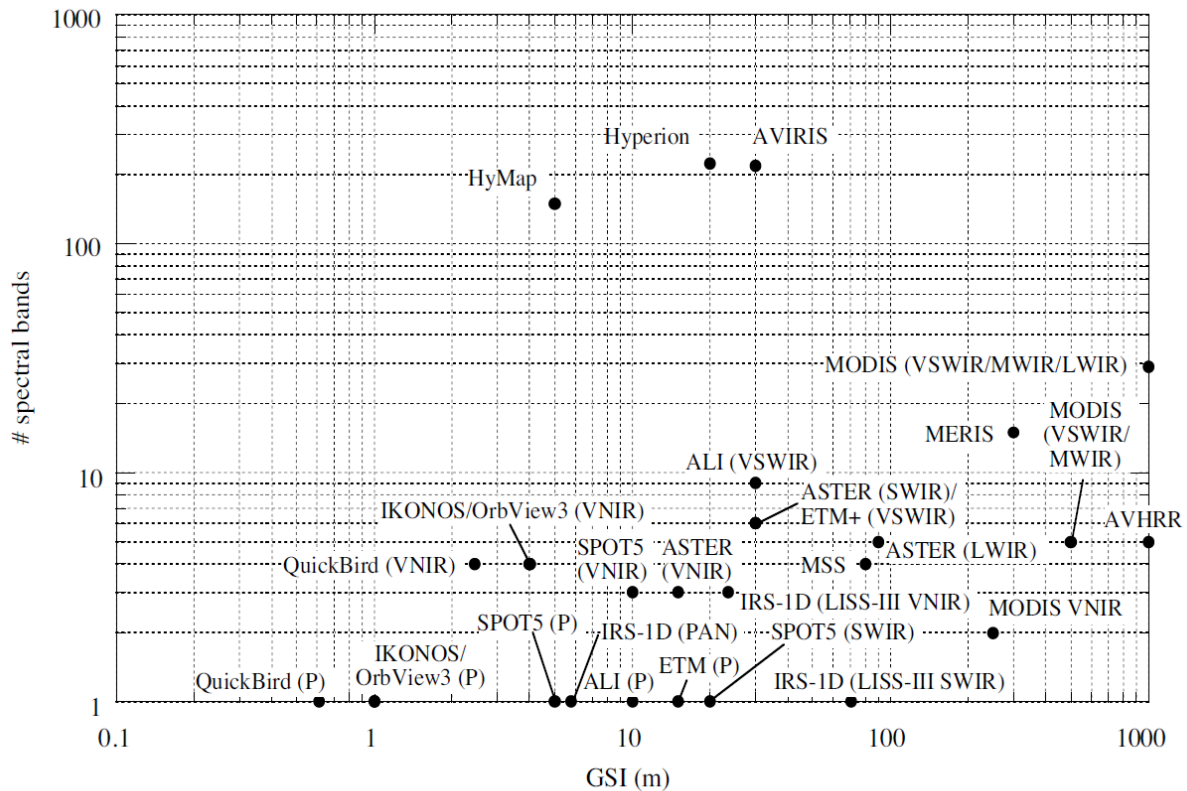


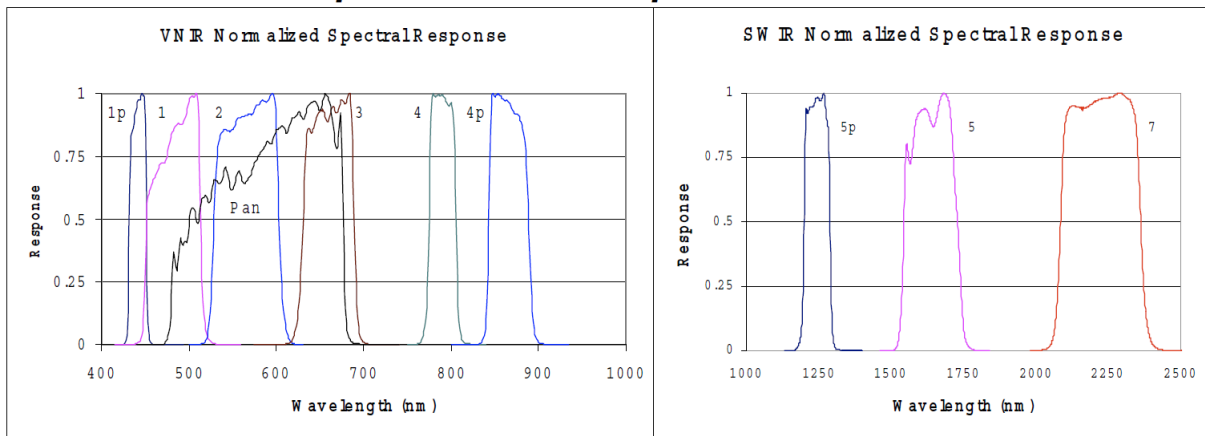
FIGURE 1-1. A plot of some remote-sensing systems in a two-dimensional parameter space. The sensor acronyms are defined in Appendix A and the notations in the graph refer to the sensor spectral regions: V = Visible, NIR = Near InfraRed, LWIR = Long Wave IR, MWIR = Mid Wave IR, SWIR = Short Wave IR, and P = Panchromatic. These terms are explained later in this chapter. All of these systems are on satellites, except AVIRIS and HyMap. There are a number of airborne simulators of satellite systems which are not shown, e.g. the MODIS Airborne Simulator (MAS), the Airborne MISR (AirMISR), and the Thematic Mapper Simulator (TMS). A list of these and other sensor acronyms is given in Appendix A. For a thorough survey of remote sensing systems, the book by Kramer is recommended (Kramer, 2002).

## Advanced Land Imager (ALI, aboard Earth Observing-1 Mission EO-1)

The New Millennium Program's first Earth Observing-1 Mission (EO-1) was launched 21 November 2000 in a geocentric Sun-synchronous orbit. "The Advanced Land Imager (ALI) was built ... to test new technology and to provide a safe technology shift for future Landsat missions... The Landsat series of satellites has provided a continuous record of changes in Earth's landscape from 1972 to the present. ALI images the Earth at the same level of detail (30 meters per pixel), and it has a more detailed set of sensors that enable crisp, photo-like images."<sup>70</sup> The ALI Multispectral Imaging capability was intended to address the traditional Landsat community. (The Hyperion Imaging Spectrometer was intended to address the research Landsat community.)<sup>71</sup>

"The Advanced Land Imager (ALI) browse images are generated from the Level 1 radiometrically corrected data and displayed as a 5,4,2 (RGB) band combination... Pixels are subsampled to a resolution of 240 meters from the original 30-meter data (a factor of 8 in each direction)... The two most typical scene lengths will be approximately 42 km for a standard scene and approximately 185 km for an extended scene... In the "Show Browse" window, browses are Level 1 radiometrically corrected in satellite orientation. Level 1T provides radiometric, systematic and geometric corrections incorporating ground control points that are applied while employing a 90-meter Digital Elevation Model (DEM) for topographic accuracy. Geodetic accuracy of the product depends on the accuracy of the ground control points and are expected to be within 2 pixels. Scenes that do not have adequate ground control will be processed to the best level of correction (L1Gst)."<sup>72</sup>

## ALI Spectral Response Functions



| ALI Bands         | 1p  | 1   | 2   | PAN | 3   | 4   | 4p  | 5p   | 5    | 7    |
|-------------------|-----|-----|-----|-----|-----|-----|-----|------|------|------|
| Wavelength ( nm ) | 442 | 485 | 567 | 592 | 660 | 790 | 866 | 1244 | 1640 | 2226 |
| Bandwidth ( nm )  | 19  | 53  | 70  | 144 | 56  | 31  | 44  | 88   | 171  | 272  |

Graph from Advanced Land Imager (ALI) Design Overview<sup>73</sup> showing center wavelength and bandwidth of all multispectral bands available (plus the Panchromatic 10-m resolution wideband).

The ALI acquires data in 9 bands 1p 1 2 3 4 4p 5p 5 7 plus a wider Panchromatic 10-m resolution wideband

<sup>70</sup> <http://earthobservatory.nasa.gov/Features/EO1Tenth/>

<sup>71</sup> <http://eo1.gsfc.nasa.gov/new/general/Disk2/EO-1%20Tech%20Transfer%20&%20Infusion%20Wrkshp.pdf>

<sup>72</sup> <http://glovis.usgs.gov/AboutBrowse.shtml#aboutbrowse>

<sup>73</sup> [http://eo1.gsfc.nasa.gov/new/general/Disk2/EO-1%20Mission%20Tech%20Forum\\_5.pdf](http://eo1.gsfc.nasa.gov/new/general/Disk2/EO-1%20Mission%20Tech%20Forum_5.pdf)

## Advanced Very High Resolution Radiometer (AVHRR) and Its Successor VIIRS

The AVHRR is a radiation-detection imager that can be used for remotely determining cloud cover and the surface temperature... This scanning radiometer uses 6 detectors that collect different bands of radiation wavelengths... The first AVHRR was a 4-channel radiometer, first carried on TIROS-N (launched October 1978, ended 1980). This was subsequently improved to a 5-channel instrument (AVHRR/2) that was initially carried on NOAA-7 (launched June 1981, ended 1986). The AVHRR/3 instrument, with 6 channels (spectral bands), was first carried on NOAA-15 launched in May 1998, still active in 2015. Resolutions: 1.09 km.<sup>74</sup> Wikipedia lists additional satellites carrying AVHRR/3, including NOAA-19 (2009 to the present) and MetOp-A (2006 to the present).<sup>75,76</sup>

The successor to AVHRR is the **Visible Infrared Imaging Radiometer Suite VIIRS**, currently aboard the **Suomi National Polar-orbiting Partnership Suomi NPP** weather satellite<sup>77</sup> (launched 2011).<sup>78</sup> It is also planned for NASA's **Joint Polar Satellite System-1 JPSS-1** Satellite (to be launched in 2017). According to Raytheon,<sup>79</sup> it has sensors for

Visible/Near IR: 9 band plus day/night pan band

Mid-Wave IR: 8 bands

Long-Wave IR: 4 bands

Details for this current generation system (VIIRS) are given to follow:

---

<sup>74</sup> <http://noaasis.noaa.gov/NOAASIS/ml/avhrr.html>

<sup>75</sup> [http://en.wikipedia.org/wiki/Advanced\\_Very\\_High\\_Resolution\\_Radiometer](http://en.wikipedia.org/wiki/Advanced_Very_High_Resolution_Radiometer)

<sup>76</sup> [http://www.esa.int/Our\\_Activities/Observing\\_the\\_Earth/The\\_Living\\_Planet\\_Programme/Meteorological\\_missions/MetOp/About\\_AVHRR\\_3](http://www.esa.int/Our_Activities/Observing_the_Earth/The_Living_Planet_Programme/Meteorological_missions/MetOp/About_AVHRR_3)

<sup>77</sup> [http://en.wikipedia.org/wiki/Suomi\\_NPP](http://en.wikipedia.org/wiki/Suomi_NPP)

<sup>78</sup> <http://npp.gsfc.nasa.gov/viirs.html>

<sup>79</sup> [http://npp.gsfc.nasa.gov/images/VIIRS\\_DS152%20Approved%208-10-11.pdf](http://npp.gsfc.nasa.gov/images/VIIRS_DS152%20Approved%208-10-11.pdf)

## VIIRS bands and bandwidths

| VIIRS Band     | Central Wavelength (µm) | Bandwidth (µm) | Wavelength Range (µm) | Band Explanation       | Spatial Resolution (m) @ nadir |
|----------------|-------------------------|----------------|-----------------------|------------------------|--------------------------------|
| <b>M1</b>      | 0.412                   | 0.02           | 0.402 - 0.422         | Visible/<br>Reflective | 750 m                          |
| <b>M2</b>      | 0.445                   | 0.018          | 0.436 - 0.454         |                        |                                |
| <b>M3</b>      | 0.488                   | 0.02           | 0.478 - 0.488         |                        |                                |
| <b>M4</b>      | 0.555                   | 0.02           | 0.545 - 0.565         |                        |                                |
| <b>M5 (B)</b>  | 0.672                   | 0.02           | 0.662 - 0.682         |                        |                                |
| <b>M6</b>      | 0.746                   | 0.015          | 0.739 - 0.754         | Near IR                |                                |
| <b>M7 (G)</b>  | 0.865                   | 0.039          | 0.846 - 0.885         | Shortwave IR           |                                |
| <b>M8</b>      | 1.240                   | 0.020          | 1.23 - 1.25           |                        |                                |
| <b>M9</b>      | 1.378                   | 0.015          | 1.371 - 1.386         |                        |                                |
| <b>M10 (R)</b> | 1.61                    | 0.06           | 1.58 - 1.64           | Medium-<br>wave IR     |                                |
| <b>M11</b>     | 2.25                    | 0.05           | 2.23 - 2.28           |                        |                                |
| <b>M12</b>     | 3.7                     | 0.18           | 3.61 - 3.79           |                        |                                |
| <b>M13</b>     | 4.05                    | 0.155          | 3.97 - 4.13           |                        |                                |
| <b>M14</b>     | 8.55                    | 0.3            | 8.4 - 8.7             | Longwave IR            |                                |
| <b>M15</b>     | 10.763                  | 1.0            | 10.26 - 11.26         |                        |                                |
| <b>M16</b>     | 12.013                  | 0.95           | 11.54 - 12.49         |                        |                                |
| <b>DNB</b>     | 0.7                     | 0.4            | 0.5 - 0.9             | Visible/<br>Reflective | 750 m across<br>full scan      |
| <b>I1 (B)</b>  | 0.64                    | 0.08           | 0.6 - 0.68            | Visible/<br>Reflective | 375 m                          |
| <b>I2 (G)</b>  | 0.865                   | 0.039          | 0.85 - 0.88           | Near IR                |                                |
| <b>I3 (R)</b>  | 1.61                    | 0.06           | 1.58 - 1.64           | Shortwave IR           |                                |
| <b>I4</b>      | 3.74                    | 0.38           | 3.55 - 3.93           | Medium-<br>wave IR     |                                |
| <b>I5</b>      | 11.45                   | 1.9            | 10.5 - 12.4           | Longwave IR            |                                |

M = Moderate (750 m) resolution bands

I = Imagery (375 m) resolution bands

DNB = Day-Night Band (or Near Constant Contrast (NCC) band)

M-bands highlighted in **pale yellow** are available as EDRs, in addition to SDRs.

True-color component bands are highlighted in red, green, and blue.

Natural-color component bands are noted with R, G, and B.

### VIIRS Spectral Bands and Resolution

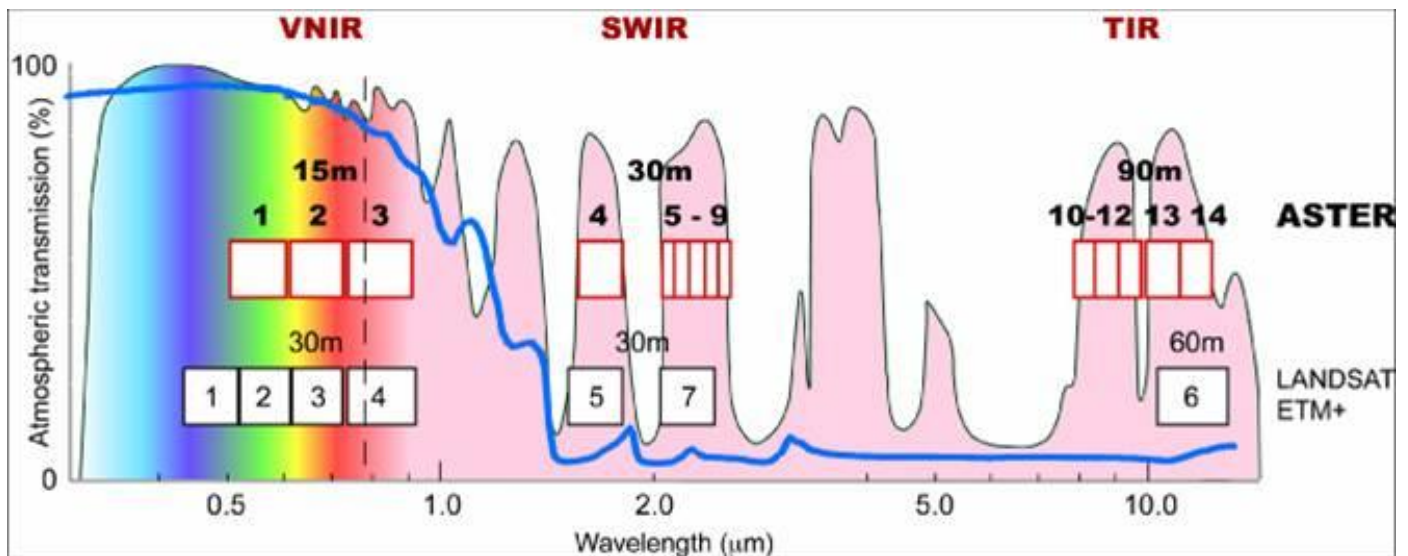
EDR = NASA Environmental Data Records;<sup>80</sup> SDR = NASA Sensor Data Records

“Natural color” is false color imaging in which MIR bands are displayed to resemble true color.<sup>81</sup>

<sup>80</sup> <http://npp.gsfc.nasa.gov/datasystems.html#dp>

<sup>81</sup> [http://rammb.cira.colostate.edu/projects/npp/VIIRS\\_bands\\_and\\_bandwidths.pdf](http://rammb.cira.colostate.edu/projects/npp/VIIRS_bands_and_bandwidths.pdf)

## Advanced Spaceborne Thermal Emission and Reflection Radiometer (ASTER, aboard Terra)



ASTER bands superimposed on a model atmosphere<sup>82</sup>. Upper curve is % atmospheric transmission.

Blue curve is probably smoothed transmission.

Lower band numbers & resolutions are for LANDSAT 7 ETM+ (Enhanced Thematic Mapper Plus).

ASTER = Advanced Spaceborne Thermal Emission and Reflection Radiometer; L1B = Level 1B Resolution. It is aboard the flagship Earth Observing Satellite (EOS), Terra. ASTER, CERES, MODIS, MISR, and MOPITT are operating well. ASTER Short Wave Infrared (SWIR) data is unavailable and MISR is currently offline.<sup>83</sup>

“The Advanced Spaceborne Thermal Emission and Reflection Radiometer obtains high-resolution (15 to 90 square meters per pixel) images of the Earth in 14 different wavelengths of the electromagnetic spectrum, ranging from visible to thermal infrared light. Scientists use ASTER data to create detailed maps of land surface temperature, emissivity, reflectance, and elevation...ASTER is the only high spatial resolution instrument on the Terra platform. ASTER’s ability to serve as a ‘zoom’ lens for the other Terra instruments is particularly important for change detection, calibration/validation and land surface studies. Unlike the other instruments aboard Terra, ASTER will not collect data continuously; rather, it collects an average of 8 minutes of data per orbit. All three ASTER telescopes [instrument subsystems] (VNIR, SWIR, and TIR) are pointable in the crosstrack direction. Given its high resolution and its ability to change viewing angles, ASTER produces stereoscopic images and detailed terrain height models... The ASTER instrument was built in Japan for the Ministry of Economy, Trade and Industry (METI). A joint United States/Japan Science Team is responsible for instrument design, calibration, and data validation.”<sup>84</sup>

<sup>82</sup> <http://asterweb.jpl.nasa.gov/images/spectrum.jpg>

on <http://asterweb.jpl.nasa.gov/characteristics.asp>

<sup>83</sup> <http://terra.nasa.gov/about>

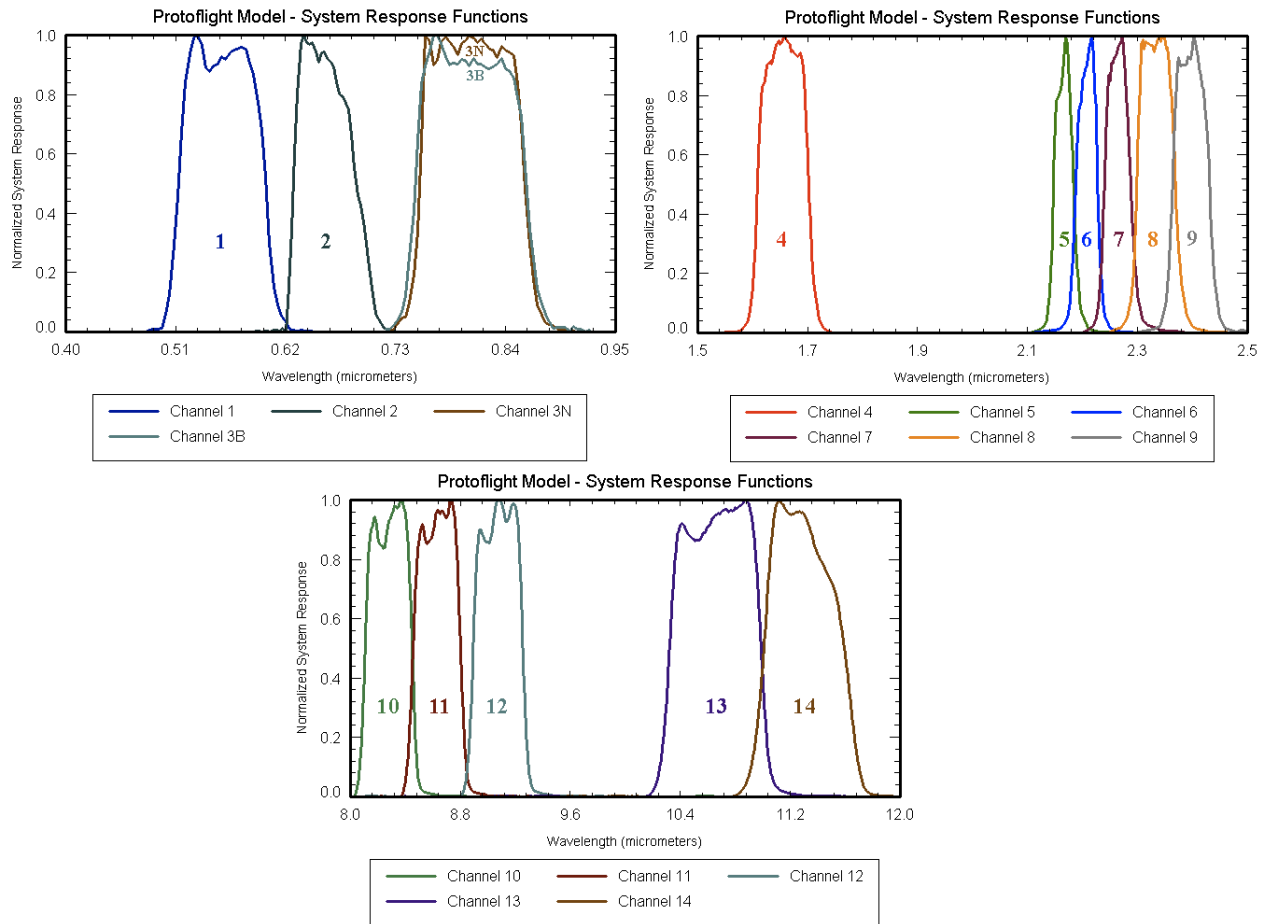
<sup>84</sup> <http://terra.nasa.gov/about/terra-instruments/aster>

## ASTER Instrument Characteristics

| Characteristic              | VNIR  | SWIR                                | TIR                                  |
|-----------------------------|---|-------------------------------------|--------------------------------------|
| Spectral Range              | Band 1: 0.52 - 0.60 $\mu\text{m}$<br>Nadir looking    | Band 4: 1.600 - 1.700 $\mu\text{m}$ | Band 10: 8.125 - 8.475 $\mu\text{m}$ |
|                             | Band 2: 0.63 - 0.69 $\mu\text{m}$<br>Nadir looking    | Band 5: 2.145 - 2.185 $\mu\text{m}$ | Band 11: 8.475 - 8.825 $\mu\text{m}$ |
|                             | Band 3: 0.76 - 0.86 $\mu\text{m}$<br>Nadir looking    | Band 6: 2.185 - 2.225 $\mu\text{m}$ | Band 12: 8.925 - 9.275 $\mu\text{m}$ |
|                             | Band 3: 0.76 - 0.86 $\mu\text{m}$<br>Backward looking | Band 7: 2.235 - 2.285 $\mu\text{m}$ | Band 13: 10.25 - 10.95 $\mu\text{m}$ |
|                             |   | Band 8: 2.295 - 2.365 $\mu\text{m}$ | Band 14: 10.95 - 11.65 $\mu\text{m}$ |
|                             | Band 9: 2.360 - 2.430 $\mu\text{m}$                   |                                     |                                      |
| Ground Resolution           | 15 m  | 30m                                 | 90m                                  |
| Data Rate (Mbits/sec)       | 62  | 23                                  | 4.2                                  |
| Cross-track Pointing (deg.) | $\pm 24$  | $\pm 8.55$                          | $\pm 8.55$                           |
| Cross-track Pointing (km)   | $\pm 318$   | $\pm 116$                           | $\pm 116$                            |
| Swath Width (km)            | 60  | 60                                  | 60                                   |
| Detector Type               | Si  | PtSi-Si                             | HgCdTe                               |
| Quantization (bits)         | 8   | 8                                   | 12                                   |
| System Response Function    | <a href="#">VNIR Chart</a>                            | <a href="#">SWIR Chart</a>          | <a href="#">TIR Chart</a>            |
|                             | <a href="#">VNIR Data</a>                             | <a href="#">SWIR Data</a>           | <a href="#">TIR Data</a>             |

ASTER Instrument Characteristics<sup>85</sup>

<sup>85</sup> <http://asterweb.jpl.nasa.gov/characteristics.asp>



Charts from *here*<sup>86</sup>

## VNIR

“The VNIR subsystem operates in three spectral bands at visible and near-IR wavelengths, with a resolution of 15 m. It consists of two telescopes--one nadir-looking with a three-spectral-band detector, and the other backward-looking with a single-band detector. The backward-looking telescope provides a second view of the target area in Band 3 for stereo observations. Thermal control of the CCD detectors is provided by a platform-provided cold plate. Cross-track pointing to 24 degrees on either side of the track is accomplished by rotating the entire telescope assembly. Band separation is through a combination of dichroic elements and interference filters that allow all three bands to view the same ground area simultaneously. The data rate is 62 Mbps when all four bands are operating. Two on-board halogen lamps are used for calibration of the nadir-looking detectors. This calibration source is always in the optical path.”<sup>87</sup>

## SWIR

“The SWIR subsystem operates in six spectral bands in the near-IR region through a single, nadir-pointing telescope that provides 30 m resolution. Cross-track pointing ( $\pm 8.550$  [degrees]) is accomplished by a pointing mirror. Because of the size of the detector/filter combination, the detectors must be widely spaced, causing a parallax error of about 0.5 pixels per 900 m of elevation. This error is correctable if elevation data, such as a DEM, are available. Two on-board halogen lamps are used for calibration in a manner similar to that used for the VNIR subsystem, however, the pointing mirror must turn to see the calibration source. The maximum data rate is 23 Mbps.”<sup>88</sup>

<sup>86</sup> [http://asterweb.jpl.nasa.gov/content/01\\_mission/03\\_instrument/01\\_Characteristics/vnirchart.htm](http://asterweb.jpl.nasa.gov/content/01_mission/03_instrument/01_Characteristics/vnirchart.htm)  
[http://asterweb.jpl.nasa.gov/content/01\\_mission/03\\_instrument/01\\_Characteristics/swirchart.htm](http://asterweb.jpl.nasa.gov/content/01_mission/03_instrument/01_Characteristics/swirchart.htm)  
[http://asterweb.jpl.nasa.gov/content/01\\_mission/03\\_instrument/01\\_Characteristics/tirchart.htm](http://asterweb.jpl.nasa.gov/content/01_mission/03_instrument/01_Characteristics/tirchart.htm)

<sup>87</sup> <http://asterweb.jpl.nasa.gov/instrument.asp>

<sup>88</sup> *ibid.*

## TIR

The TIR subsystem operates in five bands in the thermal infrared region using a single, fixed-position, nadir-looking telescope with a resolution of 90 m. Unlike the other instrument subsystems, it has a "whiskbroom" scanning mirror. Each band uses 10 detectors in a staggered array with optical bandpass filters over each detector element. The maximum data rate is 4.2 Mbps. The scanning mirror functions both for scanning and cross-track pointing (to  $\pm 8.55$  degrees). In the scanning mode, the mirror oscillates at about 7 Hz and, during oscillation, data are collected in one direction only. During calibration, the scanning mirror rotates 90 degrees from the nadir position to view an internal black body. Because of the instrument's high data rate, restrictions have been imposed so that the average data rate is manageable by the spacecraft data management system. This restriction is a one-orbit maximum average rate of 16.6 Mbps and a two-orbit maximum average rate of 8.3 Mbps, which results in approximately a 9.3% duty cycle.<sup>89</sup>

## Airborne Visible Infrared Imaging Spectrometer (AVIRIS)

This hyperspectral imaging instrument began operation in the mid-1990s. "AVIRIS is an acronym for the Airborne Visible Infrared Imaging Spectrometer. AVIRIS is a premier instrument in the realm of Earth Remote Sensing. It is a unique optical sensor that delivers calibrated images of the upwelling spectral radiance in 224 contiguous spectral channels (also called bands) with wavelengths from 400 to 2500 nanometers (nm). AVIRIS has been flown on four aircraft platforms: NASA's ER-2 jet, Twin Otter International's turboprop, Scaled Composites' Proteus, and NASA's WB-57. The ER-2 flies at approximately 20 km above sea level, at about 730 km/hr. The Twin Otter aircraft flies at 4km above ground level at 130km/hr. AVIRIS has flown all across the US, plus Canada and Europe....

The AVIRIS instrument contains 224 different detectors, each with a wavelength sensitive range (also known as spectral bandwidth) of approximately 10 nanometers (nm), allowing it to cover the entire range between 380 nm and 2500 nm. When the data from each detector is plotted on a graph, it yields a complete VIS-NIR-SWIR spectrum. Comparing the resulting spectrum with those of known substances reveals information about the composition of the area being viewed by the instrument...

AVIRIS uses a scanning mirror to sweep back and forth ("whisk broom" fashion), producing 677 pixels for the 224 detectors each scan. The pixel size and swath width of the AVIRIS data depend on the altitude from which the data is collected. The pixel size and swath width of the AVIRIS data depend on the altitude from which the data is collected. When collected by the ER-2 (20km above the ground) each pixel produced by the instrument covers an area approximately 20 meters diameter on the ground (with some overlap between pixels), thus yielding a ground swath about 11 kilometers wide. When collected by the Twin Otter (4km above the ground), each ground pixel is 4m square, and the swath is 2km wide. The ground data is recorded on board the instrument along with navigation and engineering data and the readings from the AVIRIS on-board calibrator. When all of this data is processed and stored on the ground, it yields approximately 140 Megabytes (MB) for every 512 scans (or lines) of data. Each 512 line set of data is called a "scene", and corresponds to an area about 10km long on the ground.

Recent Technical parameters: 12 Hz scanning rate; 16 bit encoding; Silicon (Si) detectors for the visible range, indium gallium arsenide (InGaAr) for the NIR, and indium-antimonide (InSb) detectors for the SWIR; 34 degrees total field of view (full 677 samples); 1 milliradian Instantaneous Field Of View (IFOV, one sample), calibrated to within 0.1 mrad.

The main objective of the AVIRIS project is to identify, measure, and monitor constituents of the Earth's surface and atmosphere based on molecular absorption and particle scattering signatures. Research with AVIRIS data is predominantly focused on understanding processes related to the global environment and climate change.<sup>90</sup>

## Cloud-Aerosol Lidar and Infrared Pathfinder Satellite Observation satellite (CALIPSO)

Aerosols in the atmosphere can also scatter light. NASA's CALIPSO satellite can observe the scattering of laser pulses to "see" the distributions of aerosols from sources such as dust storms and forest fires. See

---

<sup>89</sup> <http://asterweb.jpl.nasa.gov/instrument.asp>

<sup>90</sup> Quotes from AVIRIS website: <http://aviris.jpl.nasa.gov/index.html>

image of Iceland's Eyjafjallajökull Volcano in 2010.<sup>91</sup>

## Geostationary Operational Environmental Satellites (GOES, NOAA/NASA)

Partial List:<sup>92</sup>

*SMS (Synchronous Meteorological Satellites) type:*

GOES-1 (A) 1975-1985

GOES-2 (B) 1977-1993

GOES-3 (C) 1978-1993

*First Generation:*

GOES-4 (D) 1980-1988

GOES-7 (H) 1987-1996

*Second Generation:*

GOES-8 (I) 1994-2004

GOES-12 (M) 2001-2013

*Third Generation*

GOES-13 (N) 2006 - [GOES-EAST, located at 75°W over the equator]<sup>93</sup>

GOES-15 (P) 2010 - [GOES-WEST, located at 135°W over the Pacific Ocean over the equator]

*Fourth Generation:*

GOES- (R), planned for 2016

The **Advanced Baseline Imager (ABI)** planned for GOES-R will include 16 spectral bands, including two visible channels, four near-infrared channels, and ten infrared channels.<sup>94</sup> These bands are summarized in the table to follow: (Not all of these bands, which include VNIR, SWIR, and TIR, are present on current GOES sensors.)

---

<sup>91</sup> [http://missionscience.nasa.gov/ems/03\\_behaviors.html](http://missionscience.nasa.gov/ems/03_behaviors.html)

<http://www-calipso.larc.nasa.gov/>

[http://www.nasa.gov/mission\\_pages/calipso/main/](http://www.nasa.gov/mission_pages/calipso/main/)

<http://science.nasa.gov/missions/calipso/>

<sup>92</sup> [http://en.wikipedia.org/wiki/List\\_of\\_GOES\\_satellites](http://en.wikipedia.org/wiki/List_of_GOES_satellites)

<sup>93</sup> <http://noaasis.noaa.gov/NOAASIS/ml/genlsatl.html>

<sup>94</sup> <http://www.goes-r.gov/spacesegment/abi.html>

**TABLE 1. Summary of the wavelengths, resolution, and sample use and heritage instrument(s) of the ABI bands. The minimum and maximum wavelength range represent the full width at half maximum (FWHM or 50%) points. [The Instantaneous Geometric Field Of View (IGFOV).]**

| Future GOES imager (ABI) band | Wavelength range (µm) | Central wavelength (µm) | Nominal subsatellite IGFOV (km) | Sample use   | Heritage instrument(s)                   |
|-------------------------------|-----------------------|-------------------------|---------------------------------|--|--|
| 1                             | 0.45–0.49             | 0.47                    | 1                               | Daytime aerosol over land, coastal water mapping                       | MODIS                                    |
| 2                             | 0.59–0.69             | 0.64                    | 0.5                             | Daytime clouds fog, insolation, winds                                  | Current GOES imager/sounder              |
| 3                             | 0.846–0.885           | 0.865                   | 1                               | Daytime vegetation/burn scar and aerosol over water, winds             | VIIRS, spectrally modified AVHRR         |
| 4                             | 1.371–1.386           | 1.378                   | 2                               | Daytime cirrus cloud   | VIIRS, MODIS                             |
| 5                             | 1.58–1.64             | 1.61                    | 1                               | Daytime cloud-top phase and particle size, snow                        | VIIRS, spectrally modified AVHRR         |
| 6                             | 2.225–2.275           | 2.25                    | 2                               | Daytime land/cloud properties, particle size, vegetation, snow         | VIIRS, similar to MODIS                  |
| 7                             | 3.80–4.00             | 3.90                    | 2                               | Surface and cloud, fog at night, fire, winds                           | Current GOES imager                      |
| 8                             | 5.77–6.6              | 6.19                    | 2                               | High-level atmospheric water vapor, winds, rainfall                    | Current GOES imager                      |
| 9                             | 6.75–7.15             | 6.95                    | 2                               | Midlevel atmospheric water vapor, winds, rainfall                      | Current GOES sounder                     |
| 10                            | 7.24–7.44             | 7.34                    | 2                               | Lower-level water vapor, winds, and SO <sub>2</sub>                    | Spectrally modified current GOES sounder |
| 11                            | 8.3–8.7               | 8.5                     | 2                               | Total water for stability, cloud phase, dust, SO <sub>2</sub> rainfall | MAS                                      |
| 12                            | 9.42–9.8              | 9.61                    | 2                               | Total ozone, turbulence, and winds                                     | Spectrally modified current sounder      |
| 13                            | 10.1–10.6             | 10.35                   | 2                               | Surface and cloud  | MAS                                      |
| 14                            | 10.8–11.6             | 11.2                    | 2                               | Imagery, SST, clouds, rainfall   | Current GOES sounder                     |
| 15                            | 11.8–12.8             | 12.3                    | 2                               | Total water, ash, and SST  | Current GOES sounder                     |
| 16                            | 13.0–13.6             | 13.3                    | 2                               | Air temperature, cloud heights and amounts                             | Current GOES sounder/GOES-12+ imager     |

Source: Schmit, T.J., Gunshor, M.M., Menzel, W.P., Gurka, J.J., Li, J., Bachmeier, A.S., 2005, Introducing the Next-Generation Advanced Baseline Imager on GOES-R, Bulletin of the American Meteorological Society, v. 86, p. 1079-1096.

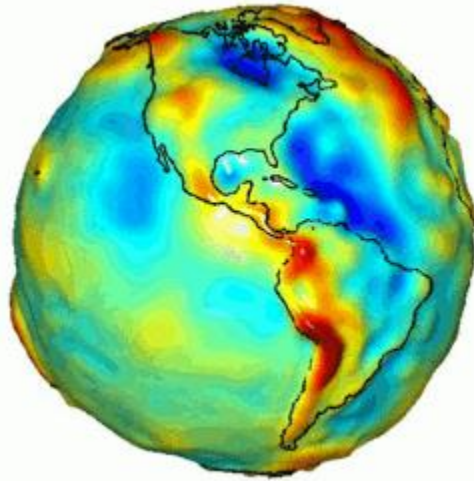
Planned GOES-R Advanced Baseline Imager ABI Bands and IGFOV Resolution<sup>95</sup>

**Gravity Recovery and Climate Experiment (GRACE)**

“One of the NASA Earth Science Enterprise’s focus areas is Earth Surface and Interior studies, which includes studying the gravity field. The Gravity Recovery and Climate Experiment (GRACE), launched by NASA on March 17, 2002, is revealing more detail about the gravity field than has ever been available before... The two GRACE satellites themselves act in unison as the primary instrument. Changes in the distance between the twin satellites are used to make gravitational field measurements... The two identical satellites orbit one behind the other in the same orbital plane at approximate distance of 220 kilometers (137 miles). As the pair

<sup>95</sup> <http://www.goes-r.gov/spacesegment/ABI-tech-summary.html>

circles the Earth, areas of slightly stronger gravity (greater mass concentration) affect the lead satellite first, pulling it away from the trailing satellite [etc.]... The geoid is a hypothetical Earth surface that represents the mean sea level in the absence of winds, currents, and most tides... GRACE provides, for the first time, global coverage of the Earth's gravity field every 30 days from a single source. GRACE is already able to measure the gravity field with a level of precision that is at least 100 times greater than any existing measurement...The finer details of the geoid that have evaded scientists for so long are on the verge of being revealed.”<sup>96</sup>



Gravity Field Anomaly (Ctrl-Click here for Animated GIF)<sup>97</sup>

### **Hyperion Grating Imaging Spectrometer (Hyperion, aboard Earth Observing-1 Mission EO-1)**

Hyperion images 220 [200 on orbit] 10nm bands covering 400nm - 2500nm, with a Swath width of 7.5 km. Orbit is 705km altitude (16 day repeat).<sup>98</sup> Level 0 and Level 1 (radiometrically corrected) data products. This is a hyperspectral grating imaging spectrometer.

“The goal of hyperspectral imaging is to obtain the spectrum for each pixel in the image of a scene, with the purpose of finding objects, identifying materials, or detecting processes... Hyperspectral [imaging] deals with imaging narrow spectral bands over a continuous spectral range, and produce the spectra of all pixels in the scene. So a sensor with only 20 bands can also be hyperspectral when it covers the range from 500 to 700 nm with 20 bands each 10 nm wide. (While a sensor with 20 discrete bands covering the VIS, NIR, SWIR, MWIR, and LWIR would be considered multispectral.)”<sup>99</sup>

### **Landsat Multispectral Scanner (MSS, on Landsat 1-5)**

(Landsat 1 was aboard Earth Resources Technology Satellite 1)

“The modern era of earth remote sensing from satellites began when the Landsat Multispectral Scanner System (MSS) provided, for the first time, in 1972 a consistent set of synoptic, high resolution earth images to the world scientific community.”<sup>100</sup>

“Images were acquired from 1972-1983 and are displayed as a 4,2,1 (RGB) color composite. Pixels are subsampled to a resolution of 480 meters from the original 80-meter data. For the 240 meter display mode, the images are JPEG compressed with an average file size of 38K. For the 1000 meter display mode, the browse images are GIFs with an average file size of 23K. The "Show Browse" images (viewed in a separate

---

<sup>96</sup> <http://earthobservatory.nasa.gov/Features/GRACE/>

<sup>97</sup> [http://en.wikipedia.org/wiki/Gravity\\_Recovery\\_and\\_Climate\\_Experiment](http://en.wikipedia.org/wiki/Gravity_Recovery_and_Climate_Experiment)

<sup>98</sup> [http://eo1.gsfc.nasa.gov/new/miscPages/TechForumPres/12-Hyp\\_Design\\_Overview.pdf](http://eo1.gsfc.nasa.gov/new/miscPages/TechForumPres/12-Hyp_Design_Overview.pdf)

<sup>99</sup> [http://en.wikipedia.org/wiki/Hyperspectral\\_imaging](http://en.wikipedia.org/wiki/Hyperspectral_imaging)

<sup>100</sup> Schowengerdt, op. cit.

browser window) were generated from full-resolution data that is orthorectified and UTM-projected, using the World Geodetic System 1984 datum.<sup>101</sup>

“Landsat 1 was launched on July 23, 1972; at that time the satellite was known as the Earth Resources Technology Satellite (ERTS). It was the first Earth-observing satellite to be launched with the express intent to study and monitor our planet’s landmasses... To perform the monitoring, Landsat 1 carried two instruments: ... the Return Beam Vidicon (RBV), and the Multispectral Scanner (MSS) built by the Hughes Aircraft Company... The MSS data were found to be superior... The MSS recorded data in four spectral bands—a green, red, and two infrared bands... Landsat 1 operated until January 1978,<sup>102</sup> Landsat 1-3 were in polar, sun-synchronous orbit.

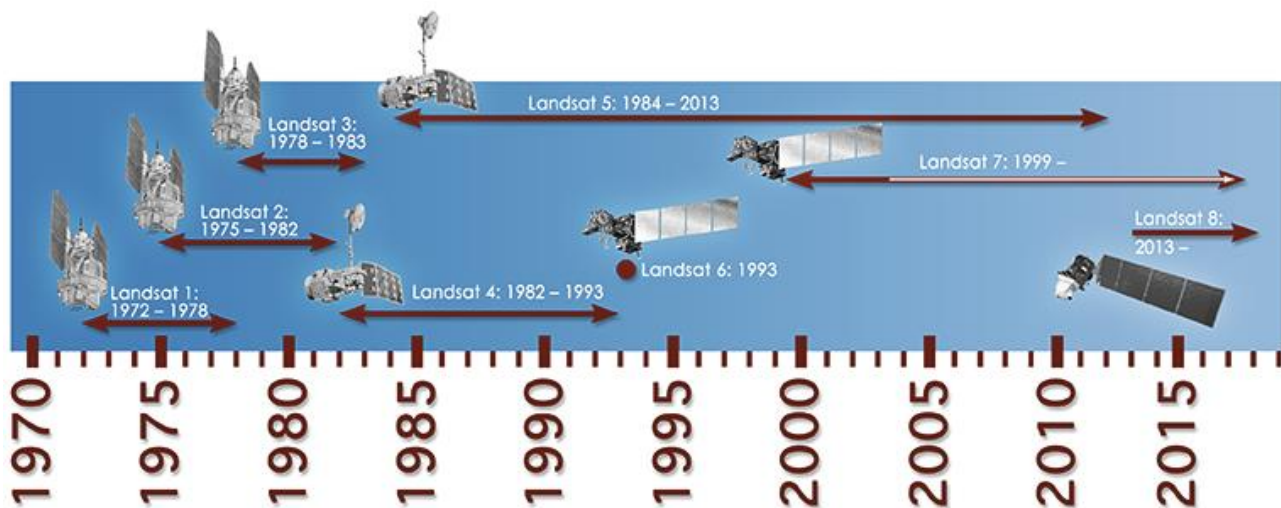
### Landsat 4-5 Multispectral Scanner (MSS)

“Images acquired from 1982-1987 are displayed as a 4,2,1 (RGB) color composite. Landsats 4-5 MSS data has sparse coverage and was used only to fill in gaps in coverage for the GLS1975 Landsat 1-3 dataset. Pixels are subsampled to a resolution of 480 meters from the original 80-meter data. The "Show Browse" images (viewed in a separate browser window) were generated from full-resolution data that is orthorectified and UTM-projected, using the World Geodetic System 1984 datum.<sup>103</sup>

Landsat 5 was “Longest Earth-observing satellite mission in history” [but had been largely superseded by Landsat 7 and 8].<sup>104</sup> Sun-synchronous orbit at 705.3 km (438.3 mi), and it took about 16 days to scan the entire Earth.

### MSS Bands for Landsats 1 to 5<sup>105</sup>

| Band # (L1-L2) | Band # (L3) | Band # (L4-L5) | µm        | Resolution* | L4/L5 <a href="#">TM</a> Band Equivalent |
|----------------|-------------|----------------|-----------|-------------|--|
| 4              | 4           | 1              | 0.5-0.6   | 68 m X 83 m | ~ 2 (0.52–0.60 µm)                       |
| 5              | 5           | 2              | 0.6-0.7   | 68 m X 83 m | ~ 3 (0.63–0.69 µm)                       |
| 6              | 6           | 3              | 0.7-0.8   | 68 m X 83 m | ~ 4 (0.76–0.90 µm)                       |
| 7              | 7           | 4              | 0.8-1.1   | 68 m X 83 m | ~ 4 (0.76–0.90 µm)                       |
| N/A            | 8           | N/A            | 10.4-12.6 | 68 m X 83 m | ~ 6 (10.41-12.5 µm)                      |



Timeline of Landsat Satellites<sup>106</sup>

<sup>101</sup> <http://glovis.usgs.gov/AboutBrowse.shtml#aboutbrowse>

<sup>102</sup> <http://landsat.gsfc.nasa.gov/?p=3172>

<sup>103</sup> <http://glovis.usgs.gov/AboutBrowse.shtml#aboutbrowse>

<sup>104</sup> [http://en.wikipedia.org/wiki/Landsat\\_program](http://en.wikipedia.org/wiki/Landsat_program)

<sup>105</sup> <http://landsat.gsfc.nasa.gov/?p=3227>

## Landsat 4-7 Thematic Mappers (TM and ETM+)

### Landsat 4-5 Thematic Mapper (TM)

“The images are displayed as RGB composites, bands 5, 4, and 3, with 2% linear stretch applied. Images are resampled to a pixel size of 240 meters from the original 28.5-meter data.”<sup>107</sup>

| Band | Wavelength | Resolution |
|------|------------|------------|
| 1    | 0.45-0.52  | 30 m       |
| 2    | 0.52-0.60  | 30 m       |
| 3    | 0.63-0.69  | 30 m       |
| 4    | 0.76-0.90  | 30 m       |
| 5    | 1.55-1.75  | 30 m       |
| 6    | 10.4-12.5  | 120 m      |
| 7    | 2.08-2.35  | 30 m       |

### Landsat 7 ETM+

“The government-owned Landsat 7 was successfully launched on April 15, 1999, from the Western Test Range of Vandenberg Air Force Base, California... The Earth observing instrument on Landsat 7, the Enhanced Thematic Mapper Plus (ETM+), replicates the capabilities of the highly successful Thematic Mapper instruments on Landsats 4 and 5. The ETM+ also includes additional features that make it a more versatile and efficient instrument for global change studies, land cover monitoring and assessment, and large area mapping than its design forebears.. Polar, sun-synchronous orbit at 705 km.”<sup>108</sup> It is still active. It includes a panchromatic band with 15m spatial resolution.

“

USGS: “Images acquired from June 1999 - May 2003 are displayed as RGB composites, bands 5, 4, and 3. Images are resampled to a pixel size of 240 meters from the original 30-meter data. Each Landsat 7 scene is color-stretched based on individual scene content. This may result in an apparent mismatch of colors between scenes. In the 240-meter display mode, browse images are JPEG compressed files with an average file size of ~130K. In the 1000-meter display mode, the browse images are GIFs with an average file size of ~35K.

The browse previews that are used to create the "Show Browse" display are uncorrected images in satellite orientation, and they can be viewed in a separate window.”<sup>109</sup>

On Landsat 7, the Enhanced Thematic Mapper Plus (ETM+) bands are:<sup>110</sup>

| ETM+ Band Number | $\mu\text{m}$ | Resolution m |
|------------------|---------------|--------------|
| 1                | 0.45-0.515    | 30 m         |
| 2                | 0.525-0.605   | 30 m         |
| 3                | 0.63-0.69     | 30 m         |
| 4                | 0.75-0.90     | 30 m         |
| 5                | 1.55-1.75     | 30 m         |

<sup>106</sup> <http://landsat.gsfc.nasa.gov/?p=3166>

<sup>107</sup> <http://glovis.usgs.gov/AboutBrowse.shtml#aboutbrowse>

<sup>108</sup> <http://landsat.gsfc.nasa.gov/?p=3184>

<sup>109</sup> <http://glovis.usgs.gov/AboutBrowse.shtml#aboutbrowse>

<sup>110</sup> <http://landsat.gsfc.nasa.gov/?p=3225>

|   |           |      |
|---|-----------|------|
| 6 | 10.4-12.5 | 60 m |
| 7 | 2.09-2.35 | 30 m |
| 8 | 0.52-0.9  | 15 m |

## Landsat 8: Operational Land Imager (OLI) and Thermal Infrared Sensor (TIRS)

Landsat 8 is an American Earth observation satellite launched on February 11, 2013. Sensors include the Operational Land Imager OLI and the Thermal Infrared Sensor TIRS.

“OLI collects data from nine spectral bands. Seven of the nine bands are consistent with the Thematic Mapper (TM) and Enhanced Thematic Mapper Plus (ETM+) sensors found on earlier Landsat satellites, providing for compatibility with the historical Landsat data, while also improving measurement capabilities. Two new spectral bands, a deep blue coastal / aerosol band [0.433 - 0.453  $\mu\text{m}$  , 30 m] and a shortwave-infrared cirrus band [1.360 - 1.390  $\mu\text{m}$  , 30 m], will be collected.”<sup>111</sup>

The TIRS has 2 spectral bands,<sup>112</sup>

Band 10 - Long Wavelength Infrared 10.6 - 11.19  $\mu\text{m}$ , 100 m

Band 11 - Long Wavelength Infrared 11.50 - 12.51  $\mu\text{m}$ , 100 m

Actual bands per USGS are:<sup>113</sup>

| OLI and TIRS Band Number     | $\mu\text{m}$ | Resolution m |
|------------------------------|---------------|--------------|
| Band 1 - Coastal aerosol     | 0.43 - 0.45   | 30           |
| Band 2 - Blue                | 0.45 - 0.51   | 30           |
| Band 3 - Green               | 0.53 - 0.59   | 30           |
| Band 4 - Red                 | 0.64 - 0.67   | 30           |
| Band 5 - Near Infrared (NIR) | 0.85 - 0.88   | 30           |
| Band 6 - SWIR 1              | 1.57 - 1.65   | 30           |
| Band 7 - SWIR 2              | 2.11 - 2.29   | 30           |
| Band 8 - Panchromatic        | 0.50 - 0.68   | 15           |
| Band 9 - Cirrus clouds       | 1.36 - 1.38   | 30           |
| Band 10 (TIRS) Thermal IR 1  | 10.60 - 11.19 | 100          |
| Band 11 (TIRS) Thermal IR 2  | 11.50 - 12.51 | 100          |

## Moderate-resolution Imaging Spectroradiometer (MODIS)

This is a multispectral imager, the Earth Observing System’s Moderate-resolution Imaging Spectroradiometer, launched with Terra in 1999. The 36 multispectral bands for the EOS MODIS system and the common uses for each band are given in a table shown earlier, under *Multispectral Images*. The band wavelengths extend from 405 nm to 14.385  $\mu\text{m}$ .

| Primary Use                       | Band | Bandwidth nm |
|-----------------------------------|------|--------------|
| Land/Cloud/Aerosols<br>Boundaries | 1    | 620 - 670    |
|                                   | 2    | 841 - 876    |
| Land/Cloud/Aerosols               | 3    | 459 - 479    |

<sup>111</sup> [http://en.wikipedia.org/wiki/Landsat\\_8](http://en.wikipedia.org/wiki/Landsat_8)

<sup>112</sup> [http://landsat.usgs.gov/band\\_designations\\_landsat\\_satellites.php](http://landsat.usgs.gov/band_designations_landsat_satellites.php)

<sup>113</sup> [http://landsat.usgs.gov/band\\_designations\\_landsat\\_satellites.php](http://landsat.usgs.gov/band_designations_landsat_satellites.php)

|   |    |             |
|---|----|-------------|
| Properties  | 4  | 545 - 565   |
|   | 5  | 1230 - 1250 |
|   | 6  | 1628 - 1652 |
|   | 7  | 2105 - 2155 |
| Ocean Color/<br>Phytoplankton/<br>Biogeochemistry | 8  | 405 - 420   |
|   | 9  | 438 - 448   |
|   | 10 | 483 - 493   |
|   | 11 | 526 - 536   |
|   | 12 | 546 - 556   |
|   | 13 | 662 - 672   |
|   | 14 | 673 - 683   |
|   | 15 | 743 - 753   |
| Atmospheric<br>Water Vapor                        | 16 | 862 - 877   |
|   | 17 | 890 - 920   |
|   | 18 | 931 - 941   |
|   | 19 | 915 - 965   |

| Primary Use                  | Band | Bandwidth $\mu\text{m}$ |
|------------------------------|------|-------------------------|
| Surface/Cloud<br>Temperature | 20   | 3.660 - 3.840           |
|                              | 21   | 3.929 - 3.989           |
|                              | 22   | 3.929 - 3.989           |
|                              | 23   | 4.020 - 4.080           |
| Atmospheric<br>Temperature   | 24   | 4.433 - 4.498           |
|                              | 25   | 4.482 - 4.549           |
| Cirrus Clouds<br>Water Vapor | 26   | 1.360 - 1.390           |
|                              | 27   | 6.535 - 6.895           |
|                              | 28   | 7.175 - 7.475           |
| Cloud Properties             | 29   | 8.400 - 8.700           |
| Ozone                        | 30   | 9.580 - 9.880           |
| Surface/Cloud<br>Temperature | 31   | 10.780 - 11.280         |
|                              | 32   | 11.770 - 12.270         |
| Cloud Top<br>Altitude        | 33   | 13.185 - 13.485         |
|                              | 34   | 13.485 - 13.785         |
|                              | 35   | 13.785 - 14.085         |
|                              | 36   | 14.085 - 14.385         |

### MODIS/ASTER Airborne Simulator (MASTER) — ARC=Ames Research Center

NASA's 50-band multispectral imager.<sup>114</sup> It is intended primarily to study geologic and other Earth surface properties. It is airborne, i.e., on airplanes,<sup>115</sup> and is designed to support the ASTER and MODIS [satellite] instrument teams in the areas of algorithm development, calibration and validation.<sup>116</sup>

### Polar Ionospheric X-ray Imaging Experiment (PIXIE)

"is an electronic camera which images the earth's aurora in x-rays... By imaging these x-rays and measuring their energies across a broad energy range, PIXIE determines the fluxes and characteristic energies of the parent electrons. This information is used to determine other important characteristics of the ionosphere, and of the interactions between the earth's upper atmosphere, ionosphere, radiation belts, and magnetosphere... PIXIE is one of 11 instruments aboard the Polar spacecraft, which is one of two satellites

<sup>114</sup> <http://asapdata.arc.nasa.gov/dsctrpns.htm>

<sup>115</sup> <http://masterweb.jpl.nasa.gov/documents/master.pdf>

<sup>116</sup> <http://masterweb.jpl.nasa.gov/>

in the Global Geospace Science (GGS) Program managed by NASA's Goddard Space Flight Center.<sup>117</sup> The POLAR launch occurred on February 24, 1996. "PIXIE ... Objectives: Study of the morphology and spectra of energetic electron precipitation and its effect on the atmosphere. Derivation of the total electron energy deposition rate, the energy distribution of the precipitating electrons, and the altitude profile of ionization and electrical conductivity."<sup>118</sup>

### **Solar Terrestrial Relations Observatory (STEREO) spacecraft**

STEREO A and STEREO B are at Lagrangian Points L4 and L5, respectively. Launched in October 2006. Instruments include Sun Earth Connection Coronal and Heliospheric Investigation (SECCHI), STEREO/WAVES (SWAVES), In-situ Measurements of Particles and CME Transients (IMPACT), and PLASMA and SupraThermal Ion Composition (PLASTIC).<sup>119</sup>

### **Terra EOS Spacecraft**

"Terra is the flagship of the Earth Observing System [=EOS], a series of spacecraft that represents the next landmark step in NASA's role to observe Earth from the unique vantage point of space. Focused on key measurements identified by a consensus of U.S. and international scientists, Terra enables new research into the ways Earth's land, oceans, air, ice, and life function as a total environmental system. Terra was launched into sun-synchronous Earth orbit on December 18, 1999, and started sending data back to earth in February 2000... Terra carries five scientific instruments: ASTER, CERES, MISR, MODIS, and MOPITT....Orbit: 705 km altitude, sun-synchronous, so that at any given latitude it crosses directly overhead at the same time each day... Orbit Inclination: 98.3 degrees from the Equator. Orbit Period: 98.88 minutes..."<sup>120</sup>

### **WIND Spacecraft and WIND-WAVES**

Comprehensive Solar Wind Laboratory for Long-Term Solar Wind Measurements.<sup>121</sup> Wind is a spin stabilized spacecraft launched in November 1, 1994 and placed in a halo orbit around the L1 Lagrange point, more than 200 R<sub>e</sub> upstream of Earth to observe the unperturbed solar wind that is about to impact the magnetosphere of Earth. Wind, together with Geotail, Polar, SoHO and Cluster, constitute a cooperative scientific satellite project designated the International Solar Terrestrial Physics (ISTP) program that aims at gaining improved understanding of the physics of solar terrestrial relation

The WAVES investigation on the WIND spacecraft [satellite launched November 1, 1994] provides comprehensive coverage of radio and plasma wave phenomena in the frequency range from a fraction of a Hertz up to about 14 MHz for the electric field and 3 kHz for the magnetic field. This package permits several kind of measurements, all of which are essential to understanding the Earth's environment—the Geospace—and its response to varying solar wind conditions. In situ measurements of different modes of plasma waves gives information on local processes and couplings in different regions and boundaries of the Geospace leading to plasma instabilities: magneto-acoustic waves, ion cyclotron waves, whistler waves, electron plasma oscillations, electron burst noise and other types of electrostatic or electromagnetic waves.<sup>122</sup>

---

<sup>117</sup> <http://pixie.spasci.com/>

[http://www-istp.gsfc.nasa.gov/istp/ggs\\_project.html](http://www-istp.gsfc.nasa.gov/istp/ggs_project.html)

<sup>118</sup> <https://directory.eoportal.org/web/eoportal/satellite-missions/p/polar>

<sup>119</sup> [http://www.nasa.gov/mission\\_pages/stereo/spacecraft/index.html](http://www.nasa.gov/mission_pages/stereo/spacecraft/index.html)

<sup>120</sup> <http://terra.nasa.gov/>

<sup>121</sup> <http://wind.nasa.gov/>

<sup>122</sup> <http://wind.nasa.gov/orbit.php>

# Aerial Photography: Vantage Point, Cameras, Filters, and Film

See Jensen Chapter 4: Aerial Photography - Vantage Point, Cameras, Filters, and Film. Not further summarized here.

## Elements of Visual Image Interpretation

See Jensen Chapter 5: Elements of Visual Image Interpretation. An important subject not further summarized here.

## Photogrammetry, Orthoimages, and Digital Elevation Models

See Jensen Chapter 6: Photogrammetry.

Photogrammetry deals with making accurate measurements from images. It requires use of *orthoimages*, that is images in which the objects and regions depicted are precisely *registered* in an accurate and well-established set of ground coordinates. It is, “the science of making measurements from photographs, especially for recovering the exact positions of surface points. Moreover, it may be used to recover the motion pathways of designated reference points located on any moving object, on its components and in the immediately adjacent environment.”<sup>123</sup>

Photogrammetry also requires creation and use of Digital Elevation Models, in which the elevations (of terrain or other surfaces) are determined and represented for points lying in a *registered* x,y coordinate system

A natural color orthoimage of the Block Mountain region in SW Montana, from the National Agriculture Imagery Program (NAIP) dataset

The USDA states, “If an image is created with the red (wavelength) band as band 1, green as band 2, blue as band 3, and near infrared as band 4, a natural color display on the computer screen would be set up with the red (display) channel as band 1 (red), green channel as band 2 (green), and blue channel as band 3 (blue). CIR would be set up with the red channel as band 4 (NIR), the green channel as band 1 (red) and the blue channel as band 2 (green). Band 3 (blue) is omitted”<sup>124</sup>

The image on the right shows an NAIP image loaded



<sup>123</sup> <http://en.wikipedia.org/wiki/Photogrammetry>

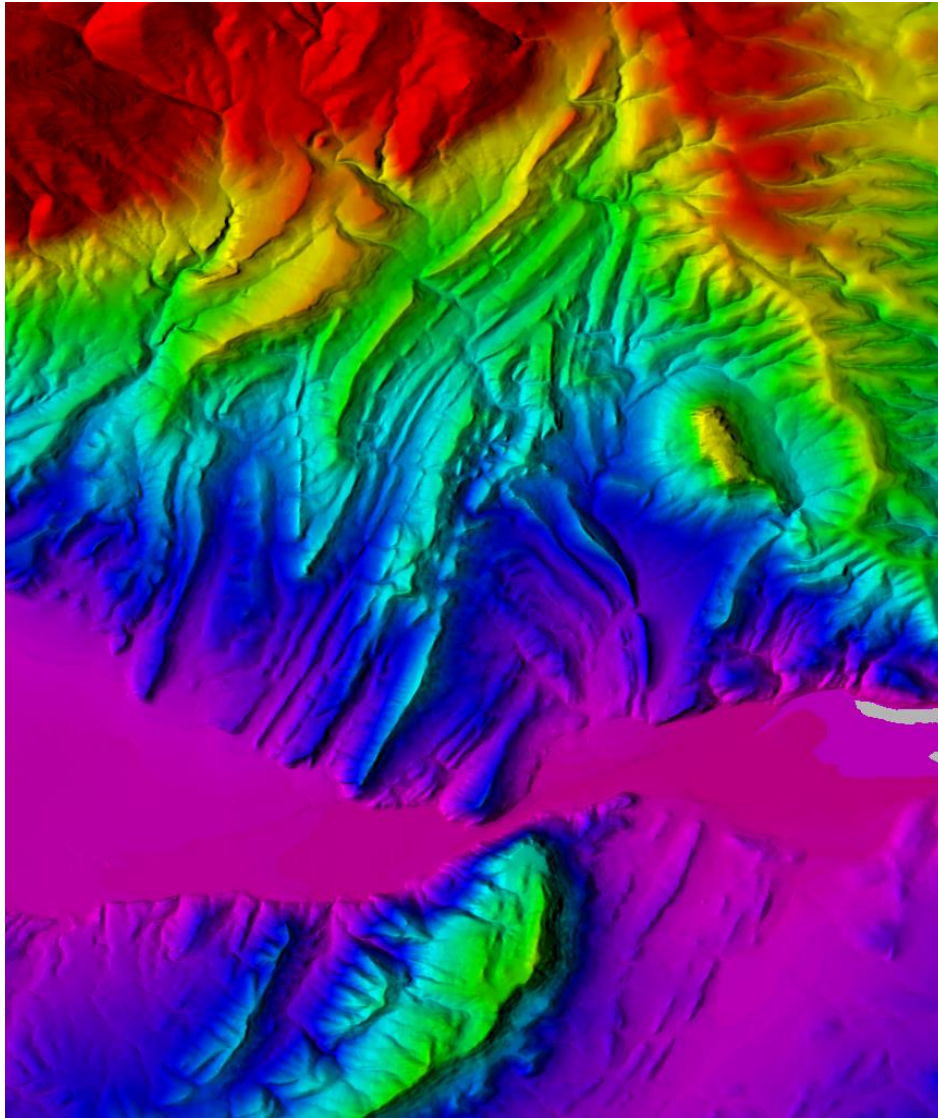
<sup>124</sup> [http://www.fsa.usda.gov/Internet/FSA\\_File/fourband\\_info\\_sheet\\_2013.pdf](http://www.fsa.usda.gov/Internet/FSA_File/fourband_info_sheet_2013.pdf)

as natural color with Band 1→R, 2→G, 3→B, no further processing. This is of the Block Mountain region in SW Montana, centered on an anticline which is exposed at the surface.

A colorized shaded relief image of the same Block Mountain region in SW Montana using the USGS National Elevation Dataset NED data<sup>125</sup>

Here the values of elevation in meters are mapped to a rainbow scale of colors, with blue being the lowest and red being the highest elevation. The distribution is further enhanced by use of shaded relief, which makes elevation differences more conspicuous:

*“Shaded relief, or hill-shading, simulates the cast shadow thrown upon a raised relief map, or more abstractly upon the planetary surface represented. The shadows normally follow the English convention of top-left lighting .... If the map is oriented with north at the top, the result is that the light appears to come from the north-west [as in this image]...”*<sup>126</sup>



Colorized shaded relief (hill-shaded) image of the Block Mountain MT area using the NED 1/3 arcsec data (rainbow scale, max 1900 m is red)

The shading here is specified by these parameters: the Sun is 45 degrees above the horizon, and is at 270 degrees from N, thus it is in the W.

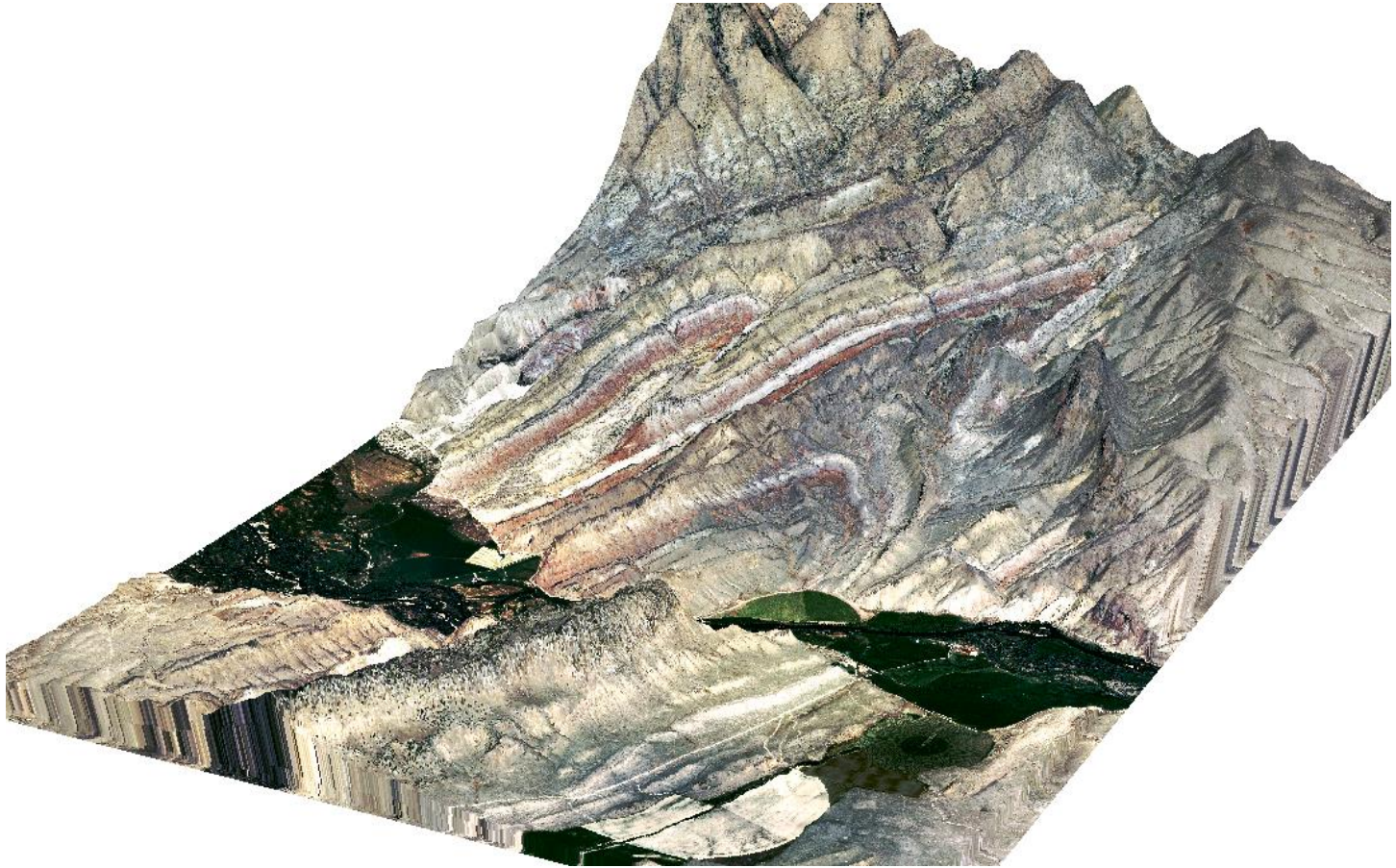
---

<sup>125</sup> <http://ned.usgs.gov/>

<sup>126</sup> [http://en.wikipedia.org/wiki/Terrain\\_cartography#Shaded\\_relief](http://en.wikipedia.org/wiki/Terrain_cartography#Shaded_relief)

### A 3-D perspective view of the Block Mountain region in SW Montana area, using the NAIP and NED datasets

This view is created, with the help of ENVI software, by “draping” the orthoimage (which gives registered x-y coordinates) over a NED elevation image (which gives the registered elevation data at the same x,y coordinates [using resampled data at a matching resolution]). The colors are those of the NAID image, although contrast is somewhat greater. The elevation data is most apparent when the viewing angles are adjusted in real-time. Here, Block Mountain is seen on the right in dark tones. The multicolored surface anticline is in the center of the region displayed. The ENVI software allows the user to view the region in an infinite number of perspectives determined by the virtual height and downward viewing angle of the viewer, as well as by the compass x,y direction of viewing.

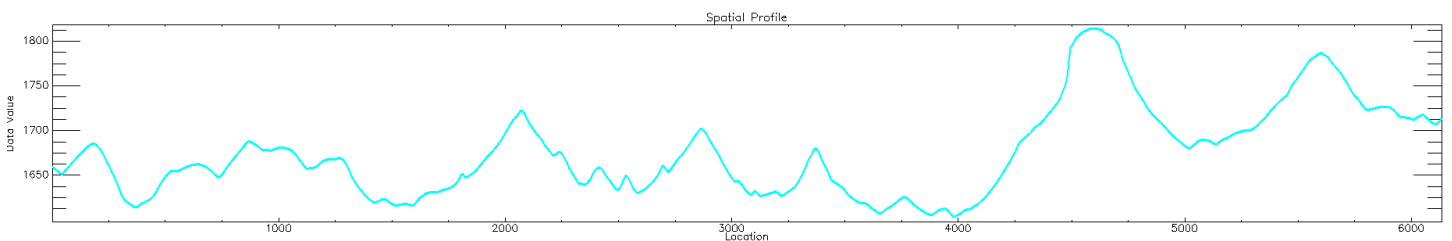


A 3D surface perspective image of Block Mountain using NAIP and NED datasets, selected from an infinite number of possible projections.

Here the viewer is looking toward the NW.

Note that part of the green low valley area is obscured by the long ridge (lower left center), which in this view projects in front of it.

Here is a representative profile from ENVI of elevation of the anticline region essentially perpendicular to the fold hinge (vertical axis is meters elevation. (Horizontal scale is uncertain.) Differential erosion of the various exposed layers of the anticline is apparent.



# Multispectral Remote Sensing Systems, Spectroscopy, and Spectroscopic Imaging

See Jensen Chapter 7: Multispectral Remote Sensing Systems (and Jensen Chapter 15: In situ Spectral Reflectance Measurement).

These proved to be core subjects of this course.

An important aspect of modern RS is the acquisition of data including images in multiple planes, each plane of which depicts the same object (i.e., at the same x, y coordinates) but in a different wavelength band. Standard digital cameras acquire 3 planes of data, Red, Green, and Blue. In Multispectral imaging, there are many planes of data. For instance, the multispectral Landsat 8 OLI acquires 8 bands or planes of Visible and IR data, ranging from 0.45  $\mu\text{m}$  to 12.5  $\mu\text{m}$ . The ASTER aboard Terra acquires 14 bands per image, ranging from 0.52  $\mu\text{m}$  to 11.65  $\mu\text{m}$ . The MODIS system on Terra acquires 36 bands per image, ranging from 0.405  $\mu\text{m}$  to 14.385  $\mu\text{m}$ .

For example, the ASTER wavelength bands are as follows (wavelength significant digits per ASTER website)<sup>127</sup>

| Band | Label<br>(nadir unless otherwise stated) | Lower Limit<br>$\mu\text{m}$ | Upper Limit<br>$\mu\text{m}$ |
|------|--|------------------------------|------------------------------|
| B1   | VNIR_Band1                               | 0.52                         | 0.60                         |
| B2   | VNIR_Band2                               | 0.63                         | 0.69                         |
| B3N  | VNIR_Band3N<br>(looking down to Nadir)   | 0.76                         | 0.86                         |
| B3B  | VNIR_Band3B<br>(backward looking)        | 0.76                         | 0.86                         |
| B4   | SWIR_Band4                               | 1.600                        | 1.700                        |
| B5   | SWIR_Band5                               | 2.145                        | 2.185                        |
| B6   | SWIR_Band6                               | 2.185                        | 2.225                        |
| B7   | SWIR_Band7                               | 2.235                        | 2.285                        |
| B8   | SWIR_Band8                               | 2.295                        | 2.365                        |
| B9   | SWIR_Band9                               | 2.360                        | 2.430                        |
| 10   | TIR_Band10                               | 8.125                        | 8.475                        |
| 11   | TIR_Band11                               | 8.475                        | 8.825                        |
| 12   | TIR_Band12                               | 8.925                        | 9.275                        |
| 13   | TIR_Band13                               | 10.25                        | 10.95                        |
| 14   | TIR_Band14                               | 10.95                        | 11.65                        |

Hyperspectral imagers acquire many more, up to several hundreds of planes per image. For instance, the airborne AVIRIS (Airborne Visible Infrared Imaging Spectrometer) acquires 224 contiguous spectral channels (also called bands) with wavelengths from 400 to 2500 nm. The brightness values (digital number or DN) may be thought to lie in a cube of 3 coordinate axes, x-position, y-position, and numbered wavelength band. Brightness values may be digitized to a bit level of 8 to 12 bits typically.

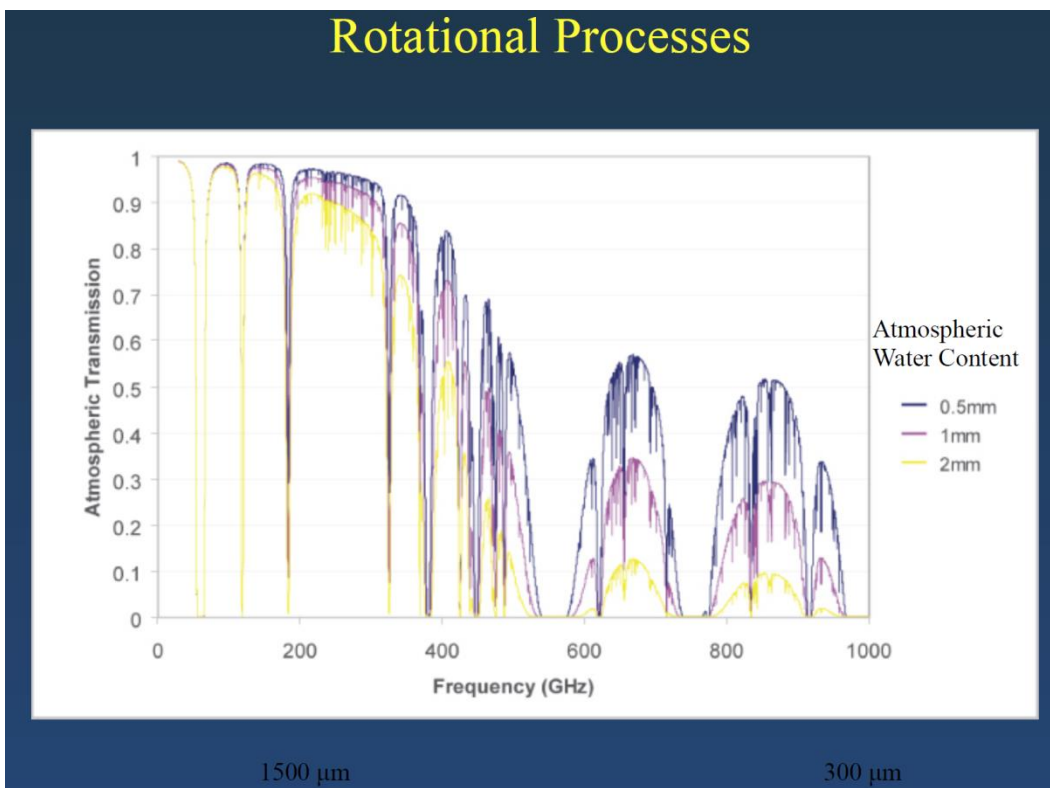
## Concept of Spectroscopy

Photons striking free molecules can cause them to rotate. Like electron orbits, these rotational states are quantized, and there are discrete photon energies that are absorbed to cause the molecules to spin. Rotational interactions are low-energy interactions and the absorption features are typically at long wavelengths (TIR and microwave).

Atmospheric light absorption attributable to water is dependent on frequency and water content:

<sup>127</sup> <http://asterweb.jpl.nasa.gov/characteristics.asp>

## Rotational Processes



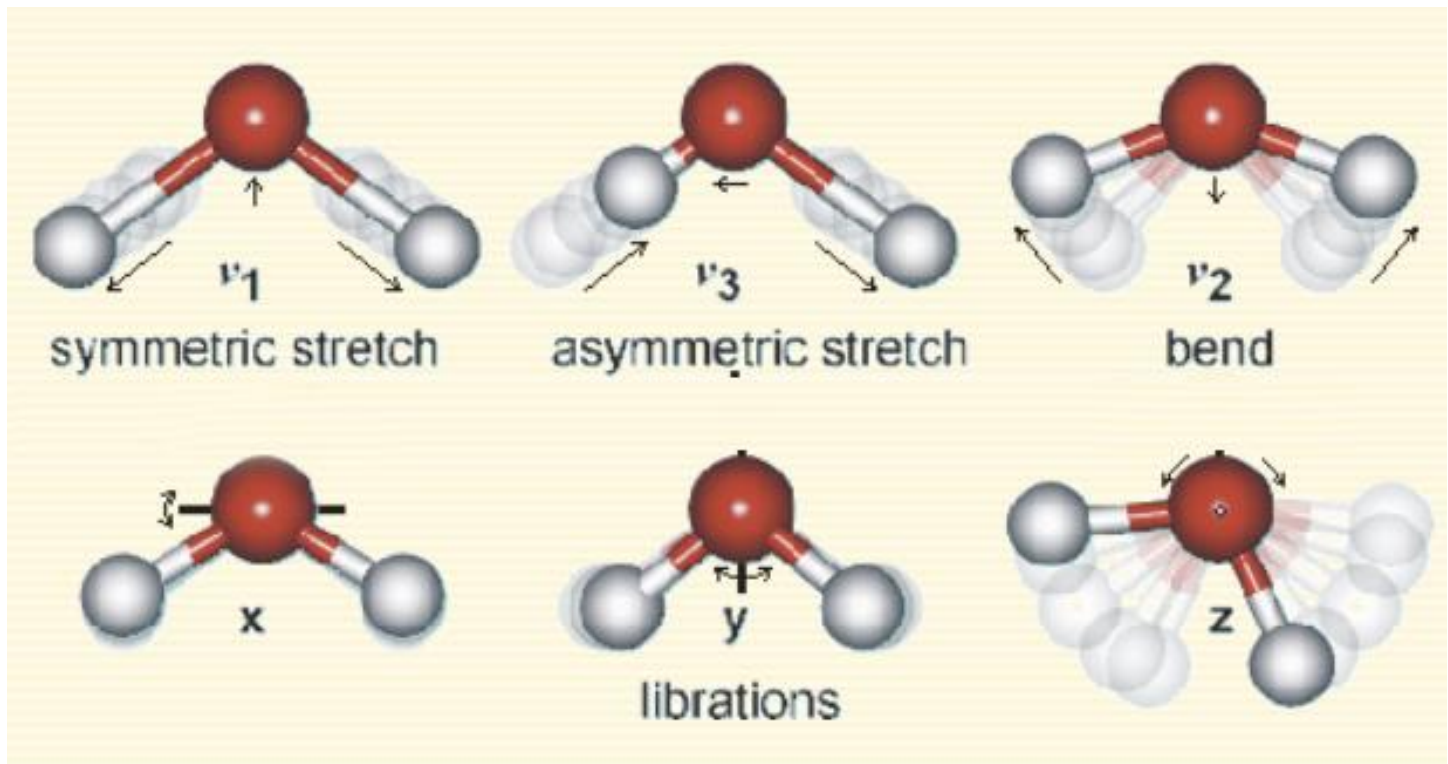
Atmospheric Spectral Transmission as a function of water content  
Note that 200 GHz is about 1500 μm and 1000 GHz is about 300 μm.  
(from lecture 6 PDF, source unknown)

Diatomic molecules of the same element ( $N_2$ ,  $O_2$ , etc.) or monoatomic molecules (Ar) are not greenhouse gases because they have no net change in their dipole moment when they vibrate and hence are almost totally unaffected by infrared radiation.<sup>128</sup>

The bonds in a molecule or a crystal lattice are like springs with attached weights: the whole system can vibrate. The frequency of vibration depends on the strength of each spring (the bond in a molecule) and their masses (the mass of each element in a molecule). For a nonlinear molecule with  $N$  atoms (such as  $H_2O$ ), there are  $3N-6$  normal vibrational modes (called fundamentals). But not all normal modes are radiatively active (in the IR). Water has 3 modes, ammonia  $NH_3$  has 6 modes, methane  $CH_4$  has 9 modes. The modes of water vibration (of the OH bonds) are: symmetric stretch ( $\nu_1$ ), asymmetric stretch ( $\nu_3$ ), and bend ( $\nu_2$ , of the angle between the 2 OH bonds), plus 3 librations. These former modes have IR absorption peaks at 2.74, 2.66, and 6.47 μm, respectively, and an even more complex fine structure results from adding in rotational modes.

<sup>128</sup> [http://en.wikipedia.org/wiki/Greenhouse\\_gas](http://en.wikipedia.org/wiki/Greenhouse_gas)

The vibrational modes of H<sub>2</sub>O are shown as follows:<sup>129</sup>



For a linear molecule with N atoms, or any diatomic molecule (N=2), the number of normal modes is  $3N-5$ . CO<sub>2</sub> and N<sub>2</sub>O each have 4 normal modes. Each vibration can also occur at multiples of the original fundamental frequency (overtones), or involve different modes of vibrations (combinations).<sup>130</sup> For example, see explanation for blue water, above.

Gases can change vibrational and rotational states simultaneously. The energy of absorption is that of the changed vibrational state  $\pm$  the rotational state energy. This can lead to complex hyperspectral patterns of absorption.

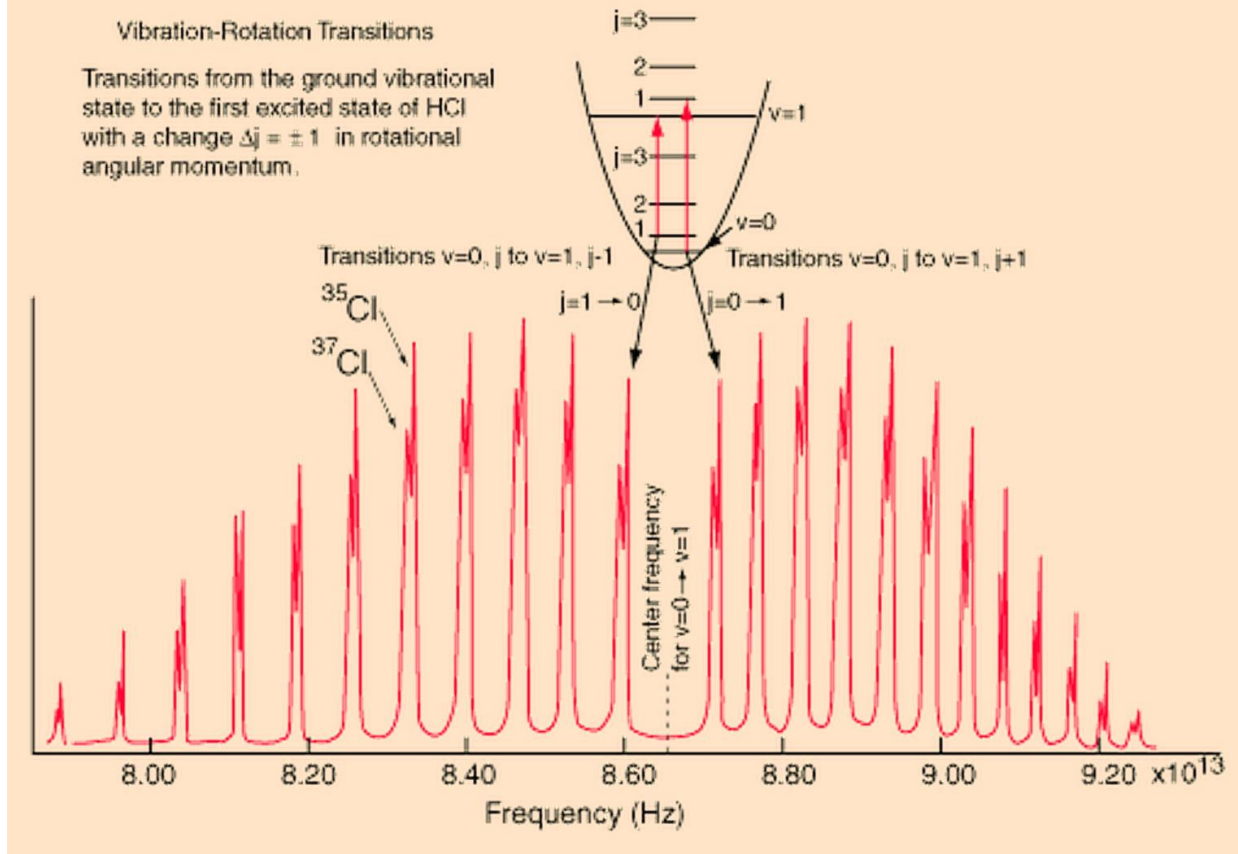
“The absorption lines shown [graph below] involve transitions from the ground to first excited vibrational state of HCl, but also involve changes in the rotational state. The rotational angular momentum changes by 1 during such transitions. If you had a transition from  $j=0$  in the ground vibrational state to  $j=0$  in the first excited state, it would produce a line at the vibrational transition energy. As observed, you get a closely spaced series of lines going upward and downward from that vibrational level difference. The splitting of the lines shows the difference in rotational inertia of the two chlorine isotopes Cl-35(75.5%) and Cl-37(24.5%).”<sup>131</sup>

<sup>129</sup> [http://www1.lsbu.ac.uk/water/water\\_vibrational\\_spectrum.html](http://www1.lsbu.ac.uk/water/water_vibrational_spectrum.html) (includes animated H<sub>2</sub>O molecule)

<sup>130</sup> Quoted or paraphrased from materials in lecture 6 PDF, source unknown

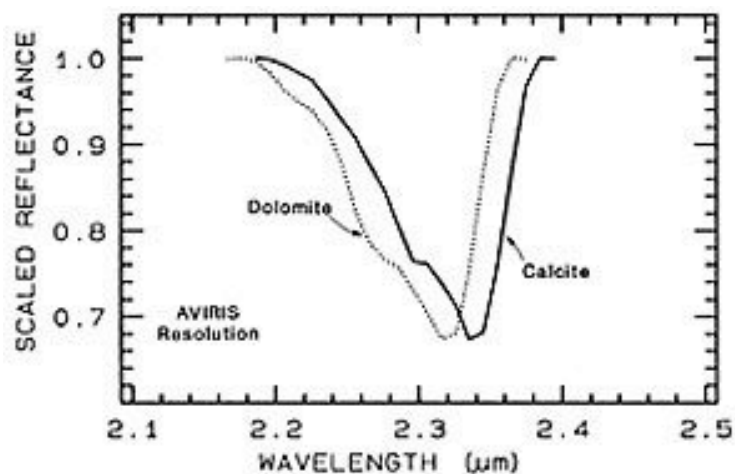
<sup>131</sup> <http://hyperphysics.phy-astr.gsu.edu/hbase/molecule/vibrot2.html#c1> including graph

# Vibration-Rotation Spectrum of HCl



Vibration and rotation IR absorption spectrum in a narrow range of wavelengths for HCl gas

When a heavier element (Ca) is substituted for a lighter (Mg) in a mineral crystal structure, the associated vibratory state has more inertia, a slightly longer period, lower frequency, and longer wavelength.<sup>132</sup>



In crystals, there are no rotations possible, but vibrational resonances occur and produce characteristic absorption wavelengths. Substituting Ca for Mg in  $(\text{Mg,Ca})\text{CO}_3$  shifts the absorption peak to longer wavelength (lower frequency), presumably because Ca is heavier and vibrates with slower frequency

<sup>132</sup> [http://fas.org/irp/imint/docs/rst/Sect13/Sect13\\_6.html](http://fas.org/irp/imint/docs/rst/Sect13/Sect13_6.html) incl. graph  
Page 65 of 110 RemoteSensing\_ESS421\_MCM\_Winter2015.docx

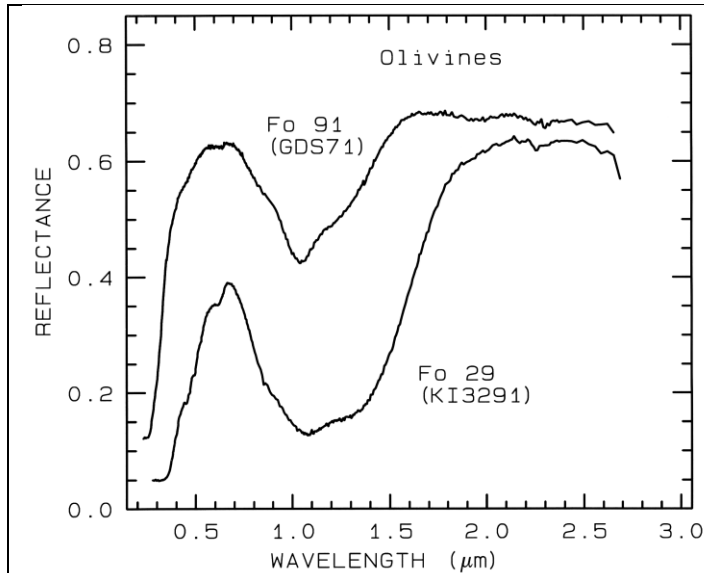
In addition to vibration and rotation resonances, Electronic Processes also contribute characteristic absorption peaks:

- **Crystal Field Effects:** The electronic energy levels of an isolated ion are usually split and displaced when located in a crystal. Unfilled d orbitals are split by interaction with surrounding ions and assume new energy values. The new energy values (transitions between them and consequently their spectra) are primarily determined by the valence state of the ion ( $\text{Fe}^{2+}$ ,  $\text{Fe}^{3+}$ ), coordination number, and site symmetry.
- **Charge Transfer Absorptions:** These are interelement transitions where the absorption of a photon causes an electron to move between ions. The transition can occur between the same metal in different valence states, such as between  $\text{Fe}^{2+}$  and  $\text{Fe}^{3+}$
- **Conduction Bands**
- **Color Centers:** Impurities leave “holes” for electrons to get stuck in. These electrons have their own sets of energy levels

Some of the spectroscopic images that follow were created and analyzed in one or more of the laboratory exercises in the course.

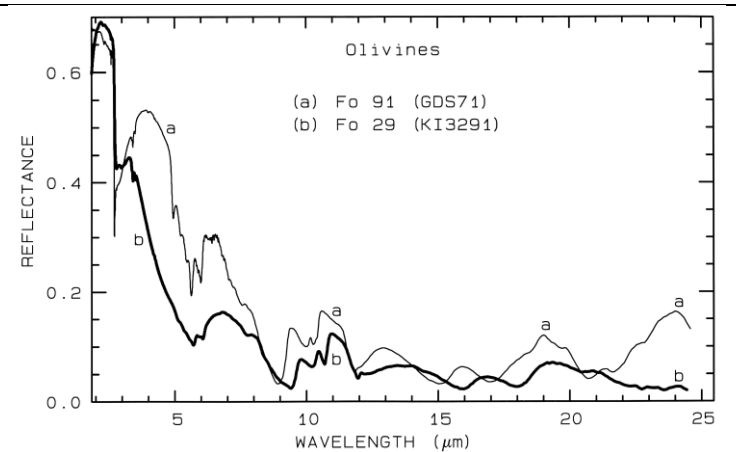
## Sample Reflectance Spectra

(per Clark, Spectroscopy of Rocks and Minerals)<sup>133</sup>

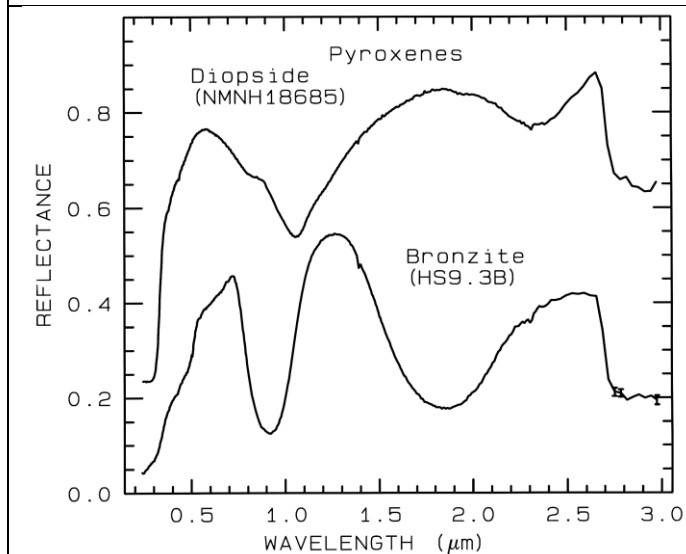


“The 1-μm band position varies from about 1.08 μm at Fo 10 to 1.05 μm at Fo 90”:

”<http://speclab.cr.usgs.gov/PAPERS.refl-mrs/giff/300dpi/fig5a3.gif>”

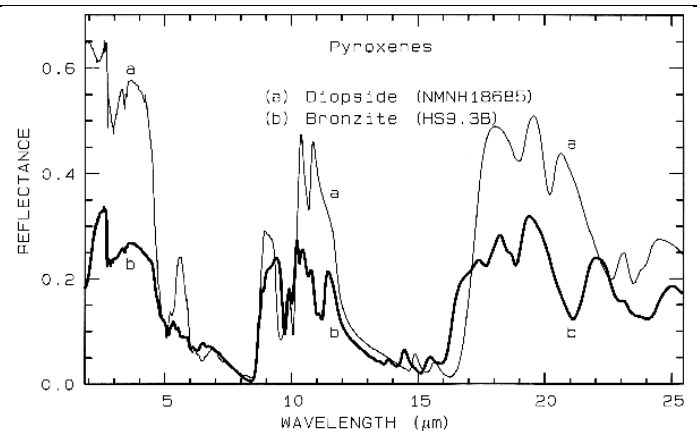


Olivine reflectance at higher mid-infrared wavelengths  
<http://speclab.cr.usgs.gov/PAPERS.refl-mrs/giff/300dpi/fig5b3.gif> :



“Reflectance spectra of two pyroxenes showing the change in Fe<sup>2+</sup>-absorption band position and shape with composition... Diopside ... is CaMgSi<sub>2</sub>O<sub>6</sub>, but some Fe<sup>2+</sup> substitutes for Mg. Bronzite ... is (Mg,Fe)SiO<sub>3</sub> with mostly Mg. ”

”<http://speclab.cr.usgs.gov/PAPERS.refl-mrs/giff/300dpi/fig6a3.gif>”



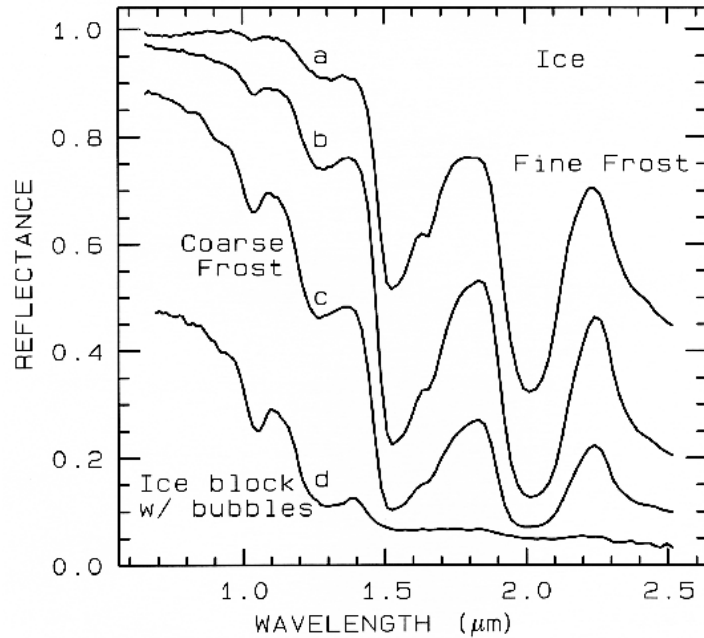
Same but at “mid-infrared wavelengths. Note the shifts in the spectral features due to the change in composition.”

”<http://speclab.cr.usgs.gov/PAPERS.refl-mrs/giff/300dpi/fig6b3.gif>”

Other examples at this website illustrate iron hydroxide vs. Iron oxide, rare-earth oxides, etc.

<http://speclab.cr.usgs.gov/PAPERS.refl-mrs/refl4.html#section3.1.1>

<sup>133</sup> <http://speclab.cr.usgs.gov/PAPERS.refl-mrs/refl4.html>



Reflectance Spectra (Figure 22a) showing effect of ice grain size<sup>134</sup>

The graph above depicts the near-infrared spectral reflectance of

- a) fine grained (~50 μm) water frost,
- b) medium grained (~200 μm) frost,
- c) coarse grained (400-2000 μm) frost and
- d) an ice block containing abundant microbubbles.

The reflectance is considerably higher for the various sizes of frost compared to an ice block. The finer the frost, the greater the reflectivity, for the three wavelengths shown. “In a smaller grain there are proportionally more surface reflections compared to internal photon path lengths, or in other words, the surface-to-volume ratio is a function of grain size. If multiple scattering dominates, as is usually the case in the visible and near- infrared, the reflectance decreases as the grain size increases.” ... “The larger the effective grain size [here, of the frost crystals], the greater the mean photon path that photons travel in the ice, and the deeper the absorptions become. Curve [d] is very low in reflectance because of the large path length in ice.”<sup>135</sup>

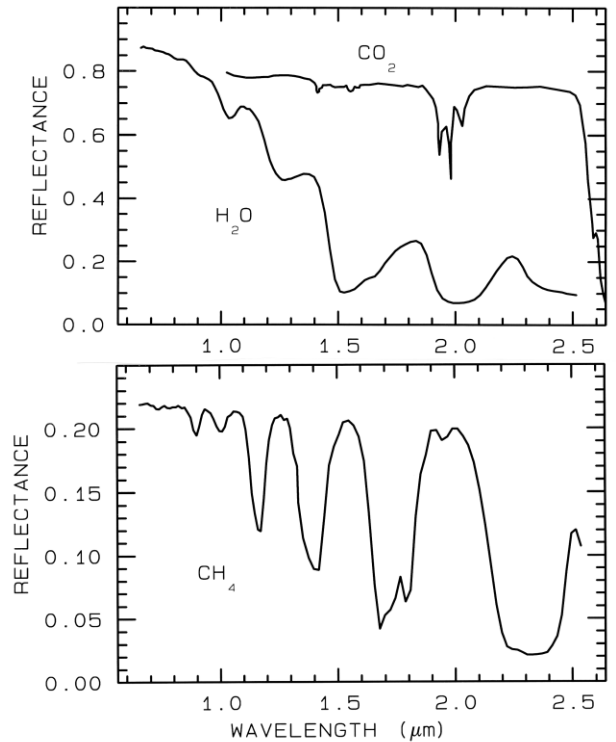
<sup>134</sup> <http://speclab.cr.usgs.gov/PAPERS.refl-mrs/giff/300dpi/fig22a3.gif>

<sup>135</sup> <http://speclab.cr.usgs.gov/PAPERS.refl-mrs/refl4.html>

“Just like water in minerals shows diagnostic absorption bands, ice (crystalline H<sub>2</sub>O) which is formally a mineral, also shows strong absorption bands. In the planetary literature it is referred as water ice, so as not to confuse it with other ices. Spectra of solid H<sub>2</sub>O, CO<sub>2</sub>, and CH<sub>4</sub> are shown in [the adjacent] figure 15.

The spectral features in [this figure] are all due to vibrational combinations and overtones, whose fundamentals have previously been discussed in general. Note the H<sub>2</sub>O spectra show broad absorptions compared to the others. The reason is that while ice is normally a hexagonal structure, the hydrogen bonds are orientationally disordered..., and the disorder broadens the absorptions. There are many ices in the solar system...

Ice, being ubiquitous in the solar system is found mixed with other minerals, on the Earth, as well as elsewhere in the solar system...:”<sup>136</sup>



## Vegetation

“Spectra of vegetation come in two general forms: green and wet (photosynthetic), and dry non-photosynthetic, but there is a seemingly continuous range between these two end members. The spectra of these two forms are compared to a soil spectrum in Figure 16 [adjacent, on top]. Because all plants are made of the same basic components, their spectra appear generally similar. However, in the spectral analysis section we will see methods for distinguishing subtle spectral details. The near-infrared spectra of green vegetation are dominated by liquid water vibrational absorptions. The water bands are shifted to slightly shorter wavelengths than in liquid water, due to hydrogen bonding. The absorption in the visible is due to chlorophyll [discussed elsewhere]... The dry non-photosynthetic vegetation spectrum shows absorptions due to cellulose, lignin, and nitrogen. Some of these absorptions can be confused with mineral absorptions, unless a careful spectral analysis is done...

[Figure 16, top diagram, shows] Reflectance spectra of photosynthetic (green) vegetation, non-photosynthetic (dry) vegetation, and a soil. The green vegetation has absorptions short of 1  $\mu\text{m}$  due to chlorophyll. Those at wavelengths greater than 0.9  $\mu\text{m}$  are dominated by liquid water. The dry vegetation shows absorptions dominated by cellulose, but also lignin and nitrogen. These absorptions must also be present in the green vegetation, but can be detected only weakly in the presence the stronger water bands. The soil spectrum shows a weak signature at 2.2  $\mu\text{m}$  due to montmorillonite.”<sup>137</sup> Both graphs depict the abrupt “red edge” where low reflectance at red wavelength transitions to a strong reflectance at near IR.

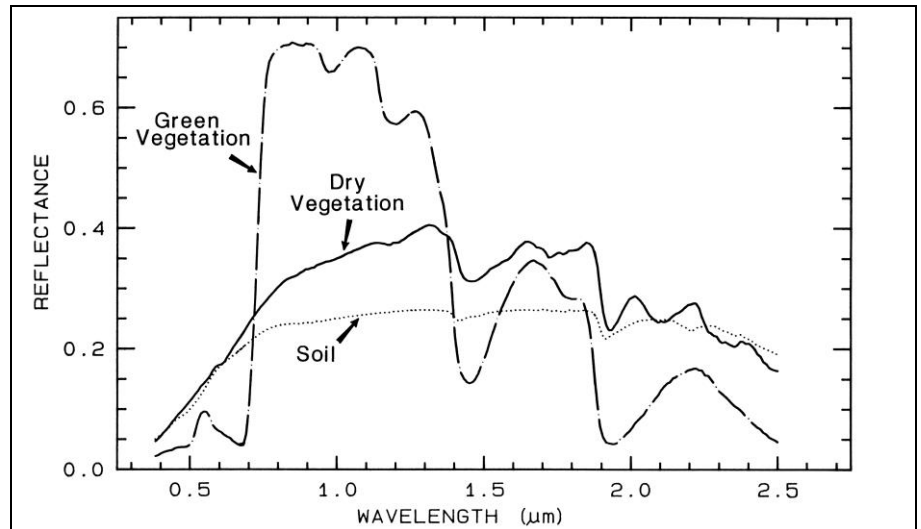
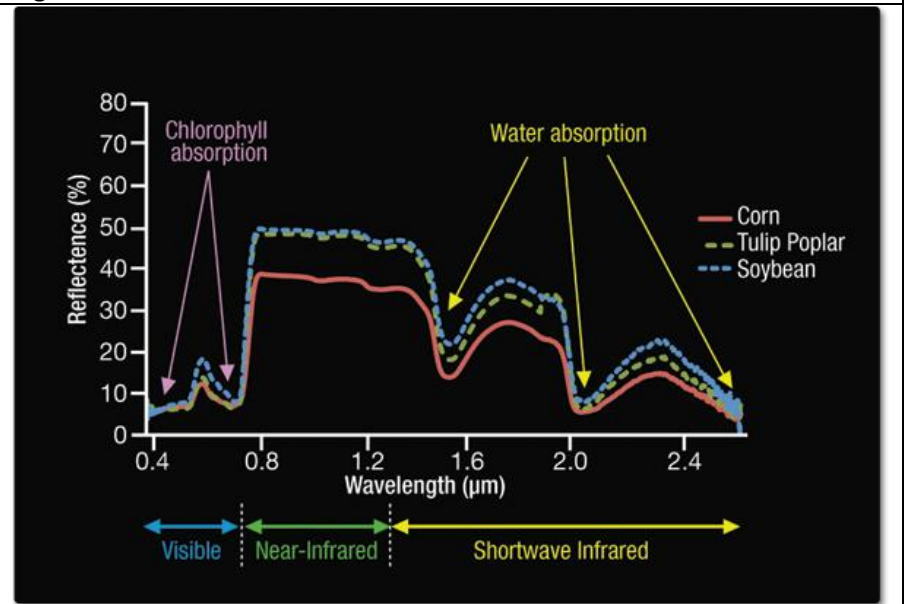


Figure 16<sup>137</sup>



Spectral Signatures of [Living] Vegetation

“[This graph] shows the differences among the spectral signatures of [living] corn, soybeans, and Tulip Poplar trees.”<sup>138</sup>

## Grain Size Effects

Mineral spectra are affected by grain size as follows:

“The amount of light scattered and absorbed by a grain is dependent on grain size... [see Figures 21a and 21b that follow, also Figure 22a previously shown]. A larger grain has a greater internal path where photons may be absorbed according to Beers Law. It is the reflection from the surfaces and internal imperfections that control scattering. In a smaller grain there are proportionally more surface reflections compared to internal photon path lengths, or in other words, the surface-to-volume ratio is a function of grain size. If multiple scattering dominates, as is usually the case in the visible and near-infrared, the reflectance decreases as the

<sup>137</sup> <http://speclab.cr.usgs.gov/PAPERS.refl-mrs/giff/300dpi/fig16-3.gif>

<sup>138</sup> [http://missionscience.nasa.gov/ems/08\\_nearinfraredwaves.html](http://missionscience.nasa.gov/ems/08_nearinfraredwaves.html)

<sup>139</sup> <http://speclab.cr.usgs.gov/PAPERS.refl-mrs/refl4.html#section4.3>

grain size increases, as shown in the pyroxene visible to near-infrared spectra in Figure 21a. However, in the mid-infrared, where absorption coefficients are much higher and the index of refraction varies strongly at the Christensen frequencies [defined below], first surface reflection is a larger or even dominant component of the scattered signal. In these cases, the grain size effects are much more complex, even reversing trends commonly seen at shorter wavelengths (e.g. Figure 21b) [i.e., so that reflectance increases with increasing grain size].<sup>140</sup>

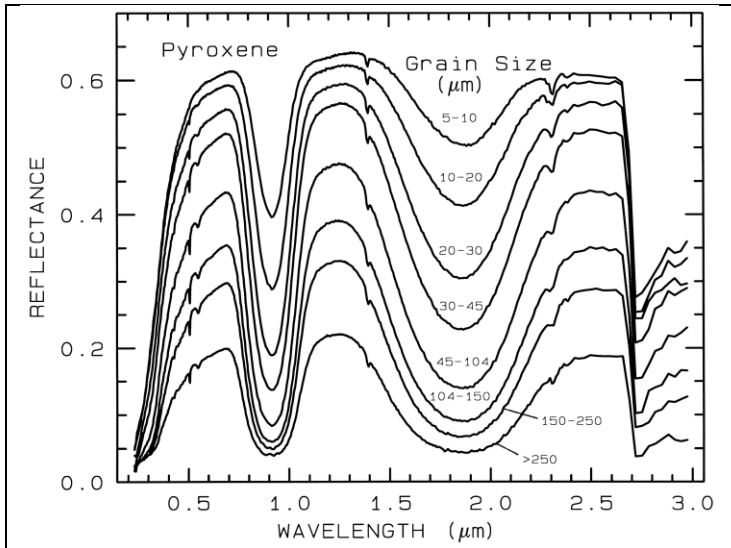


Figure 21a [VNIR and SWIR]  
 “Reflectance Spectra of pyroxene as a function of grain size. As the grain size becomes larger, more light is absorbed and the reflectance drops”

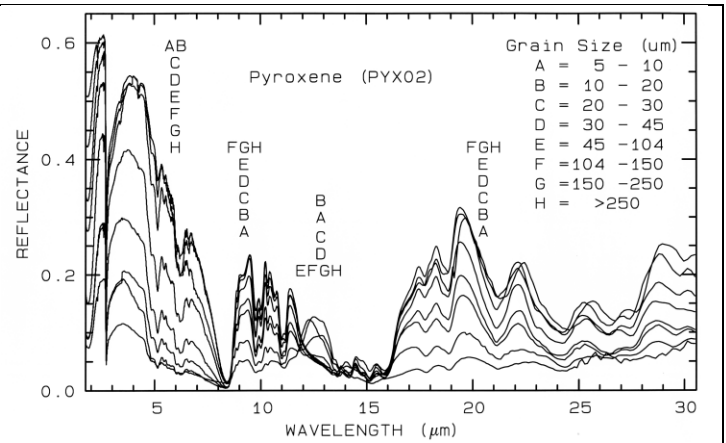


Figure 21b [VNIR, SWIR, MIR and some LWIR]  
 “Same series as in Figure 21a, but [including also] the mid-IR. The position of letter identifiers indicates the relative position of the spectra at the various wavelengths. Note the reversal in the trends at some wavelengths and not others. Grain size effects on the shapes of spectral features in the mid-IR can be quite large.”

*Christensen frequency* is defined as follows. (Here,  $n$  is the real component of the index of refraction  $m$  and  $K$  is the imaginary component, also called the Extinction Coefficient. Thus, index of refraction  $m = n + iK$  in complex number notation.) “The complex index of refraction in Figure 4a [below] shows important properties of materials. As one moves to longer wavelengths (left to right in Figure 4a), the index of refraction decreases to a minimum just before a sharp rise (e.g. at 8.5 and 12.6  $\mu\text{m}$  in Figure 4a). The minimum is often near or even below  $n = 1$  [where  $n$  is the real part of the index]. The wavelength where  $n = 1$  is called the Christensen frequency and usually results in a minimum in reflected light because of the small (to zero) difference in the index of refraction compared to the surrounding medium (e.g. air or vacuum). The location of the observed reflectance minimum is also controlled by the extinction coefficient... Note that the Christensen frequency sometimes occurs at a wavelength shorter than the maximum in the extinction coefficient (e.g. Figure 4a, below). This maximum is called the [Reststrahlen] band: the location of fundamental vibrational stretching modes in the near and mid-infrared. The combination of  $n$  and  $K$  at these wavelengths often results in high reflectance.”<sup>141</sup>

<sup>140</sup> Text and images: <http://speclab.cr.usgs.gov/PAPERS.refl-mrs/refl4.html#section4.3>

<sup>141</sup> <http://speclab.cr.usgs.gov/PAPERS.refl-mrs/refl4.html#section2.1>

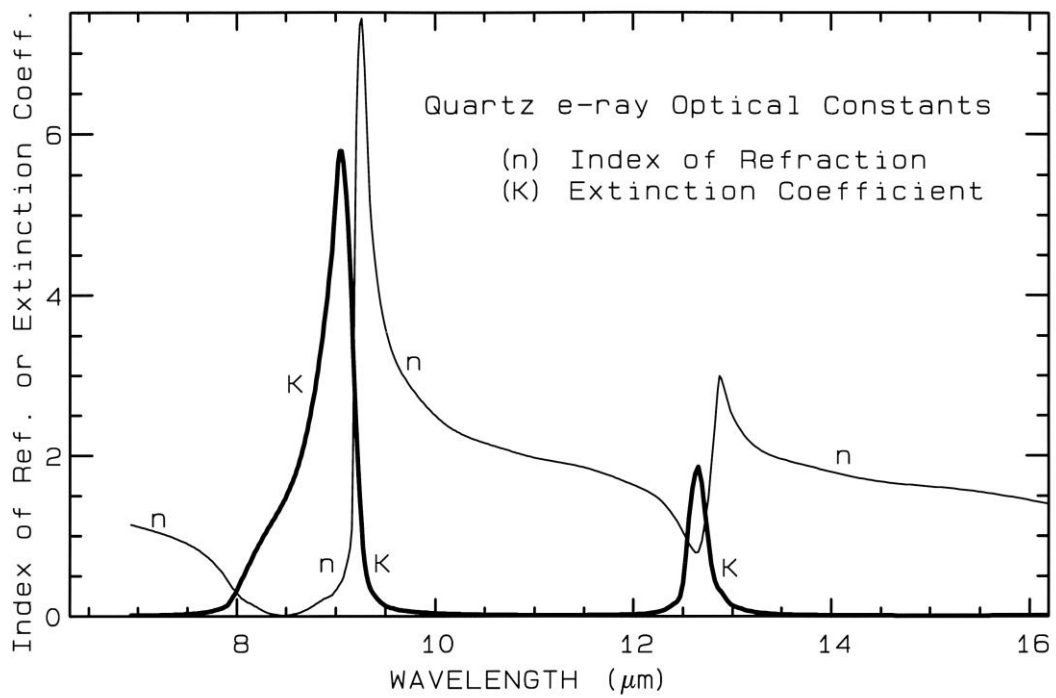
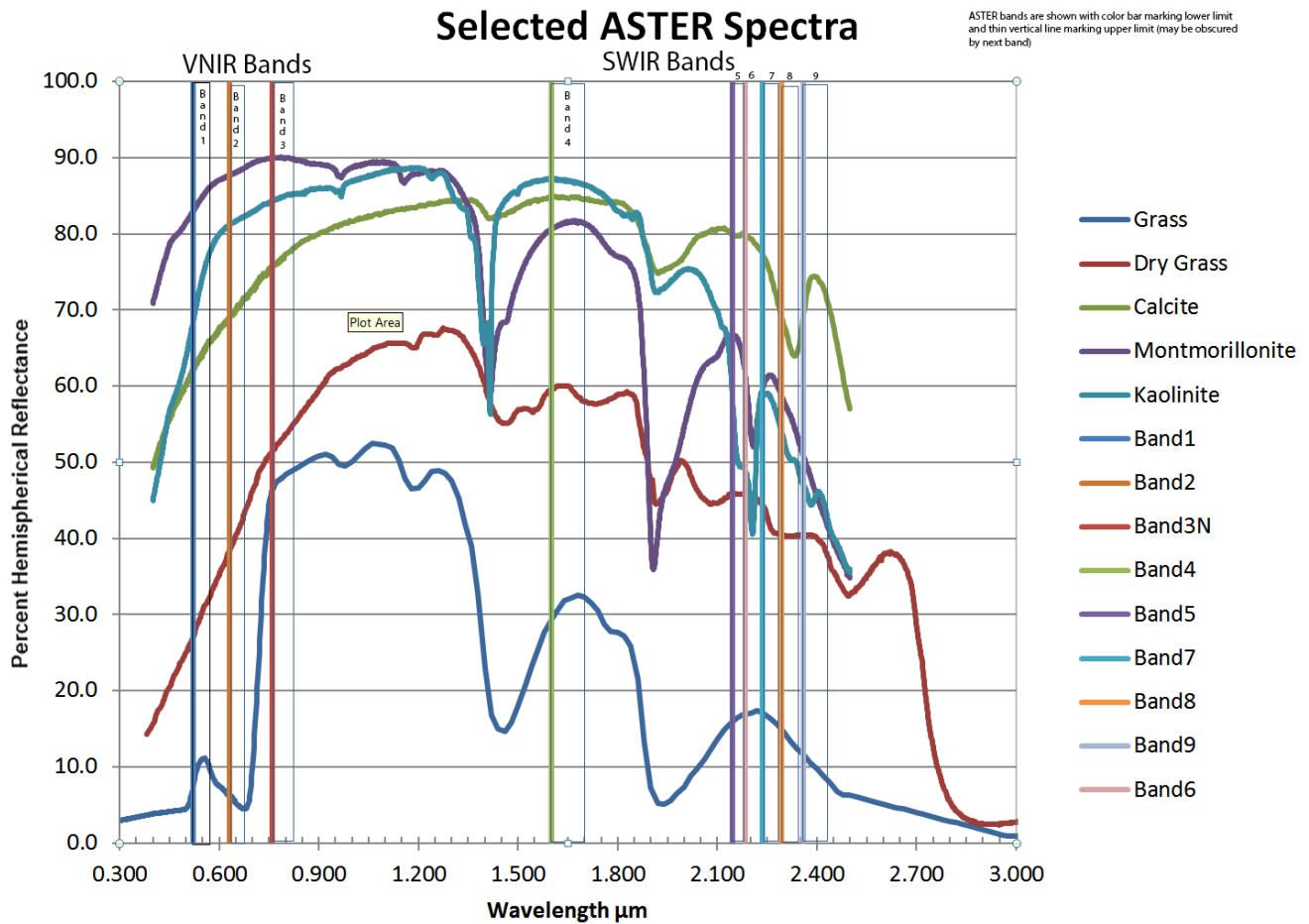


Figure 4a, Optical constants n and K for quartz, SiO<sub>2</sub>  
 Note the peak in n and K in the range of 8 to 10 μm.

In the graph that follows are depicted the 9 ASTER bands in VNIR and SWIR, along with representative reflectance curves for selected minerals and living and dry grass. Note the sharp *red edge* for living grass. Not depicted here are the 5 ASTER TIR bands.



### Mathematical Indexes

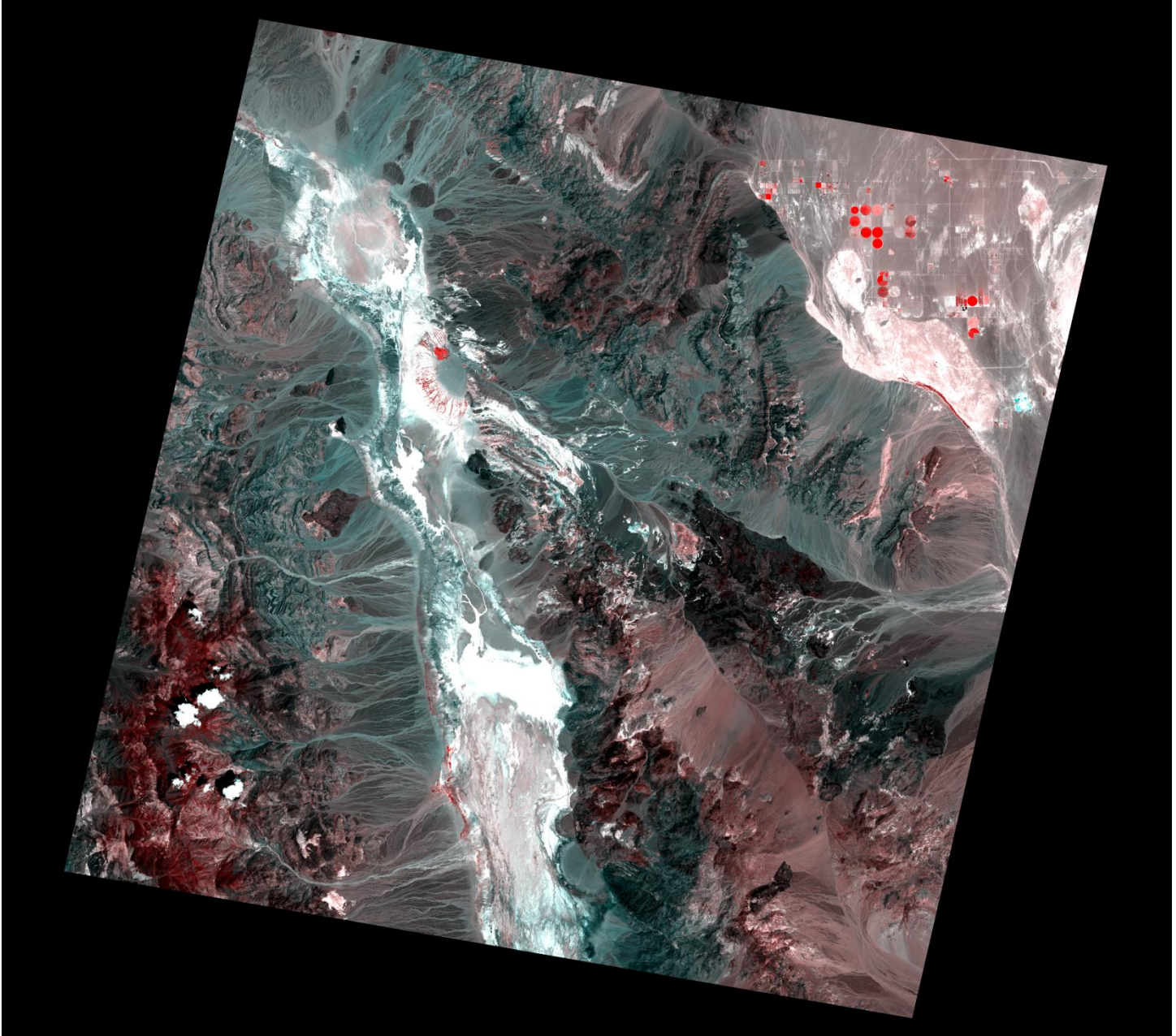
The differences in spectral reflectivity allow creation of images using various mathematical combinations of bands (Indexes) to enhance the conspicuity of a particular mineral type or other *theme* such as living vegetation health. Using ASTER band terminology (where B3 = Band 3), suitable indices (indexes) can include a Vegetation Index defined as B3/B2. This optimizes distinction between living and dry grass.

Indexes for particular minerals might include:

|                        | <b>Kaolinite Index<br/>(B4+B6)/B5</b> | <b>Montmor. Index<br/>(B5+B7)/B6</b> | <b>Calcite index 1<br/>(B7+B9)/B8</b> | <b>Calcite index 4<br/>(B6+B9)/B8<br/>(alternate version)</b> |
|------------------------|---------------------------------------|--------------------------------------|---------------------------------------|---|
| <b>Kaolin</b>          | 2.61                                  | 2.10                                 | 2.07                                  | 1.85  |
| <b>Montmorillonite</b> | 2.10                                  | 2.27                                 | 1.96                                  | 1.86  |
| <b>Calcite</b>         | 1.93                                  | 1.96                                 | 2.17                                  | 2.24  |

In addition, an SiO<sub>2</sub> index may be constructed using TIR bands, namely B14/B12.

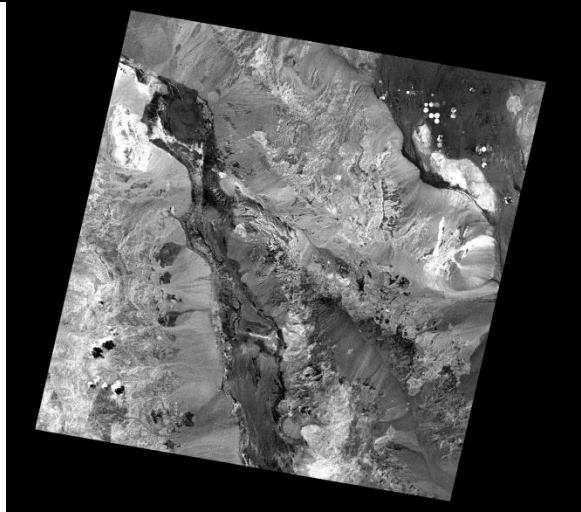
Here is a false color image of the Death Valley area using ASTER imagery:



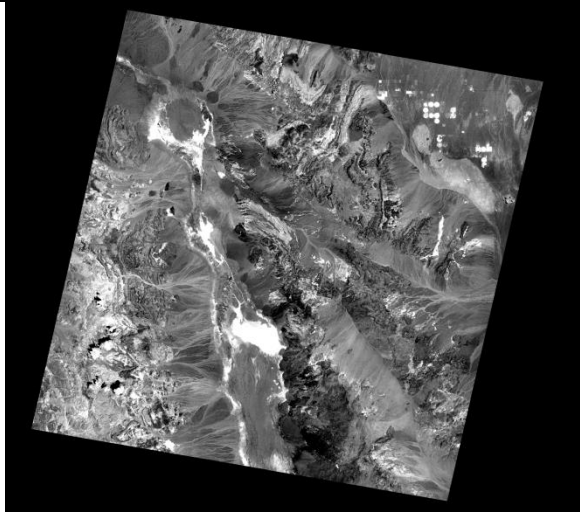
False color image with ASTER Band 3N shown as R, Band 2 as G, and Band 1 as B  
This has been rotated so that North is straight up.  
The slant of this and other ASTER images is determined by the  
sun synchronous oblique orbit of satellite Terra.

The following are some representative spectroscopic index images made of the Death Valley CA region derived from ASTER imagery, the ASTER Spectral Library, and indexes defined above. The grayscale images are each of a single image plane defined by the mineral index specified. Note how much the distributions of bright and dark values vary among these 4 images. The single index of values for  $\text{SiO}_2$  has additionally been mapped to a color scale termed “rainbow” (for which blue is lowest, red is highest in value).<sup>142</sup> Three different mineral indexes have been mapped to R-G-B in the image labeled ASTER\_SWIR\_rotated\_MontR\_KaolG\_CarbB.png.

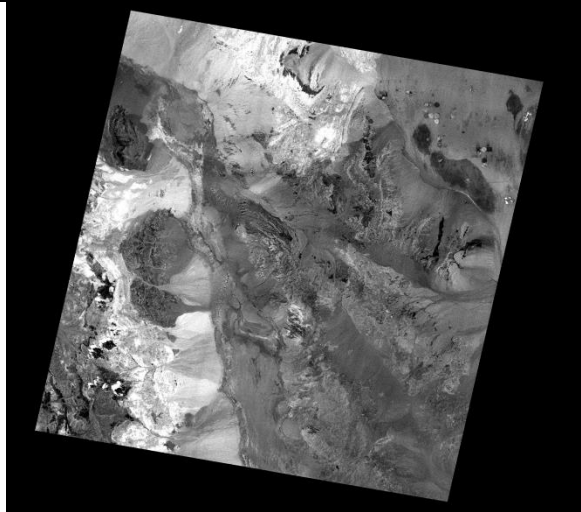
<sup>142</sup> <http://www.exelisvis.com/docs/LoadingDefaultColorTables.html>  
Page 74 of 110 RemoteSensing\_ESS421\_MCM\_Winter2015.docx



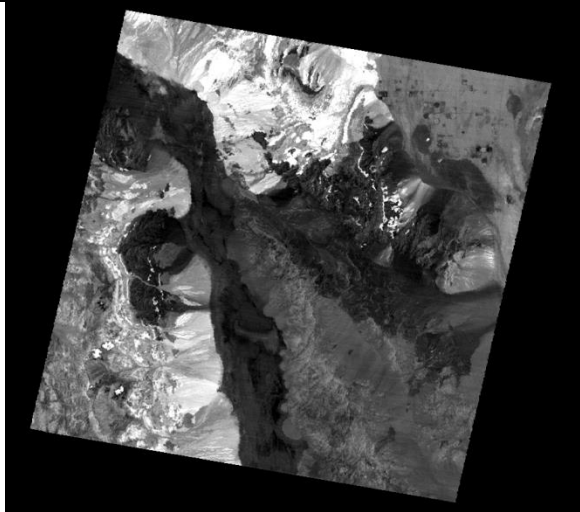
carbonate\_index2.png



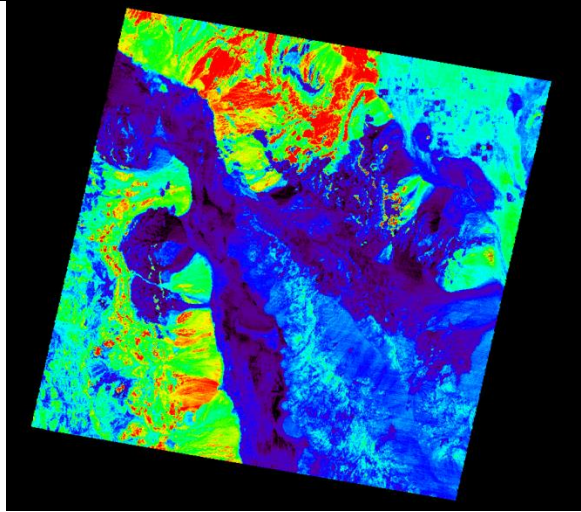
kaolinite\_index2.png



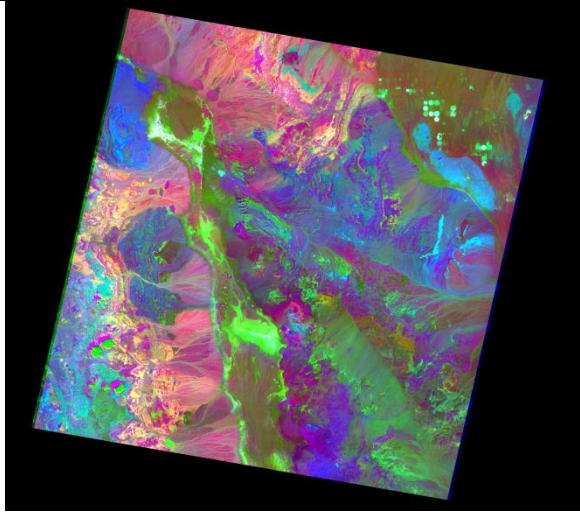
montmorillonite\_index2.png



TIR\_SiO2\_index\_grayscale.png



TIR\_SiO2\_index\_RainbowRGB.png

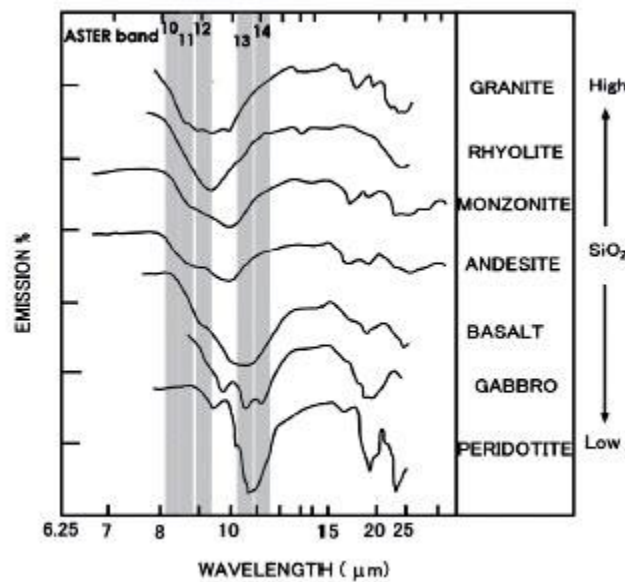


ASTER\_SWIR\_rotated\_MontR\_KaolG\_CarbB.png

Interpretation of the somewhat confusing multicolor 3 index image may be summarized as follows:

| Resulting Color | Interpretation  |
|-----------------|---|
| Red             | Montmorillonite alone   |
| Green           | Kaolinite alone   |
| Blue            | Carbonate (Calcite) alone   |
| Cyan            | Mix of Kaolinite G and Carbonate B in similar proportions               |
| Magenta         | Mix of Montmorillonite R and Carbonate B in similar proportions         |
| Yellow          | Mix of Montmorillonite R and Kaolinite G in similar proportions         |
| White           | Mix of Montmorillonite, Kaolinite, and Carbonate in similar proportions |
| Black           | Absence of Montmorillonite, Kaolinite, and Carbonate                    |

The SiO<sub>2</sub> index, which uses TIR bands 12 and 14, can be seen to serve a potentially useful role in distinguishing the following SiO<sub>2</sub> containing minerals.



Koyabashi et al state, “The absorption of TIR by silicate minerals is correlated to the molecular structure and silica content. For example, mafic minerals have large absorption at band 13 (11.5 μm) and felsic minerals at band 12 (9 μm)... Since igneous rocks are classified by the assemblages of silicate minerals and their quantity, the type of igneous rocks and approximate silica content can be indirectly inferred from the TIR absorption position. [The figure above] shows the emission spectrum of various igneous rocks in the TIR.”<sup>143</sup>

Koyabashi et al give the following equation for estimating SiO<sub>2</sub> weight %, for which R<sup>2</sup>=0.74 using TIR and VNIR band spectroscopic data. (These are somewhat different bands from the index mentioned above.)

$$\text{SiO}_2 \text{ (wt\%)} = 138.42 \times (\text{Band13}/\text{Band12}) + 34.61 \times (\text{Band2}/\text{Band1}) - 129.02$$

“where band 2/band1 is a proxy for the state of oxidation of iron in rock surface and hence a proxy for the weathering intensity.”

<sup>143</sup> Koyabashi C et al, *Andean geology* 37 (2): 433-441. July, 2010

[http://www.scielo.cl/scielo.php?pid=S0718-71062010000200009&script=sci\\_arttext](http://www.scielo.cl/scielo.php?pid=S0718-71062010000200009&script=sci_arttext)

## Ferric iron (Fe<sup>3+</sup>; B2/B1) index image using ASTER data

The graphical figure shown to follow [source of figure unknown] illustrates the reflectance of red sandstone compared to a blue/green colored shale. Note how the reflectance at the wavelengths of ASTER bands 1 and 2 are different between the two rock types. This index does not distinguish sandstone from shale, but simply can show that one rock type contains oxidized iron and the other does not.

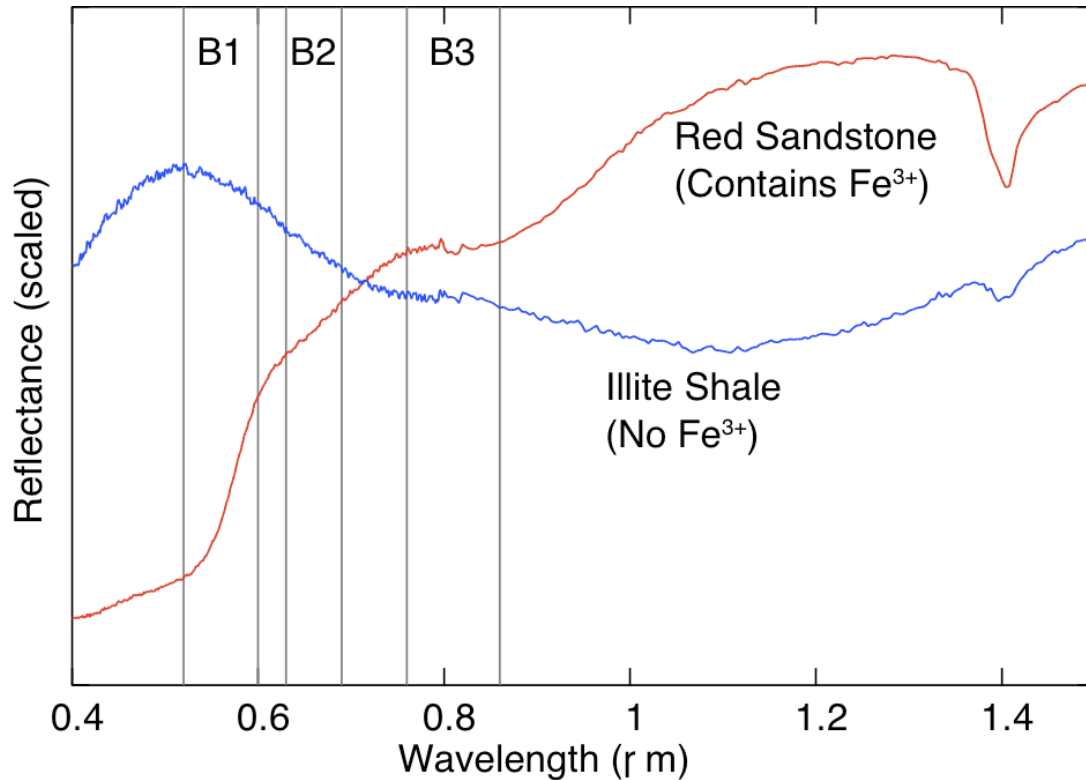
Relevant ASTER bands are:

Band 1: 0.52 - 0.60  $\mu\text{m}$  [Green]

→ Should be relatively dark with Ferric iron oxide Fe(III)<sub>2</sub>O<sub>3</sub>

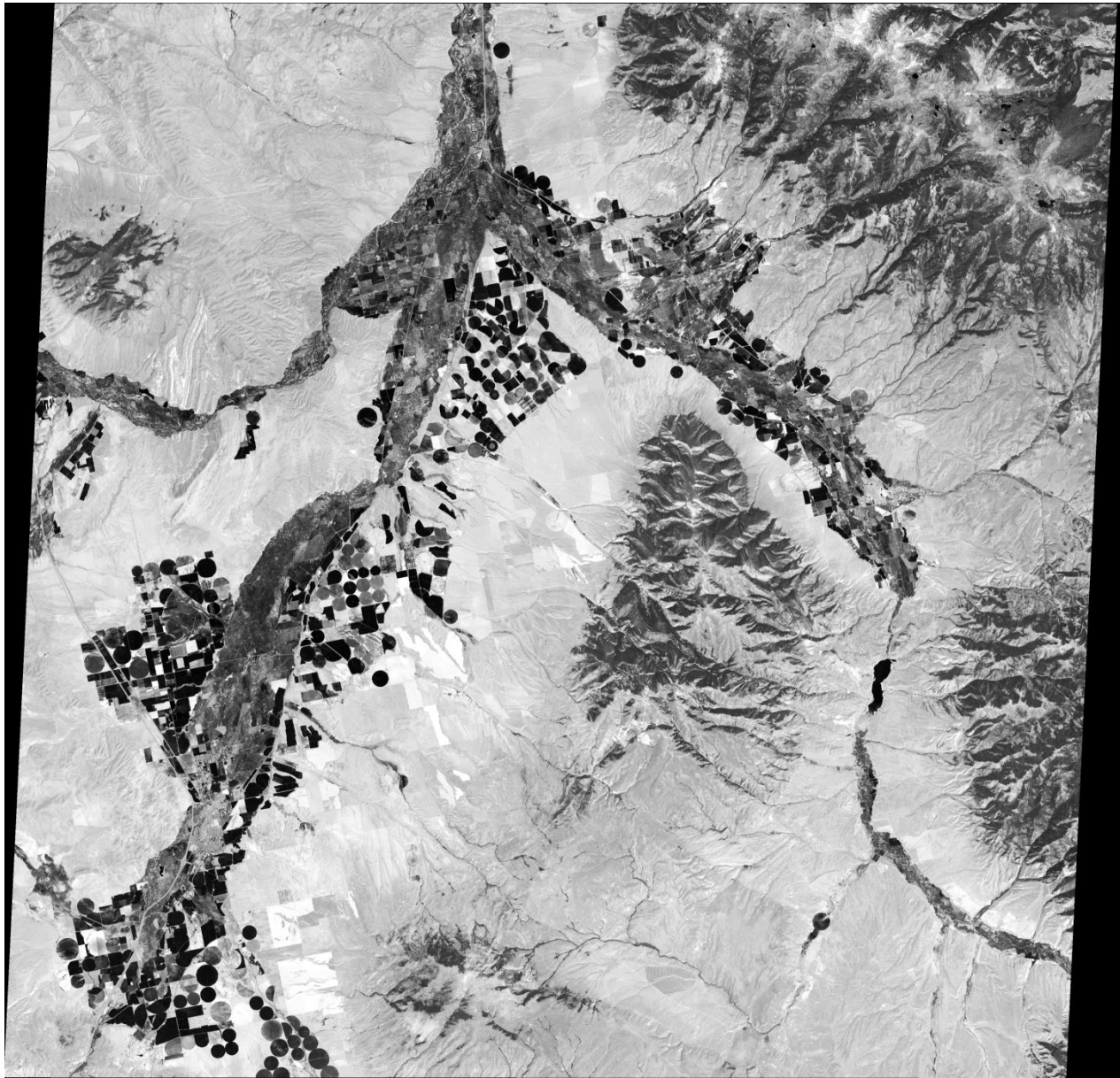
Band 2: 0.63 - 0.69  $\mu\text{m}$  [Red]

→ Should be brighter with Ferric iron oxide Fe(III)<sub>2</sub>O<sub>3</sub>



Viewing the graph, one expects B2/B1 to be higher for red sandstone and lower for Illite Shale.

An image using this index (ASTER Band2/Band 1) follows. This is used to highlight Ferric Iron oxide Fe(III)<sub>2</sub>O<sub>3</sub>. The region of interest does not have very distinctive absorptions in the short-wave infrared, unlike the Death Valley indices. However, iron oxides are prominent in some of the rocks in the area and can be used to distinguish some of the rock units.:



ASTER Band2/Band 1 index image for highlighting Ferric Iron oxide  $\text{Fe(III)}_2\text{O}_3$ ,  
Block Mountain MT region (Block Mountain is upper left)  
(ENVI Enhance > Linear 2%, Black bars trimmed, no other processing)

Of course, multispectral data with more and narrower bands or even better with hyperspectral data would allow even more precise index creation.

## Thermal Infrared Remote Sensing

See Jensen Chapter 8: Thermal Infrared Remote Sensing. Minimally summarized here, topic deserves more time than I have been able to devote to it. See also example in Spectroscopy topic of SiO<sub>2</sub> index imaging using ASTER data.

“Thermal infrared energy is emitted from all objects ... that have a temperature greater than absolute zero. Therefore, all features we encounter in the landscape on a typical day (the Sun, vegetation, soil, rocks, water, people) emit thermal infrared electromagnetic radiation... Humans sense thermal energy primarily through the sense of touch. Our eyes cannot detect differences in thermal infrared energy because they are primarily sensitive to short wavelength visible light from 0.4  $\mu\text{m}$  to 0.7  $\mu\text{m}$ . Our eyes are not sensitive to the reflective infrared (0.7 - 3.0  $\mu\text{m}$ ) or thermal infrared energy (3.0 - 14  $\mu\text{m}$ )... Engineers have developed detectors that are sensitive to thermal infrared radiation. These thermal infrared sensors allow humans to sense a previously invisible world as they monitor the thermal characteristics of the landscape.”<sup>144</sup>

Thermal IR RS requires very fast detectors cooled to low temperatures using liquid He or N:

- Indium antimonide (In:Sb), with peak sensitivity near 5  $\mu\text{m}$ , operating at  $T < 90$  K
- Mercury-doped germanium (Ge:Hg), with peak sensitivity near 10  $\mu\text{m}$ , operating at  $T \sim 73$  K (note: the boiling point of LN<sub>2</sub> is about 77 K at 1 atmosphere)
- Mercury-cadmium-telluride (Hg:Cd:Te) sensitive over the range from 8 to 14  $\mu\text{m}$ , operates at  $T > 150$  K (for 1.0 - 3.0  $\mu\text{m}$ ),  $\leq 120$  K (for 3 - 5  $\mu\text{m}$ ), and 50 - 80 K (for 8 - 12  $\mu\text{m}$ )
- Arsenic-doped Silicon (Si:As), sensitive over 12 - 25  $\mu\text{m}$ , operates at 10 K.

Spatial resolution and radiometric resolution are inversely related, and IFOV also plays a role in determining how many photons are captured per pixel.

In 1968, the [US] government declassified thermal infrared remote sensing systems that did not exceed a certain spatial resolution and temperature sensitivity.”

In 1980, NASA and the JPL developed the “thermal infrared multispectral scanner (TIMS) that acquires thermal infrared energy in six bands at wavelength intervals of  $< 1.0$   $\mu\text{m}$ . Landsat Thematic Mapper 4 and 5 sensors were launched on July 16, 1982 and March 1, 1984, respectively, and collected 120 x 120 m thermal infrared data (10.4 - 12.5  $\mu\text{m}$ ) along with two bands of middle infrared data... Today, the NOAA Geostationary Operational Environmental Satellite (GOES) collects thermal infrared data at a spatial resolution of 8 x 8 km for weather prediction. Full-disk images of the earth are obtained every 30 minutes both day and night by the thermal infrared sensor.” The Advanced Very High Resolution Radiometer AVHRR and its successor, Visible Infrared Imaging Radiometer Suite VIIRS, are important current instruments which include Thermal IR (discussed above).

The analyst must think thermally in order to interpret TIR images. Thermal IR (3 to 14  $\mu\text{m}$ ) is emitted energy, not reflected energy (which is found in 0.7 to 3  $\mu\text{m}$ ). Natural and man-made materials can differ in emissivity from 1.0. Their emission curve (i.e., spectral radiant exitance) may deviate substantially from that of a perfect *blackbody*, thus they are called *graybodies*. Surface emissivity depends variably on surface color, roughness, moisture content, soil compaction, field of view, viewing angle, as well as chemical composition and wavelength.

The Earth is like a  $\sim 300$  K blackbody and the Sun appears as a 6000 K blackbody. The “relative radiated energy” given off by a hotter blackbody is always greater for all wavelengths than by a colder blackbody (provided emissivities are close to 1). The following is also true: “Thermal or longwave infrared (TIR or LWIR) light includes wavelengths between 8,000 and 15,000 nanometers. Most of the energy in this part of the spectrum is emitted (not reflected) by the Earth as heat, so it can be observed both day and night.”<sup>145</sup>

Two different rocks with the same kinetic temperature  $T_{\text{kin}}$  but with different emissivities can appear to have different temperatures  $T_{\text{rad}}$  when remotely sensed by a thermal radiometer. Adjustment in remote sensing of temperature must make use Kirchoff’s radiation law, which may be paraphrased: “in the infrared portion of

---

<sup>144</sup> Jensen JRJPPT *Thermal Infrared Remote Sensing* 2007, as are the immediately following quotes and figure

<sup>145</sup> <http://earthobservatory.nasa.gov/Features/FalseColor/page5.php>

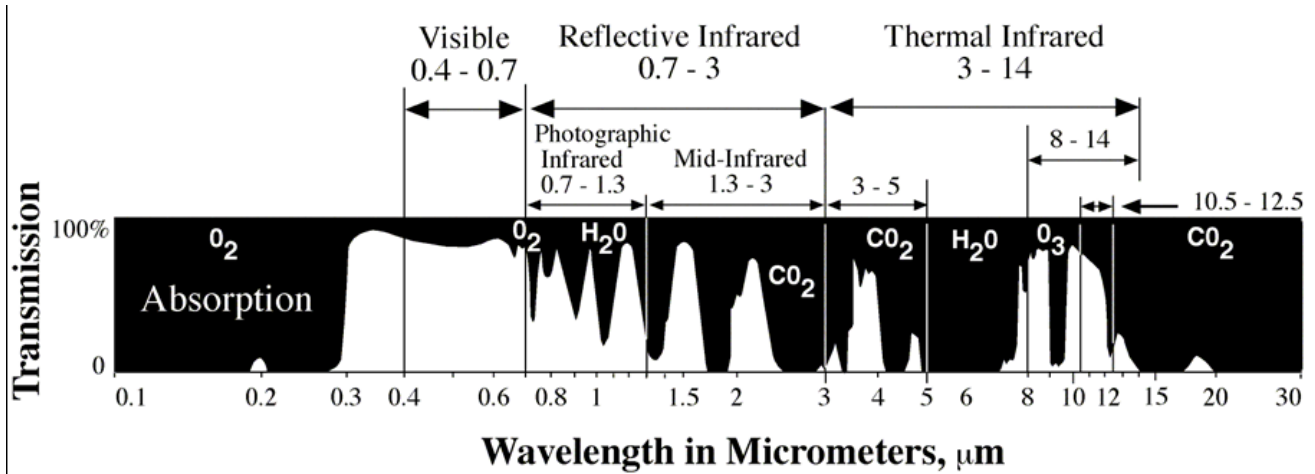
the spectrum the spectral emissivity of an object generally equals its spectral absorptance”, or  $\alpha_\lambda \approx \epsilon_\lambda$  (in thermal equilibrium and for real surfaces). This can also be expressed as, “good absorbers are good emitters and good reflectors are poor emitters [thus the latter can make a good emergency blanket].” “If reflectivity increases then emissivity must decrease. If emissivity increases then reflectivity must decrease.”<sup>146</sup> Thus, the relationship between  $T_{kin}$  and  $T_{rad}$  is given by

$$T_{rad} = \epsilon \sigma T_{kin}^{1/4}$$

The temperature of terrain is affected not only by solar irradiance and exitance but also by thermal inertia P, which depends on thermal conductivity K, density, and Thermal capacity c.

Water has strong TIR absorption and high TIR emissivity, thus it reflects little TIR. Mirror-like metal surfaces that reflect light well have low emissivities.

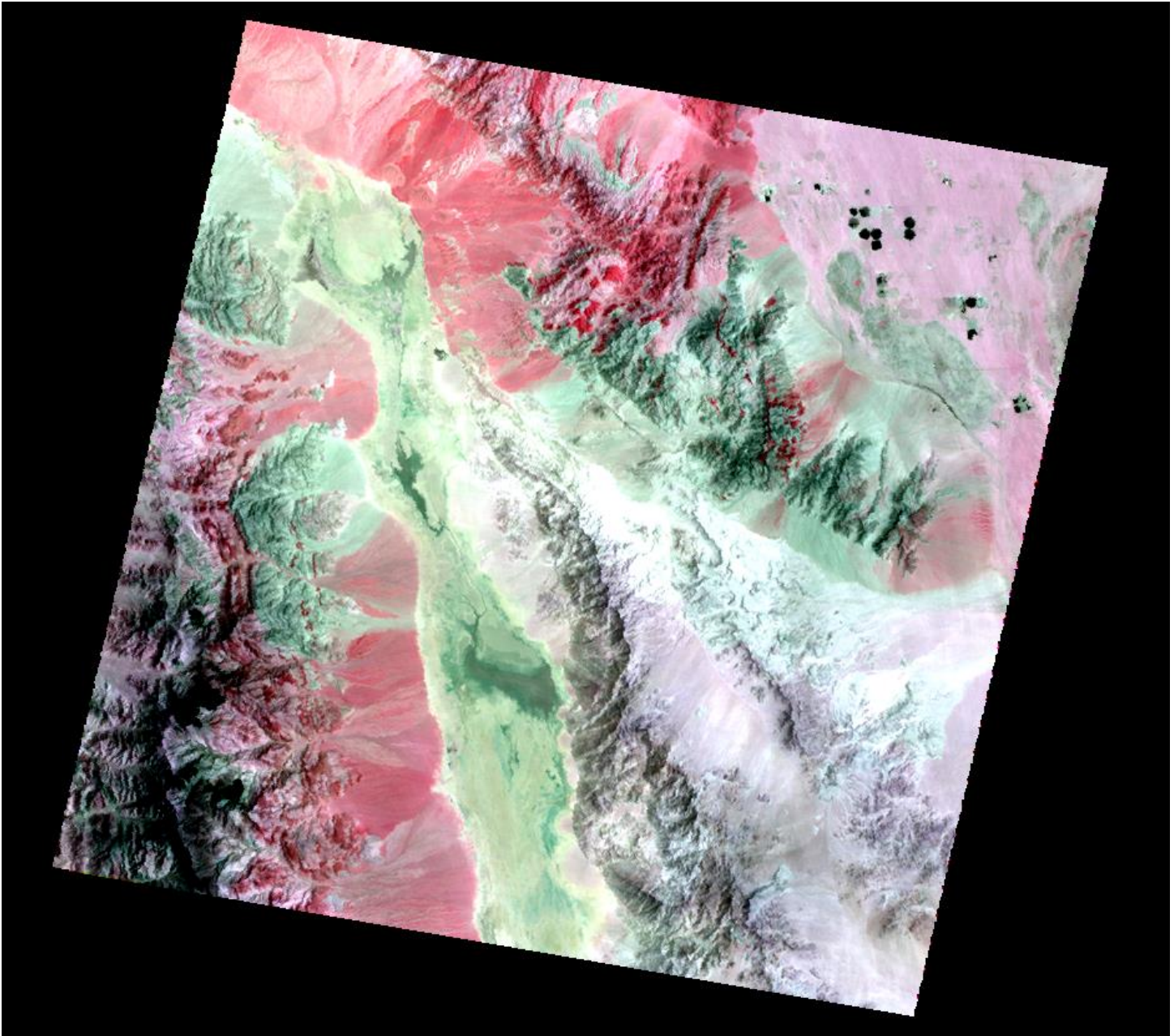
The absorption of Thermal IR by the atmosphere (specifically, by ozone, water, and CO<sub>2</sub>) is an important consideration:



Atmospheric “Windows” in the EM Spectrum, including Thermal IR (3 to 14 μm)

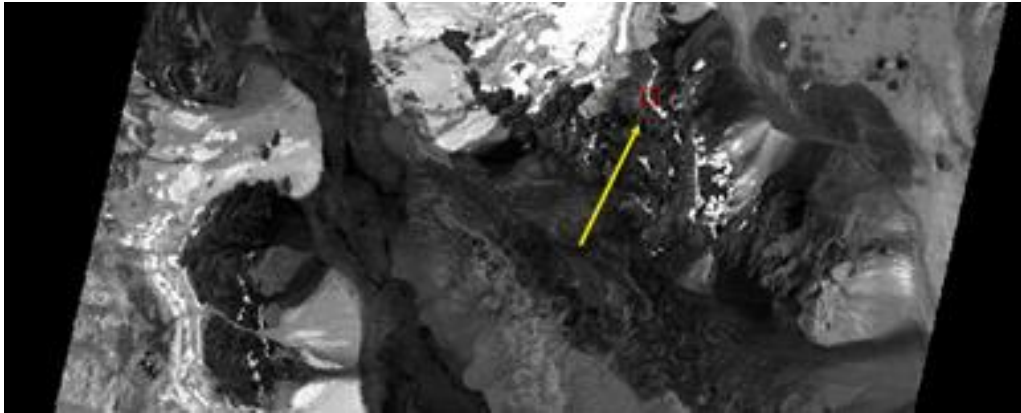
<sup>146</sup> *ibid.*

Here follows another example of Thermal IR imaging, in which images at 3 different ASTER TIR band of Death Valley CA are mapped to a single R, G, and B false color image:

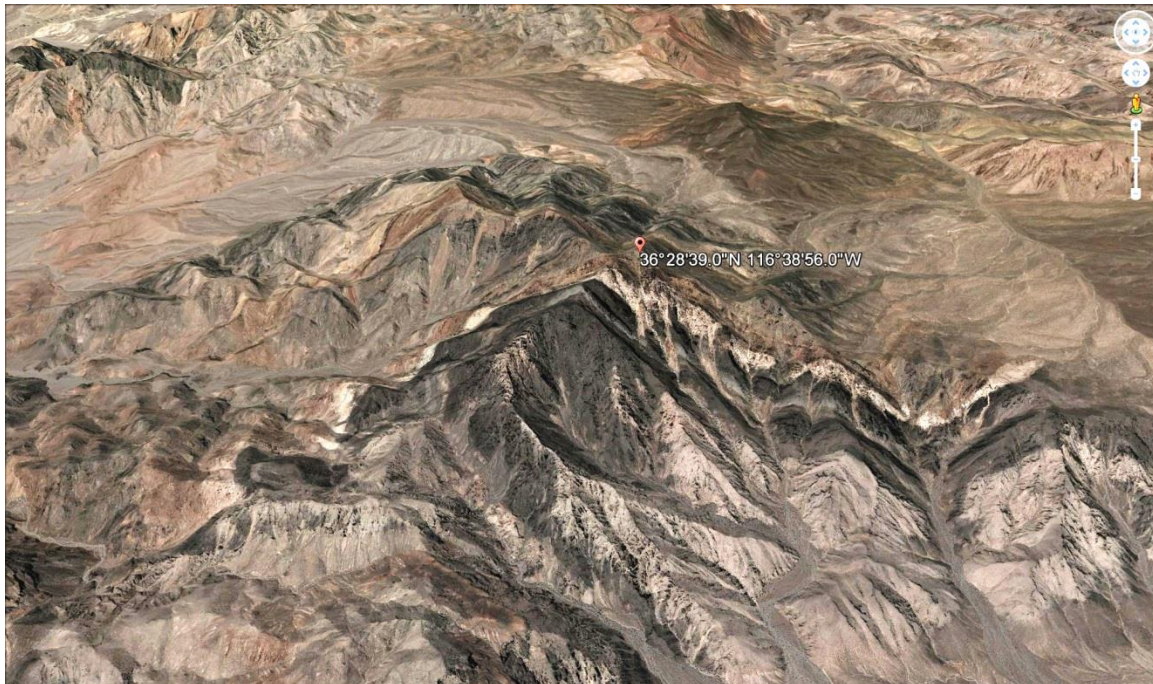


ASTER image of Death Valley area  
False color, TIR band 14 mapped as R, band 12 as G, and band 10 as blue.

A high signal curving structure in the SiO<sub>2</sub> TIR index image is seen to correspond with a band of quartzite in the Funeral mountains near Death Valley:



SiO<sub>2</sub> Index image (TIR bands) with approximate area of lat. and long. marked in small red cursor box. Bright curving thin line passing through red box displays high SiO<sub>2</sub> signal.



Oblique view facing W of the prominent bright appearing SiO<sub>2</sub> index band (visible light, screen capture from Google Earth, cropped and contrast enhanced).

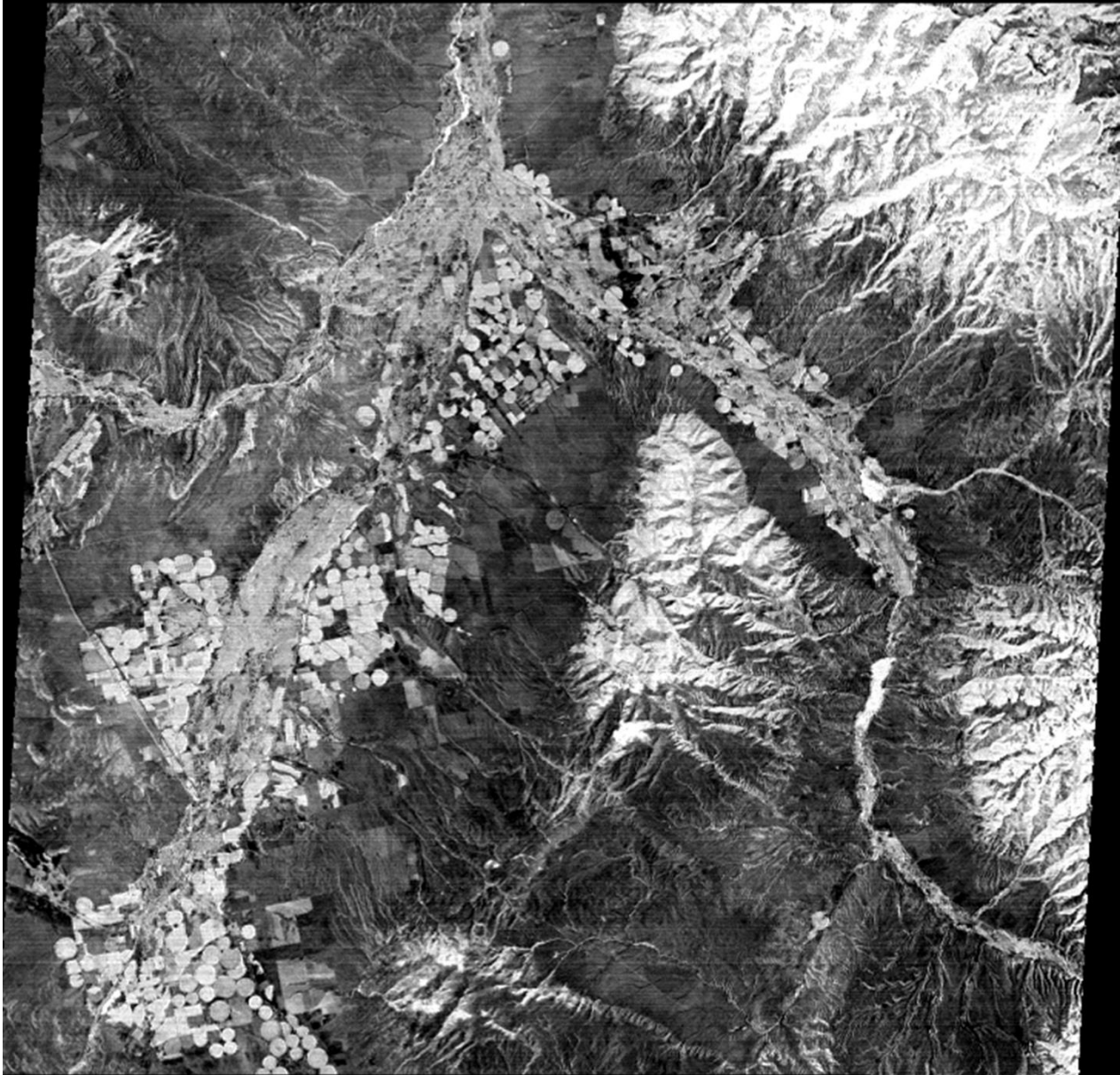
The visible light band is about 2 miles long.

This is probably an exposed band of high quartz material or quartzite. The Stirling, Zabriskie, Wood Canyon Formation, and Eureka quartzite formations are all found in the area, but I am unsure which band this might be.



A different oblique view (facing generally W) of a bright appearing visible light structure, higher magnification (screen capture from Google Earth, cropped and contrast enhanced)

Here is another example of a SiO<sub>2</sub> index image using ASTER TIR bands 14 and 12:



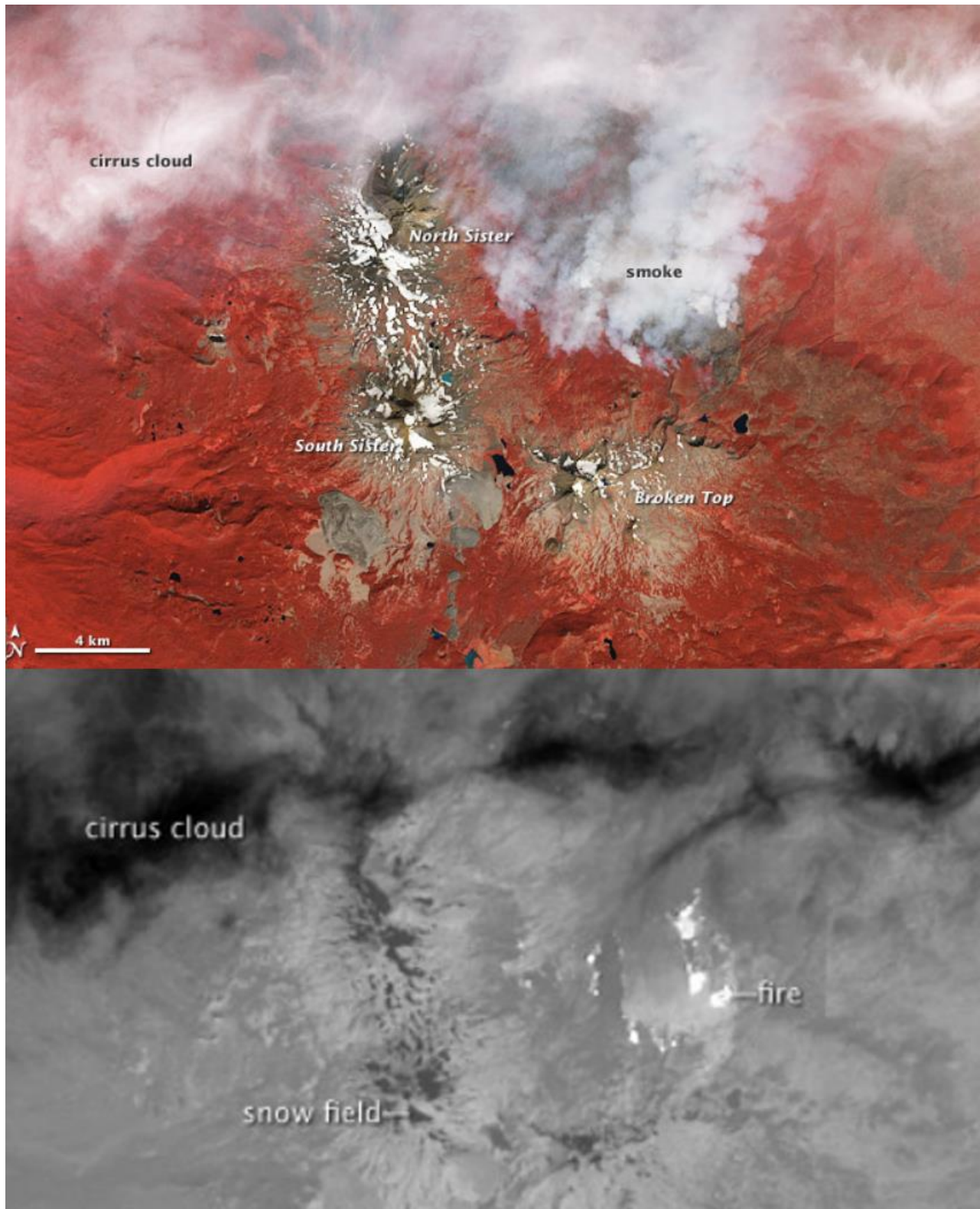
ASTER SiO<sub>2</sub> Band 14 / Band 12 index image , Block Mountain MT region  
(Enhance > Linear 2%, Black bars trimmed, no other processing)

#### VNIR and TIR images of the Pole Creek fire in OR

- ASTER images of the Pole Creek OR fire in false color VNIR and in grayscale TIR in Deschutes National Forest: “In the top image, vegetated areas appear bright red; snow and ice looks white; and clouds are a wispy off-white. Exposed rock and barren land near the summits of the mountains are shades of brown. Smoke billowing from the fire appears gray.”

“A view of the same area created from ASTER’s thermal band (bottom) shows how temperature varies across the scene. Warmer temperatures are shown with brighter colors [whiter], and cooler temperatures are darker. Actively-burning hot spots from the Pole Creek fire are the hottest features in the image, while high-floating cirrus clouds near North Sister are the coldest... The smoke is transparent to ASTER’s thermal band because smoke plumes consist of ash particles and other combustion products so fine that they are easily penetrated by the relatively long wavelengths of thermal infrared radiation. By contrast, ASTER cannot see through

clouds [in VNIR or TIR] because they tend to have larger particles that thermal infrared cannot easily pass through.”<sup>147</sup>



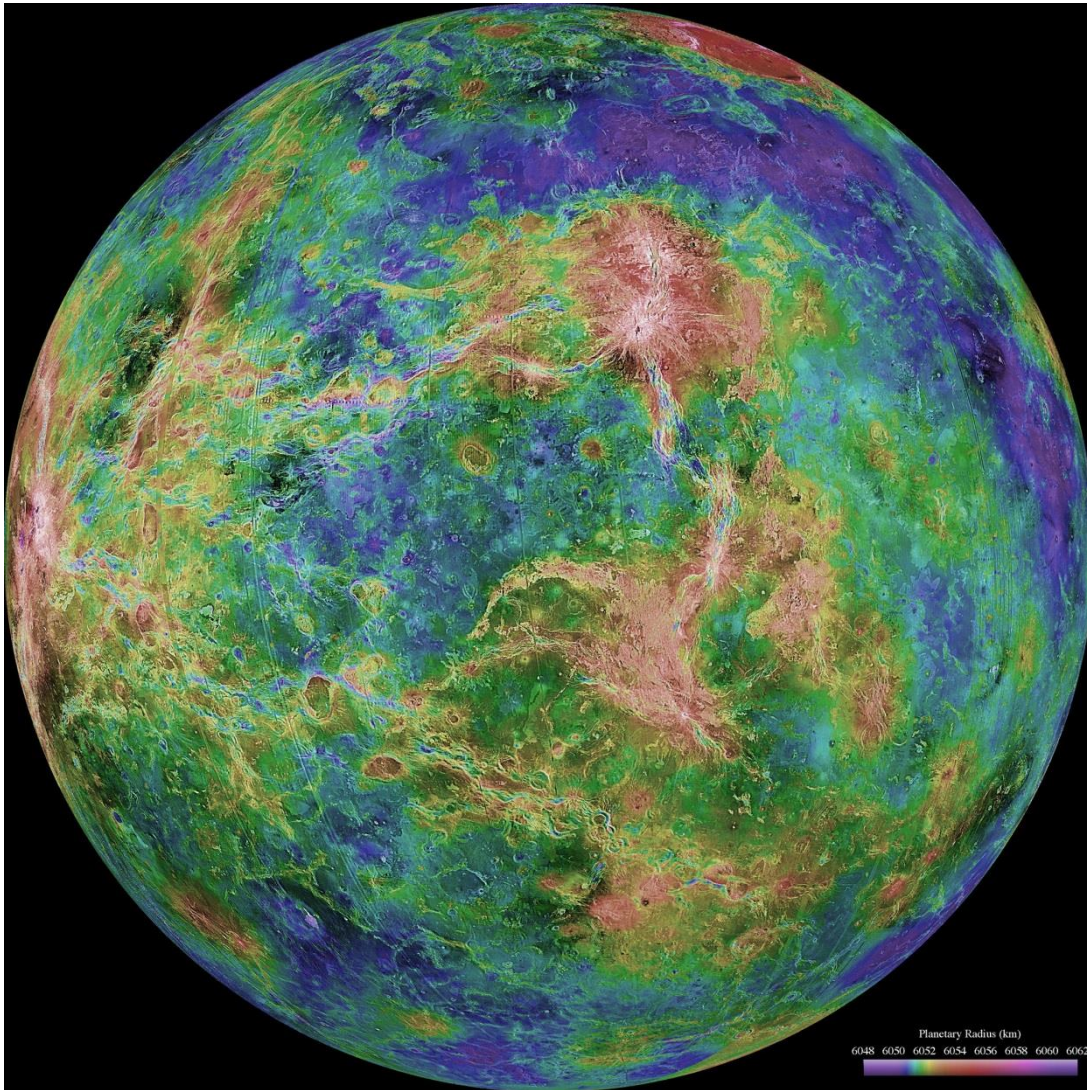
Band information about the new generation GOES weather satellites, which include TIR thermal imaging, is summarized above under GOES Geostationary Operational Environmental Satellites.

<sup>147</sup> <http://earthobservatory.nasa.gov/IOTD/view.php?id=79306>

## Active and Passive Microwave (RADAR) Remote Sensing

See Jensen Chapter 9: Active and Passive Microwave Remote Sensing.

The following is constructed from the 1990-1994 Magellan mission. It is a Synthetic Aperture Radar (SAR) image of Venus, with radar operating at 2.385 GHz (12.6 cm, thus in S band) with a PRF of 4400-5800 Hz. It is "a mosaic of the Magellan images (most with illumination from the west) forms the image base... Gaps in the Magellan coverage were filled with images from the Earth-based Arecibo radar in a region centered roughly on 0 degree latitude and longitude, and with a neutral tone elsewhere (primarily near the south pole). The composite image was processed to improve contrast and to emphasize small features, and was color-coded to represent elevation."<sup>148</sup>



The term *microwave* signifies "small" (shorter wavelengths  $\lambda$ , 1 mm – 1 meter), as compared to waves used in typical radio broadcasting (1 mm – 100,000 km), but quite long in comparison to visible light  $\lambda$  (0.4 to 0.7  $\mu\text{m}$ ) and IR (0.7 to 1000  $\mu\text{m}$  [1 mm]).

<sup>148</sup> <http://photojournal.jpl.nasa.gov/catalog/PIA00160>

RS Systems can be *passive*, recording electromagnetic energy that is reflected (e.g., blue, green, red, and near-infrared light) or emitted (e.g., thermal infrared energy) from the surface of the Earth. Passive microwave has been used to map the Amazon Basin in 85 GHz radiation.<sup>149</sup>

More common are active remote sensing systems that are not dependent on the Sun's electromagnetic energy or the thermal properties of the Earth. "Active remote sensors create their own electromagnetic energy that 1) is transmitted from the sensor toward the terrain (and is largely unaffected by the atmosphere), 2) interacts with the terrain producing a backscatter of energy, and 3) is recorded by the remote sensor's receiver."<sup>150</sup>

Radar is widely used as an active RS techniques (along with LiDAR and SONAR). RADAR was developed starting in 1922. Active microwave (RADAR) RS, based on the transmission of long-wavelength microwaves (e.g., 3 – 25 cm) through the atmosphere and then recording the amount of energy back-scattered from the terrain. Microwave RS includes *Real Aperture Side-Looking Airborne Radar (SLAR)* systems, *Synthetic Aperture Radar (SAR)*, and *Interferometric synthetic aperture radar (InSAR/IfSAR)*.

The following<sup>151</sup> are some of the radar/microwave band EM wavelengths and frequencies (boldface are the most commonly used in RS per Jensen p. 294):

| <b>Band name</b> | <b>Frequency range</b> | <b>Wavelength range</b> | <b>Notes</b>  |
|------------------|------------------------|-------------------------|---|
| HF               | 3–30 MHz               | 10–100 m                | Coastal radar systems, over-the-horizon radar (OTH) radars; 'high frequency'  |
| VHF              | 30–300 MHz             | 1–10 m                  | Very long range, ground penetrating; 'very high frequency'  |
| UHF              | 300–1000 MHz           | 0.3–1 m                 | Very long range (e.g. ballistic missile early warning), ground penetrating, foliage penetrating; 'ultra high frequency'   |
| <b>P</b>         | < 300 MHz              | > 1 m                   | 'P' for 'previous', applied retrospectively to early radar systems; essentially HF + VHF  |
| <b>L</b>         | 1–2 GHz                | <b>15–30 cm</b>         | Long range air traffic control and surveillance; 'L' for 'long'   |
| <b>S</b>         | 2–4 GHz                | <b>7.5–15 cm</b>        | Moderate range surveillance, Terminal air traffic control, long-range weather, marine radar; 'S' for 'short'  |
| <b>C</b>         | 4–8 GHz                | <b>3.75–7.5 cm</b>      | Satellite transponders; a compromise (hence 'C') between X and S bands; weather; long range tracking  |
| <b>X</b>         | 8–12 GHz               | <b>2.5–3.75 cm</b>      | Missile guidance, marine radar, weather, medium-resolution mapping and ground surveillance; in the USA the narrow range 10.525 GHz ±25 MHz is used for airport radar; short range tracking. Named X band because the frequency was a secret during WW2. Used for orbital and suborbital imaging radars. |
| <b>Ku</b>        | 12–18 GHz              | 1.67–2.5 cm             | High-resolution, also used for satellite transponders, frequency under K band (hence 'u')   |
| <b>K</b>         | 18–24 GHz              | 1.11–1.67 cm            | From German kurz, meaning 'short'; limited use due to absorption by water vapour, so Ku and Ka were used instead for surveillance. K-band is used for detecting clouds by meteorologists, and by police for detecting speeding motorists. K-band radar guns operate at 24.150 ± 0.100 GHz.              |
| <b>Ka</b>        | 24–40 GHz              | 0.75–1.11 cm            | Mapping, short range, airport surveillance;   |

<sup>149</sup> Special Sensor Microwave Imager (SSM/I). The SSM/I is a seven-channel, four-frequency, orthogonally polarized, passive microwave radiometric system that measures atmospheric, ocean and terrain microwave brightness temperatures at 19.35, 22.2, 37.0, and 85.5 GHz.

[https://nsidc.org/data/docs/daac/ssmi\\_instrument.gd.html](https://nsidc.org/data/docs/daac/ssmi_instrument.gd.html)

<sup>150</sup> Jensen JRJPPT 2009.

<sup>151</sup> <http://en.wikipedia.org/wiki/Radar>

|    |            |            |  |
|----|------------|------------|--|
|    |            |            | frequency just above K band (hence 'a') Photo radar, used to trigger cameras which take pictures of license plates of cars running red lights, operates at $34.300 \pm 0.100$ GHz.   |
| mm | 40–300 GHz | 1.0–7.5 mm | Millimetre band, subdivided as below. The frequency ranges depend on waveguide size. Multiple letters are assigned to these bands by different groups. These are from Baytron, a now defunct company that made test equipment. |
| V  | 40–75 GHz  | 4.0–7.5 mm | Very strongly absorbed by atmospheric oxygen, which resonates at 60 GHz.   |
| W  | 75–110 GHz | 2.7–4.0 mm | Used as a visual sensor for experimental autonomous vehicles, high-resolution meteorological observation, and imaging.   |

Microwave  $\lambda$  are usually expressed in cm. Radar is transmitted in pulses which are of  $\mu$ sec duration.

*Range resolution* depends on pulse length  $\tau$ , depression angle  $\gamma$ , H, etc.

*Azimuth resolution* is determined by the width of the terrain illuminated by the radar beam [in the front to back direction of the laterally directed beam]. “In real aperture (brute force) radars a shorter wavelength pulse will result in improved azimuth resolution. Unfortunately, the shorter the wavelength, the poorer the atmospheric and vegetation penetration capability.... Fortunately, the beam width is also inversely proportional to antenna length (L). This means that the longer the radar antenna, the narrower the beam width and the higher the azimuth resolution...”<sup>152</sup> Azimuth resolution is given by  $S\lambda/L$ , where S is slant-range distance to the point of interest and L is the antenna length.

Advantages of microwave/RADAR RS include:<sup>153</sup>

- Active microwave energy penetrates clouds and can be an all-weather remote sensing system.
- Synoptic views of large areas, for mapping at 1:25,000 to 1:400,000; cloud-shrouded countries may be imaged.
- Coverage can be obtained at user-specified times, even at night.
- Permits imaging at shallow look angles, resulting in different perspectives that cannot always be obtained using aerial photography.
- Senses in wavelengths outside the visible and infrared regions of the electromagnetic spectrum, providing information on surface roughness, dielectric properties, and moisture content.
- May penetrate vegetation, sand, and surface layers of snow. For instance, a hidden channel of the Nile was apparent under the sand with SIR-C imaging.
- Has its own illumination, and the angle of illumination can be controlled.
- Enables resolution to be independent of distance to the object, with the size of a resolution cell being as small as 1 x 1 m.
- Images can be produced from different types of polarized energy
  - HH = Like polarized Horizontal transmit/Horizontal receive
  - HV = Cross polarized Horizontal out / Vertical in
  - VV = Like polarized Vertical transmit/Vertical receive
  - VH = Cross polarized Vertical out / Horizontal in).
- May operate simultaneously in several wavelengths (frequencies) and thus has multi-frequency potential. (For instance, imaging of a pine forest in L, C, and X bands returns signal from the top of the canopy in the X 3 cm band, from the upper- and mid-portions in the C 5.8 cm band, and the entire tree structure in the L 23.5 cm band.)

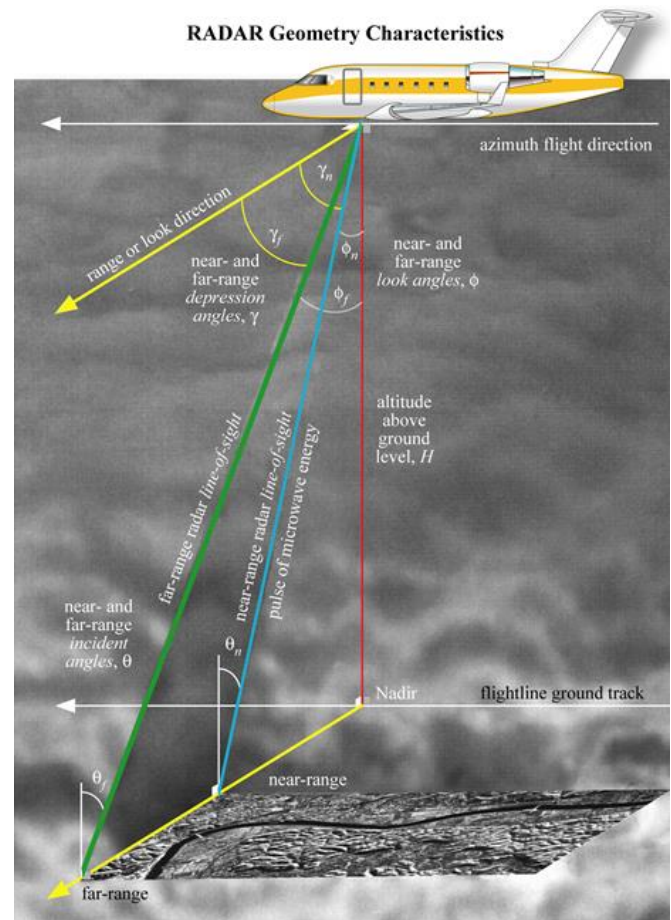
<sup>152</sup> Jensen JRJPPT 2009

<sup>153</sup> Jensen JRJPPT 2009, including image “RADAR Geometry Characteristics”

- Can measure ocean wave properties, even from orbital altitudes.
- Can produce overlapping images suitable for stereoscopic viewing and radargrammetry.
- Supports interferometric operation using two antennas for 3-D mapping, and analysis of incident-angle signatures of objects.

Radar Imaging Nomenclature is summarized in the diagram and the following list:<sup>154</sup>

- Nadir [vertical downward direction]
- azimuth flight direction [forward direction directly overlying the *flightline ground track*]
- range (near and far) [ground extent of imaging]
- depression angles ( $\gamma$ ) formed with respect to horizontal look direction
- look angles ( $\phi$ ) formed with respect to vertical
- incidence angle ( $\theta$ ) (angle between incident beam and vertical). (Not the same as the *local incident angle* formed between the beam and the *local slope angle*  $\alpha$  formed between the ground slope and the horizontal.)
- altitude above-ground-level,  $H$
- polarization (backscattering can alter polarization)



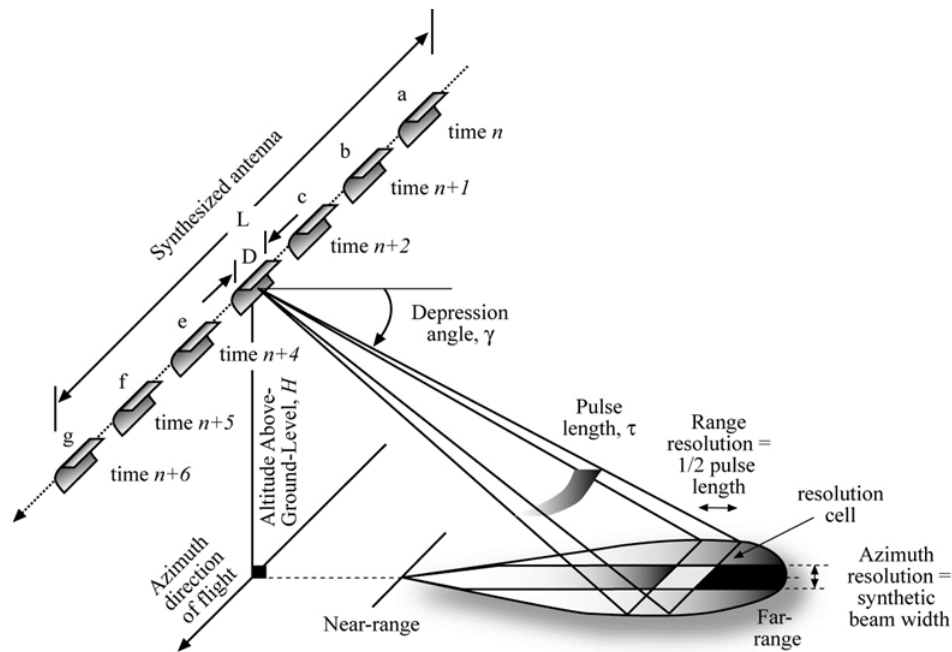
A variety of physical phenomena and/or artifacts can be found and must be considered, including

- radar foreshortening: All terrain that has a slope inclined toward the radar will appear compressed or foreshortened relative to slopes inclined away from the radar.
- image layover (an extreme case of image foreshortening, in which for instance the top of a mountain can appear closer than its base, thus it “layover” the base)
- shadowing (portions of the ground are in the beam’s shadow and totally obscured)
- Image speckle (caused by constructive and destructive interference, and hence random bright and dark areas in a radar image. The speckle can be reduced by processing separate portions of an aperture and recombining these portions so that interference does not occur. This process, called multiple looks or non-coherent integration, aids interpretation but reduces resolution.)
- Surface roughness (measured in cm) strongly influences the strength of the returning signal. A surface is rough if the modified Rayleigh criteria give  $h > \lambda / (4.4 \sin \gamma)$  where  $h$  is the height in cm of surface objects and  $\gamma$  is the depression angle. Rough surfaces return a strong signal. The surface is smooth if  $h < \lambda / (25 \sin \gamma)$  and acts as a specular reflector, returning a weak or nonexistent signal.
- The Cardinal Effect can cause bright corner-type reflection from cities in which all streets and structures are aligned N-S and E-W (e.g., Santa Monica and San Fernando), compared to cities with more randomly oriented structures.

**Synthetic aperture radar (SAR)** A major advance in radar remote sensing has been the improvement in azimuth resolution through the development of *synthetic aperture radar (SAR)* systems. The antenna length  $L$  is effectively much longer through synthesis electronically of a longer aperture. “Like a brute force or real aperture radar, a synthetic aperture radar also uses a relatively small antenna (e.g., 1 m) that sends out a

<sup>154</sup> Jensen JRJPPT 2009

relatively broad beam perpendicular to the aircraft. The major difference is that a greater number of additional beams are sent toward the object. Doppler principles are then used to monitor [and separate] the returns from all these additional microwave pulses to synthesize the azimuth resolution to become one very narrow beam.”<sup>155</sup>



Some of the Microwave RS systems have included:

- SASS Radar scatterometer aboard Seasat (launched 1978)
- *ALT-A, ALT-B* on TOPEX/ Poseidon launched 1992 (Radar altimeters for ocean topography)
- *Poseidon-1 and Poseidon-2* Radar altimeters aboard TOPEX/Poseidon (launched 1992) and Jason-1 (launched 2001), resp.
- NSCAT radar scatterometer aboard ADEOS-1 (launched 1996, failed 1997)
- SeaWinds radar scatterometer aboard QuikSCAT 1999 and ADEOS-2 2002.
- *ERS-1 RA and SAR* (European remote sensing satellite SAR system 1991)
- *ERS-2 RA and SAR* (European remote sensing satellite SAR system 1995)
- *JERS-1* (Japanese Earth Resources Satellite 1 SAR system 1992)
- RADARSAT-1 SAR system (1995)
- RADARSAT-2 SAR system (2007)
- ASAR *Advanced Synthetic Aperture Radar* aboard Envisat (, 2002 - 2012)
- *PALSAR Phased Array type L-band Synthetic Aperture Radar* is an L-band SAR aboard Advanced Land Observing Satellite (ALOS) 2006-2011 )
- UAVSAR *Uninhabited Aerial Vehicle Synthetic Aperture Radar*, airborne, launched 2007).
- *Precipitation Radar PR* phased-array radar, and *TRMM Microwave Imager TMI*, aboard Tropical Rainfall Measuring Mission TRMM launched 1997.<sup>156</sup>
- *Special Sensor Microwave Imager SSM/I* aboard multiple Defense Meteorological Satellite Program (DMSP) Block 5D-2 satellites<sup>157</sup> F8 to F16 (1987 to 2003) operating with passive microwaves at 19.35, 22.235, 37.0 and 85.5 GHz<sup>158</sup>
- *AMSR Advanced Microwave Scanning Radiometer* passive microwave on ADEOS-2
- *AMSR-E Advanced Microwave Scanning Radiometer-EOS* passive microwave aboard Aqua 2006.
- *Shuttle SIR-C/X-SAR (Spaceborne Imaging Radar C/X band Synthetic Aperture Radar*, 1994 and 1995, flown on Space Shuttle Endeavour).<sup>159</sup> SIR-C ... collected data polarized both horizontally

<sup>155</sup> Jensen PPT 2009, including image of SAR imaging technique

<sup>156</sup> <http://trmm.gsfc.nasa.gov/>

<sup>157</sup> [https://nsidc.org/data/docs/daac/ssmi\\_instrument.gd.html](https://nsidc.org/data/docs/daac/ssmi_instrument.gd.html)

<sup>158</sup> [http://en.wikipedia.org/wiki/Special\\_sensor\\_microwave\\_imager](http://en.wikipedia.org/wiki/Special_sensor_microwave_imager)

and vertically on C and L bands. X-SAR used a slotted waveguide antenna to collect vertically polarized signals using X-band radar. Preceding missions were *SIR-A* and *SIR-B* (thus “SIR-C” does not refer to C band).

- *Shuttle Radar Topography Mission SRTM 2000*, generated the most complete high-resolution digital topographic database until the ASTER GDEM in 2009. SRTM consisted of a specially modified radar system that flew on board the Space Shuttle Endeavour during the 11-day STS-99 mission in February 2000, based on the older Spaceborne Imaging Radar-C/X-band Synthetic Aperture Radar (SIR-C/X-SAR), previously used on the Shuttle in 1994.

See also the list<sup>160</sup> of Satellite Microwave RS Sensors at *Microwave Radar and Radiometric Remote Sensing*

---

<sup>159</sup> [http://www.jpl.nasa.gov/news/fact\\_sheets/radar.pdf](http://www.jpl.nasa.gov/news/fact_sheets/radar.pdf)

<sup>160</sup> <http://mrs.eecs.umich.edu/sensors.html>

# LiDAR Remote Sensing

See Jensen Chapter 10: LIDAR Remote Sensing.

The term *LiDAR* or *LIDAR* derives from *RADAR*, thus light detection and ranging, using visible light or more commonly NIR (from 1040 to 1060 nm). A laser pulse is sent out, reflected off a surface and detected and position of reflection and intensity are determined. The time between send and receive is measured. Platforms can be terrestrial, airborne, or satellite based. Scales imaged can extend from small dirt clods to whole planets and moons.

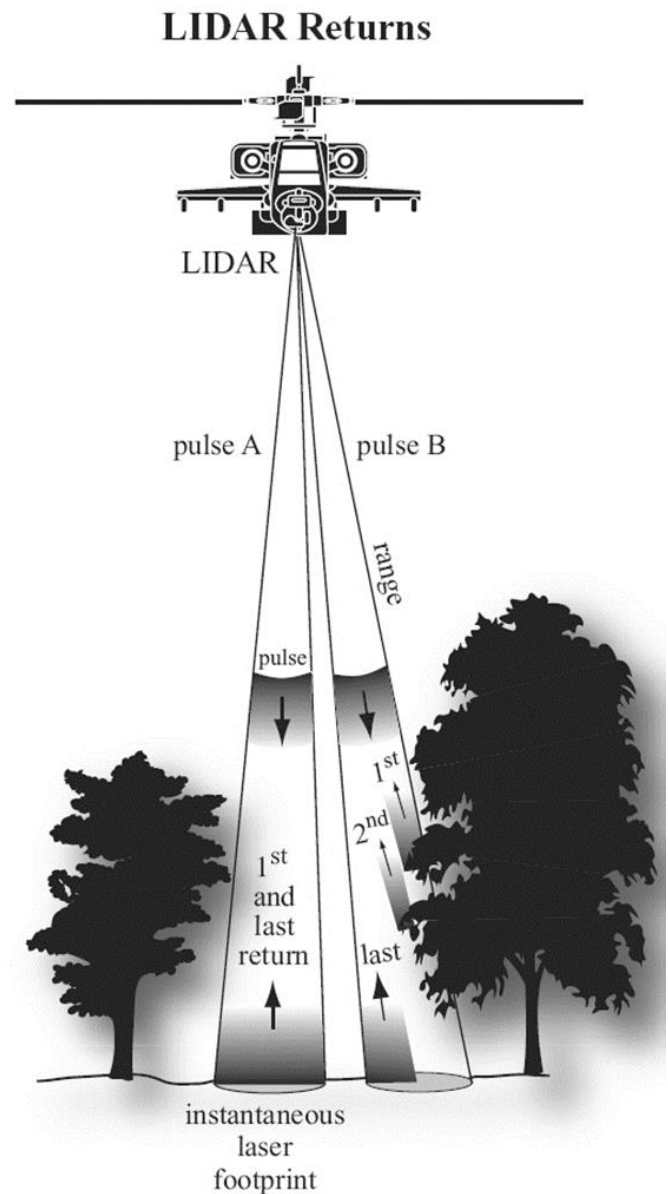
LiDAR provides a highly accurate means of elevation model collection for sub-meter contours. Acquisition can take place day or night—shadows that are problematic in mountainous areas are not an issue with LiDAR. Unlike photography, acquisition can take place below cloud cover—cloud shadows are no issue. It is very cost effective for larger projects. Return signal can be used for more than just ranging.<sup>161</sup> The intensity of the return signal carries useful information in addition to its position.

LiDAR with **Airborne Laser Swath Mapping ALSM** uses pulsed laser, differential GPS (using a GPS base station), and Inertial measurement unit (IMU) can measure elevations with ~15 cm vertical accuracy. (See diagram below, from Jensen 2009 JRJPTT).

LiDAR allows the creation of highly accurate **Digital Elevation Models DEMs** with submeter resolution. In vegetated areas, the first return may be from the top of a vegetation canopy, intermediated returns from branches and leaves, last return may be from the ground (terrain), etc. The latter may be used to construct a type of DEM, the **Digital Terrain Models DTM** (of the bare-earth land surface without vegetation or structures). The other type of DEM, **Digital Surface Models (DSM)**, depict the surfaces of land + structures present.

Precision DEMs may be overdraped by orthoimages to create highly detailed 3D images viewable from many angles. Hillshaded DEM display can be used to demonstrate hidden faults. LiDAR was used to monitor the growing elevation of the lava dome inside the crater of Mt. St. Helens in 2003-2005. It has been used to map caves, archaeological sites, geomorphological features.

In space and solar system exploration, it has been used to map several planets, the Moon, even an asteroids (433 Eros, by **NEAR Near Earth Asteroid Rendezvous - Shoemaker** using **NEAR Laser Rangefinder NLR**, launched 1996, landed on surface 2001). The Moon was mapped by Apollo LiDAR 1971-2, by Space Shuttle mission including 1994, by **Shuttle Laser Altimeter SLA** 1996-7, and **Clementine** LiDAR in 1994. The **Lunar Reconnaissance Orbiter (LRO)** launched 2009, utilizes **Lunar Orbiter Laser Altimeter (LOLA)**;<sup>162</sup> and other spacecraft.



<sup>161</sup> Text from J. F. Banfield presentation "LiDAR (Light Detection and Ranging)"

<sup>162</sup> <http://lunar.gsfc.nasa.gov/> NASA image from Banfield "LiDAR (Light Detection and Ranging)"

## Comparison of Techniques for measuring surfaces and detecting changes in surfaces

|                    | GPS                       | InSAR                         | Airborne LiDAR           | Ground-based LiDAR       |
|--------------------|---------------------------|-------------------------------|--------------------------|--------------------------|
| Sample Density     | 1 site/10 km <sup>2</sup> | 10,000 pixels/km <sup>2</sup> | 1-10 hits/m <sup>2</sup> | 1000 hits/m <sup>2</sup> |
| Position Precision | 1-20 mm                   | 2-3 m                         | 5-15 cm                  | 0.6-5 cm                 |
| Change Detection   | 1 mm                      | 1-2 cm                        | 10 cm                    | 1 cm                     |
| Scale              | Global                    | 100 km                        | 10-100 km                | 1 km                     |

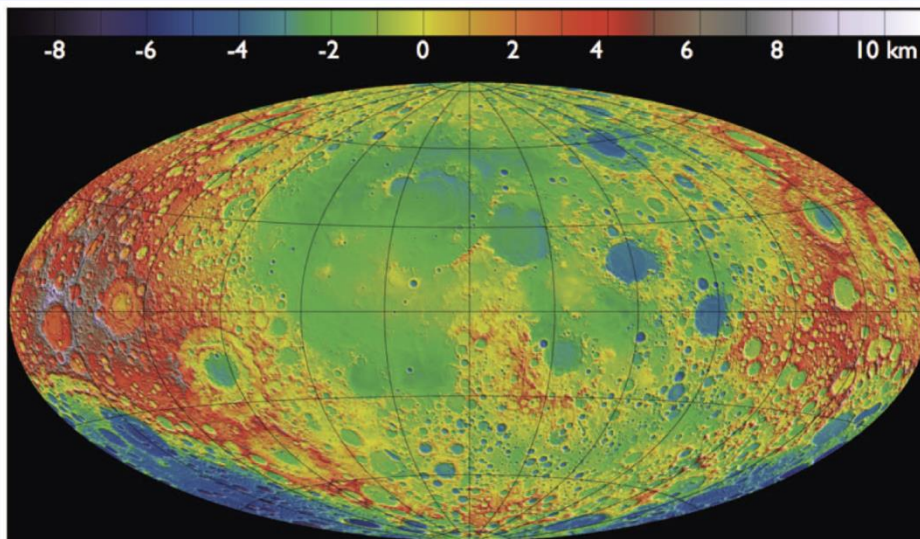
Table from J. F. Banfield presentation “LiDAR (Light Detection and Ranging”

Precision DEMs may be overdraped by orthoimages to create highly detailed 3D images viewable from many angles. Hillshaded DEM display can be used to demonstrate hidden faults. LiDAR was used to monitor the growing elevation of the lava dome inside the crater of Mt. St. Helens in 2003-2005. It has been used to map caves, archaeological sites, geomorphological features.

In space and solar system exploration, it has been used to map planets, moons, even asteroids (433 Eros, by **NEAR Near Earth Asteroid Rendezvous - Shoemaker** using **NEAR Laser Rangefinder NLR**, launched 1996, landed on surface 2001). The Moon was mapped by Apollo LiDAR 1971-2, by Space Shuttle mission including 1994, by **Shuttle Laser Altimeter SLA** 1996-7, and **Clementine** LiDAR in 1994. The **Lunar Reconnaissance Orbiter (LRO)** launched 2009, utilizes **Lunar Orbiter Laser Altimeter (LOLA)**;<sup>163</sup> and other spacecraft.



### Lunar Topography Map From LOLA Measurements



Equal-Area projection of lunar topography developed from 1 billion LOLA measurements  
Resolution: N/S ~20m; E/W ~0.1 deg (4.5km at equator, 200m at >85 Lat)

**Mars Orbiter Laser Altimeter MOLA** was an important instrument on the **Mars Global Surveyor (MGS) spacecraft**, which operated in Mars orbit from September 1997 to November 2006.

Earth has been mapped with **CALIPSO (Cloud-Aerosol Lidar and Infrared Pathfinder Satellite Observation) spacecraft** mission in a Sun-synchronous orbit launched 2006 and **ICESat (Ice, Cloud, and land Elevation Satellite)** with **Geoscience Laser Altimeter System (GLAS)**, 2003-2010, operating at 1064 & 532 nm to make precision altimetry of the Cryosphere.<sup>164</sup>

The MESSENGER spacecraft (**MERCURY Surface, Space ENVIRONMENT, GEOchemistry, and RANGING**) utilizes the **MLA Mercury Laser Altimeter**. Launched 2004, in orbit 2011.

Bathymetry is possible with 0.5  $\mu\text{m}$  laser (blue-green 532 nm). A 1064 nm NIR pulse is reflected from surface to give this distance, whereas a concurrent green pulse at 532 nm is transmitted and may reveal bottom contours as deep as 80 m, often less.

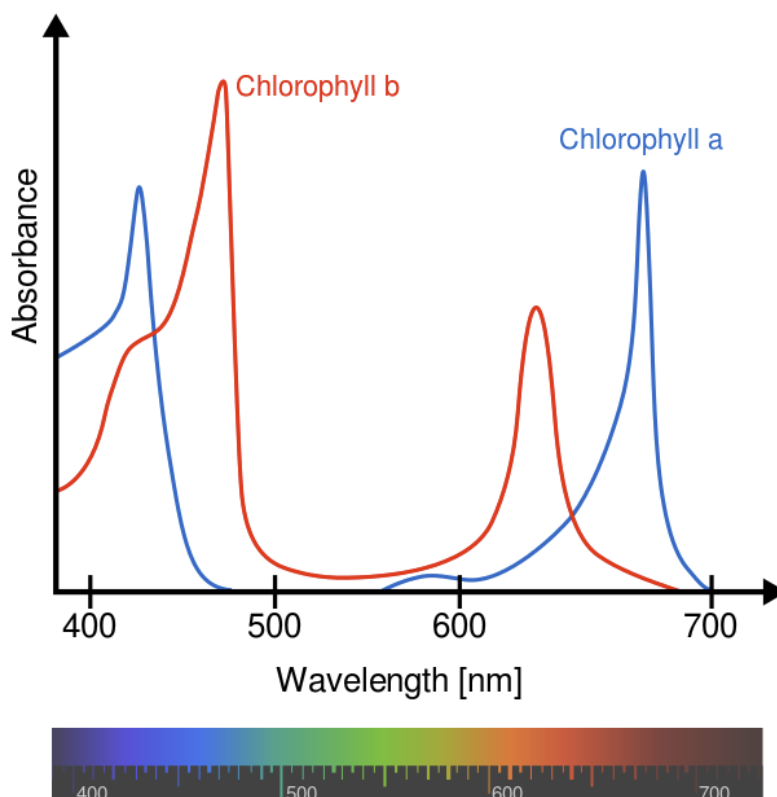
---

<sup>164</sup> <http://icesat.gsfc.nasa.gov/icesat/>  
Page 94 of 110

## Remote Sensing of Vegetation

See Jensen Chapter 11: Remote Sensing of Vegetation. Minimal summarization here, much more would be desirable for this important topic but out of time. But see also under Spectroscopy.

In leaf structure, the upper palisade parenchymal cell have the bulk of the chlorophyll-a (having peak absorption at 0.43 and 0.66  $\mu\text{m}$ ), chlorophyll-b (having peak absorption at 0.45 and 0.65  $\mu\text{m}$ ), and  $\beta$ -carotene, whereas the lower disordered spongy parenchymal mesophyll cells are responsible for much of the NIR reflectance. In infrared photography, plants appear bright due to reflection of NIR. Optimal absorption windows are at 0.45 - 0.52  $\mu\text{m}$  and 0.63 - 0.69  $\mu\text{m}$ .



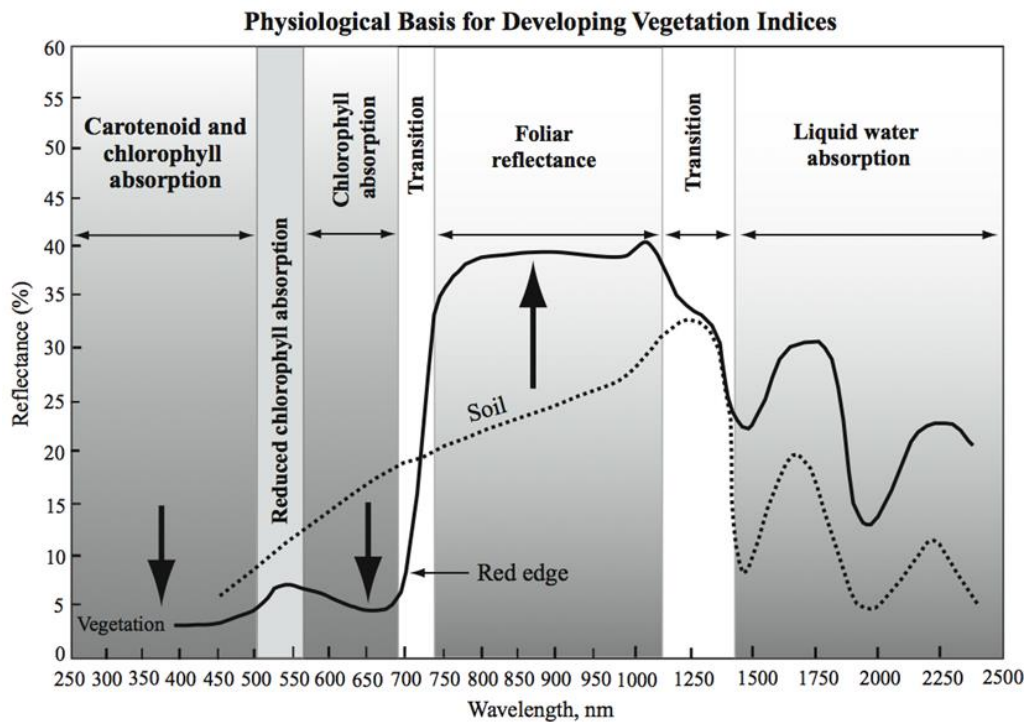
Chlorophyll absorption vs wavelength (free in a solvent)<sup>165</sup>

Beta-carotene absorbs most strongly between 400-500 nm. Other pigments in leaves include phycoerythrin (peaking about 560 nm) and anthocyanins. "At a pH of 1.0, anthocyanins strongly absorb light between 460 and 550 nm (long blue, cyan and green light) and have an absorption maximum of about 520nm. Thus, at a pH of 1.0, anthocyanins are colored; they transmit violet, short blue and red light to the eye. However, at a pH of 4.5, anthocyanins uniquely absorb no light in the visible range."<sup>166</sup>

<sup>165</sup> <http://en.wikipedia.org/wiki/Chlorophyll>

<sup>166</sup> <http://cellbiologyolm.stevegallik.org/anthocyanin/page17>

The following spectrum representative of living green plants demonstrates important spectral features:



The Red Edge in near-IR is a diagnostic feature characteristic of living photosynthetic plants.<sup>167</sup>

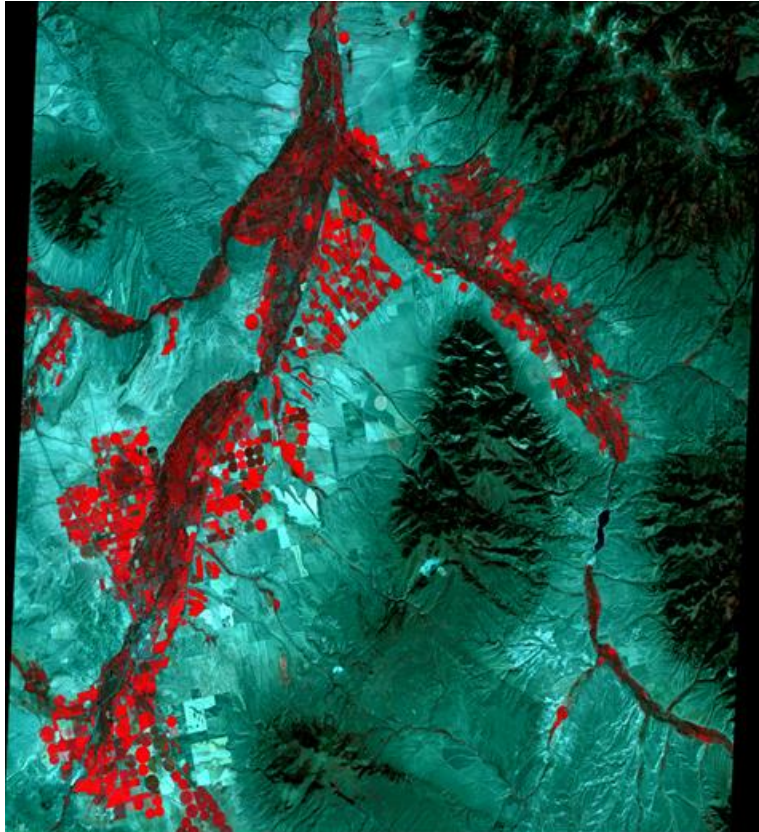
There are a number of useful vegetation indices which utilize spectral data. These include:

- the NIR to Red ratio,
- the normalized difference vegetation index NDVI,
- the Normalized Difference Moisture or Water Index (NDMI or MDWI),
- the soil adjusted vegetation index (SAVI),
- the Atmospherically Resistant Vegetation Index (ARVI),
- New Vegetation Index NVI,
- MODIS Enhanced Vegetation Index (EVI),
- Triangular Vegetation Index (TVI),
- Visible Atmospherically Resistant Index (VARI),
- Red Edge Position Determination (REP)

The following is an ASTER false color image with Band 3→R, Band 2→G, Band 1→B

The relevant ASTER bands are:<sup>168</sup>

|  |     |
|--|-----|
| Band 3: 0.76 - 0.86 $\mu\text{m}$ [true NIR]   | → R |
| Band 2: 0.63 - 0.69 $\mu\text{m}$ [true Red]   | → G |
| Band 1: 0.52 - 0.60 $\mu\text{m}$ [true Green] | → B |



ASTER false color image, near Block Mountain MT, with Band 3→R, Band 2→G, Band 1→B  
Demonstrates bright signal in near IR (shown as Red) by living plants (in numerous circularly irrigated crops)  
(Block Mountain is in the top left and not well seen)

---

<sup>168</sup> <http://asterweb.jpl.nasa.gov/characteristics.asp>

The same region is seen below in grayscale displaying a vegetation index (ASTER Band3/Band2).

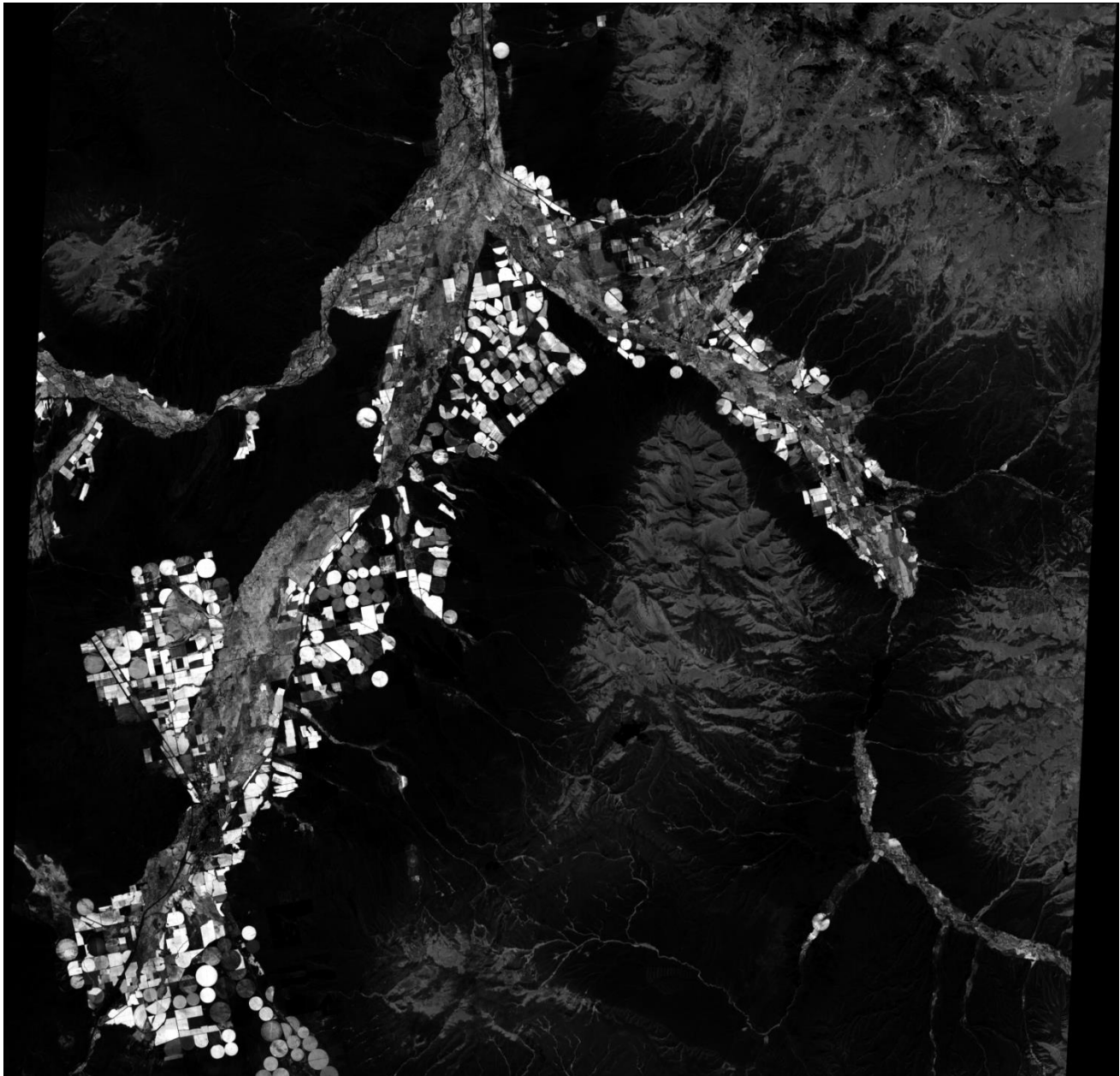
Relevant ASTER bands are:

Band 3: 0.76 - 0.86  $\mu\text{m}$  [NIR]

[should be bright reflectance with vegetation]

Band 2: 0.63 - 0.69  $\mu\text{m}$  [Red]

[should be relatively dark with vegetation]



ASTER Band3/Band2 index image, near Block Mountain MT, for Vegetation (displays as bright), Enhance>Linear 2%, black bars trimmed, no other processing (Block Mountain is in the top left and not well seen)

## Remote Sensing of Water

See Jensen Chapter 12: Remote Sensing of Water. Important topic but not further summarized here, out of time.

“Scattering in the water column is important in the violet, dark blue, and light blue portions of the spectrum (400 - 500 nm). This is the reason water appears blue to our eyes...”

The best wavelength region for discriminating land from pure water is in the near-infrared and middle-infrared from 740 - 2,500 nm... In the near- and middle-infrared regions, water bodies appear very dark, even black, because they absorb almost all of the incident radiant flux, especially when the water is deep and pure and contains little suspended sediment or organic matter.”<sup>169</sup>

## Remote Sensing the Urban Landscape

See Jensen Chapter 13: Remote Sensing the Urban Landscape. Not assigned, not further summarized here.

# Remote Sensing of Soils, Minerals, and Geomorphology

See Jensen Chapter 14: Remote Sensing of Soils, Minerals, and Geomorphology. Not further summarized here, out of time

Photosynthetic plants tend to have a characteristic reflectance spectrum, with low reflectance in Red and Blue (wavelengths used in PS), moderately low in Green, and High in nearby NIR. The jump from low red to high NIR is called the “Red Edge”.

Wavelength dependence of reflectance by various plants:<sup>170</sup>

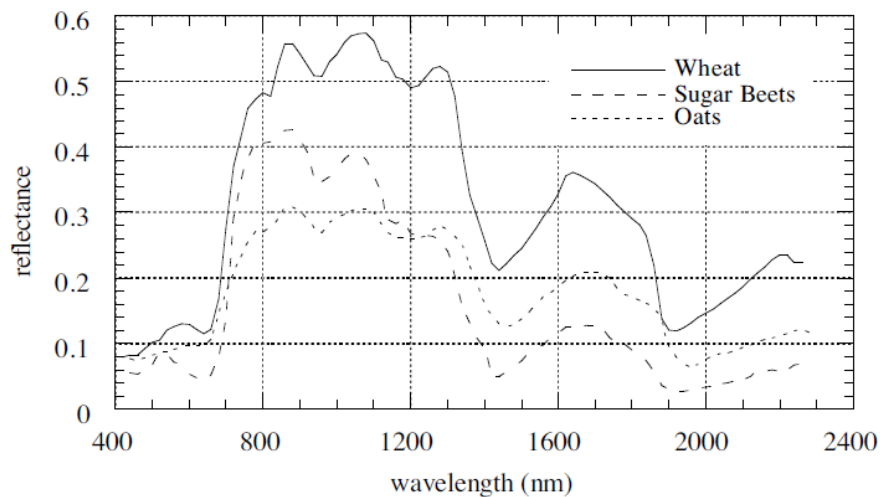
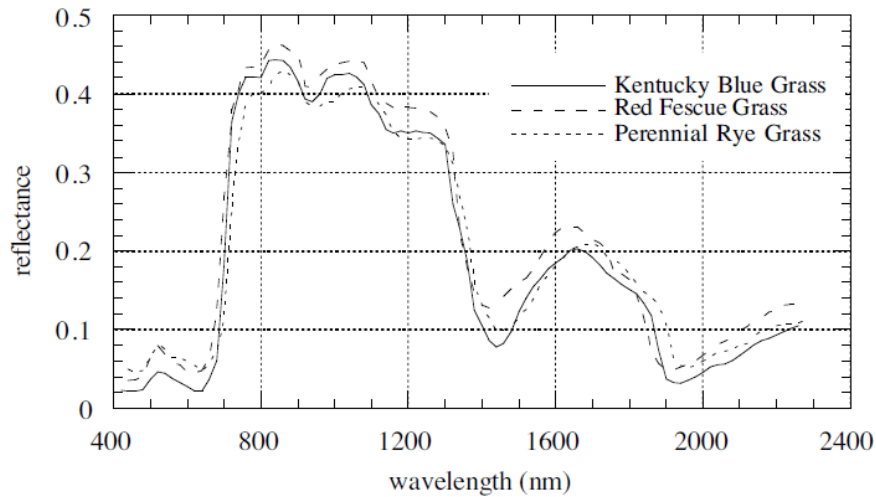


FIGURE 1-7. Example vegetation spectral reflectance curves (Bowker et al., 1985). The curves in the upper graph show variability among three types of grasses; even under relatively well-controlled laboratory conditions, the reflectance of corn leaves has been found to vary as much as  $\pm 17\%$  near the reflectance edge at  $0.67\ \mu\text{m}$  (Landgrebe, 1978).

<sup>170</sup> Schowengerdt, op. cit.  
Page 100 of 110

# Glossary and Mini-Topics including Spacecraft Missions & Instruments

Topics and terms are included here for added emphasis or for when they are not fully treated in the body of this summary. Emphasis such as italics may be added by MCM in quoted material.

## Anaglyph 3D

“Anaglyph 3D is the name given to the stereoscopic 3D effect achieved by means of encoding each eye's image using filters of different (usually chromatically opposite) colors, typically red and cyan. Anaglyph 3D images contain two differently filtered colored images, one for each eye. When viewed through the "color-coded" "anaglyph glasses", each of the two images reaches the eye it's intended for, revealing an integrated stereoscopic image. The visual cortex of the brain fuses this into perception of a three-dimensional scene or composition.”<sup>171</sup>

## Bayer Filters

“A Bayer filter mosaic is a color filter array (CFA) for arranging RGB color filters on a square grid of photosensors [usually charge coupled devices CCDs]. Its particular arrangement of color filters is used in most single-chip digital image sensors used in digital cameras, camcorders, and scanners to create a color image. The filter pattern is 50% green, 25% red and 25% blue, hence is also called RGBG, GRGB, or RGGB.”

## Cassini–Huygens Mission to Saturn

Cassini launched October 1997 with the European Space Agency's Huygens probe. The [Huygens] probe was equipped with six instruments to study Titan, Saturn's largest moon. It landed on Titan's surface on Jan. 14, 2005, and returned spectacular results... Cassini completed its initial four-year mission to explore the Saturn System in June 2008 and the first extended mission, called the Cassini Equinox Mission, in September 2010. Now, the healthy spacecraft is seeking to make exciting new discoveries in a second extended mission called the Cassini Solstice Mission.” It is a flagship-class NASA–ESA–ASI robotic spacecraft sent to the Saturn system.<sup>172</sup>

## Chandra X-ray Observatory

“The Chandra X-ray Observatory is part of NASA's fleet of "Great Observatories" along with the Hubble Space Telescope, the Spitzer Space Telescope and the now deorbited Compton Gamma Ray Observatory. Chandra allows scientists from around the world to obtain X-ray images of exotic environments to help understand the structure and evolution of the universe.”<sup>173</sup> Launched 23 July 1999. Instruments include High Resolution Camera (HRC, 0.1–10 keV), AXAF CCD Imaging Spectrometer (ACIS, 0.2–10 keV).<sup>174</sup>

## Compton Gamma Ray Observatory (CGRO): EGRET, BATSE, OSSE, COMPTEL:

Successful exploratory missions in gamma-ray astronomy led to the **Energetic Gamma Ray Experiment Telescope (EGRET)** instrument on the **CGRO**. Launched in 1991, EGRET made the first complete survey of the sky in the 30 MeV - 10 GeV range [max. range out of 4 instrument, 20 MeV - 30 GeV]... Most of the gamma-ray sources detected by EGRET remain unidentified... Also on the CGRO was the **Burst and Transient Source Experiment BATSE**: Gamma ray detection (25 keV - 10 MeV or 20 to >600 keV) was also a predecessor. **CGRO** was de-orbited June 2000..<sup>175</sup>

---

<sup>171</sup> [http://en.wikipedia.org/wiki/Anaglyph\\_3D](http://en.wikipedia.org/wiki/Anaglyph_3D)

<sup>172</sup> <http://en.wikipedia.org/wiki/Cassini%E2%80%93Huygens>  
<http://saturn.jpl.nasa.gov/mission/introduction/>

<sup>173</sup> [http://www.nasa.gov/mission\\_pages/chandra/main/](http://www.nasa.gov/mission_pages/chandra/main/)

<sup>174</sup> [http://en.wikipedia.org/wiki/Chandra\\_X-ray\\_Observatory](http://en.wikipedia.org/wiki/Chandra_X-ray_Observatory)

<sup>175</sup> <http://gammaray.msfc.nasa.gov/batse/>

[http://en.wikipedia.org/wiki/Compton\\_Gamma\\_Ray\\_Observatory](http://en.wikipedia.org/wiki/Compton_Gamma_Ray_Observatory)

## Computer & Login Setup:

### USGS Registration

<https://earthexplorer.usgs.gov/register/>

This allows you to register and save information that can be used to access a specific USGS site or to place orders for USGS products. Additional features, such as the ability to save search information, may also be available to registered users depending on the site accessed. Login info on file

## Digital elevation model DEM

a digital model or 3D representation of a terrain's surface — commonly for a planet (including Earth), moon, or asteroid — created from terrain elevation data. The surface may be (1) the actual bare earth terrain (called a *digital terrain model DTM*) or (2) for Earth at least it may be a *digital surface model DSM* representing the earth's surface and includes all objects on it (forest canopy etc.)

## Fermi gamma-ray space telescope spacecraft

Formerly named Gamma-Ray Large Area Space Telescope (GLAST). NASA's Fermi gamma-ray space telescope mapped out the Milky Way galaxy by creating a full 360-degree view of the galaxy from our perspective here on Earth.<sup>176</sup> Launched June 11, 2008. Instruments: Large Area Telescope (LAT [20 MeV - 300 GeV]) and Gamma-ray Burst Monitor (GBM [ $< 10$  keV -  $> 25$  MeV]). It “is an international and multi-agency space mission that studies the cosmos in the energy range 10 keV - 300 GeV. Fermi has an imaging gamma-ray telescope vastly more capable than instruments flown previously [such as BATSE], as well as a secondary instrument to augment the study of gamma-ray bursts. The main instrument, the *Large Area Telescope (LAT)*, has superior area, angular resolution, field of view, and deadtime... The Gamma-ray Burst Monitor (GBM) has a field of view several times larger than the LAT and provides spectral coverage of gamma-ray bursts that extends from the lower limit of the LAT down to 10 keV.”<sup>177</sup>

## Geosynchronous and Geostationary satellites [GEOs], Analemma, Tundra orbits

A satellite in **geosynchronous** orbit [GEO, Clarke orbit] has an orbital period the same as the Earth's rotation period, so stays over the same longitude (though possibly varying in latitude). Such a satellite returns to the same position in the sky after each sidereal day, and over the course of a day traces out a path in the sky that is typically some form of **analemma**. A special case of geosynchronous satellite GEO is the **geostationary satellite**, which has a geostationary orbit [no special acronym]—a circular geosynchronous orbit directly above the Earth's equator. Such an orbit remains over a spot on Earth fixed in both longitude and latitude (which is 0°).

Another type of geosynchronous orbit used by satellites is the **Tundra elliptical orbit**.<sup>178</sup> A Tundra orbit is “a highly elliptical geosynchronous orbit with a high inclination (usually near 63.4°) and an orbital period of one sidereal day (about 4 minutes less than a solar day). A satellite placed in this orbit spends most of its time over a chosen area of the Earth, a phenomenon known as apogee dwell. The ground track of a satellite in a tundra orbit is a closed “figure-eight”. These are conceptually similar to Molniya orbits which have the same inclination but half the period (about 12 hours).”<sup>179</sup> “Tundra orbits—with an apogee of about 29,200 miles (46,990 km) and a perigee of about 14,900 miles (23,980 km)—provide high-latitude users with higher elevation angles than can be offered by a geostationary orbit. The three Sirius/Radiosats spend about 16 hours of each solar day over the continental United States, with at least one of them over the country at all times.”<sup>180</sup>

**Geosynchronous satellites** revolve around the Earth with a period of one sidereal day. Seen from a fixed point on the Earth's surface, they trace paths in the sky which repeat every day, and are therefore simple and meaningful analemmas. They are generally roughly elliptical, teardrop shaped, or figure-8 in shape. Their shapes and dimensions depend on the parameters of the orbits.

A subset of geosynchronous satellites are **geostationary** ones, which ideally have perfectly circular orbits, exactly in the Earth's equatorial plane. A geostationary satellite therefore ideally remains stationary relative to the Earth's surface, staying over a single point on the equator. No real satellite is exactly geostationary, so real ones trace small analemmas in the sky. Since geosynchronous satellites are close to

---

<sup>176</sup> [http://missionscience.nasa.gov/ems/12\\_gammarays.html](http://missionscience.nasa.gov/ems/12_gammarays.html)

<sup>177</sup> <http://fermi.gsfc.nasa.gov/science/>

<sup>178</sup> [http://en.wikipedia.org/wiki/Geosynchronous\\_satellite](http://en.wikipedia.org/wiki/Geosynchronous_satellite)

<sup>179</sup> [http://en.wikipedia.org/wiki/Tundra\\_orbit](http://en.wikipedia.org/wiki/Tundra_orbit)

<sup>180</sup> <http://www.americaspace.com/?p=43791>

the Earth compared to the Sun, their analemmas vary substantially depending on the location of the observer on the Earth's surface... The paraboloidal dishes that are used for radio communication with geosynchronous satellites often have to move so as to follow the satellite's daily movement around its analemma. The mechanisms that drive them must therefore be programmed with the parameters of the analemma. Exceptions are dishes that are used with (approximately) geostationary satellites, since these satellites appear to move so little that a fixed dish can function adequately at all times.”<sup>181</sup> Images by a stationary telescope show such satellites to remain in one place compared to the streaks made by stars. Examples include METEOSAT

### High Resolution Imaging Science Experiment HiRISE

is a camera on board the Mars Reconnaissance Orbiter [launched 12 August 2005]. It consists of a 0.5 m (19.7 in) aperture reflecting telescope, the largest so far of any deep space mission, which allows it to take pictures of Mars with resolutions of [25 cm or] 0.3 m /pixel (about 1 foot), resolving objects below a meter across.<sup>182</sup> Spectral ranges are 400 to 600 nm, 550 to 850 nm, and 800 to 1000 nm [thus VNIR].<sup>183</sup>

### Hubble Space Telescope HST

“The first element of the program [of Great Observatories]— and arguably the best known—is the Hubble Space Telescope (HST). The Hubble telescope was deployed by a NASA Space Shuttle in 1990. A subsequent Shuttle mission in 1993 serviced HST and recovered its full capability. A second successful servicing mission took place in 1997. Subsequent servicing missions have added additional capabilities to HST, which observes the Universe at ultraviolet, visual, and near-infrared wavelengths. Instruments include ACS - Advanced Camera for Surveys, Cosmic Origins Spectrograph (COS, two channels, the Far Ultraviolet FUV channel covering wavelengths from 115 to 177 nm, and the Near Ultraviolet NUV) channel, covering 175-300 nm), NICMOS — Near Infrared Camera/Multi-Object Spectrometer, STIS — Space Telescope Imaging Spectrograph, and Wide Field Camera 3 (WFC3, operating at UVIS or NIR).<sup>184</sup>

### Kepler Laws:

(1) Orbits are ellipses, having semi-major axis  $a$  and semi-minor axis  $b$  and eccentricity  $e$ . Eccentricity<sup>185</sup> is given by  $\sqrt{1 - b^2/a^2}$ . Although it is often said that the Sun is at one of the foci, the focus is in fact at the barycenter. The barycenter is usually inside the Sun (just outside the Sun for Jupiter<sup>186</sup>) but not at the center of it.

(2) Objects when in elliptical orbits move fastest when closest to the Sun.

Perihelion distance =  $a(1-e)$ ; Aphelion distance =  $a(1+e)$

A line joining a planet and the Sun sweeps out equal areas during equal intervals of time.

(3) The square of the orbital period  $p$  of a planet is directly proportional to the cube of the semi-major axis  $a$  of its orbit.<sup>187</sup> The constant of proportionality is  $k_{\text{Sun}} = 4\pi^2/GM_{\text{Sun}}$

<sup>181</sup> <http://en.wikipedia.org/wiki/Analemma>

<sup>182</sup> <http://en.wikipedia.org/wiki/HiRISE>

<sup>183</sup> <http://www.uahirise.org/teknikos.php>

<sup>184</sup> [http://www.nasa.gov/mission\\_pages/hubble/spacecraft/index.html](http://www.nasa.gov/mission_pages/hubble/spacecraft/index.html)

<sup>185</sup> [http://en.wikipedia.org/wiki/Eccentricity\\_%28mathematics%29](http://en.wikipedia.org/wiki/Eccentricity_%28mathematics%29)

<sup>186</sup> [http://en.wikipedia.org/wiki/Barycentric\\_coordinates\\_%28astronomy%29](http://en.wikipedia.org/wiki/Barycentric_coordinates_%28astronomy%29)

<sup>187</sup> [http://en.wikipedia.org/wiki/Kepler%27s\\_laws\\_of\\_planetary\\_motion](http://en.wikipedia.org/wiki/Kepler%27s_laws_of_planetary_motion)

## Lagrange points applied to Earth-Sun orbits

**Lagrange points L4 and L5** are relatively stable high earth orbits respectively about 60° ahead of and behind the Earth in its orbit about the Sun, thus at about 1 A.U from the Earth.<sup>188</sup> Satellites include STEREO A and STEREO B. Stability arises from the Coriolis force.

**Lagrange point L1** is an unstable orbital point on a line from Sun to Earth and about 1.5 million km (the Hill sphere radius) closer to the Sun (thus always in full sunlight, good for solar observatories). Satellites orbiting at or about L1 include WIND, SOHO, and ACE

**Lagrange point L2** is also an unstable orbital point, on a line from Sun passing through and extended beyond Earth and about 1.5 million km further from Earth (thus always in the dark, good for observatories needing to be shielded from solar radiation. Satellites include WMAP (formerly), Planck, and ESA Gaia, and may eventually be the destination of JWST.<sup>189,190</sup>

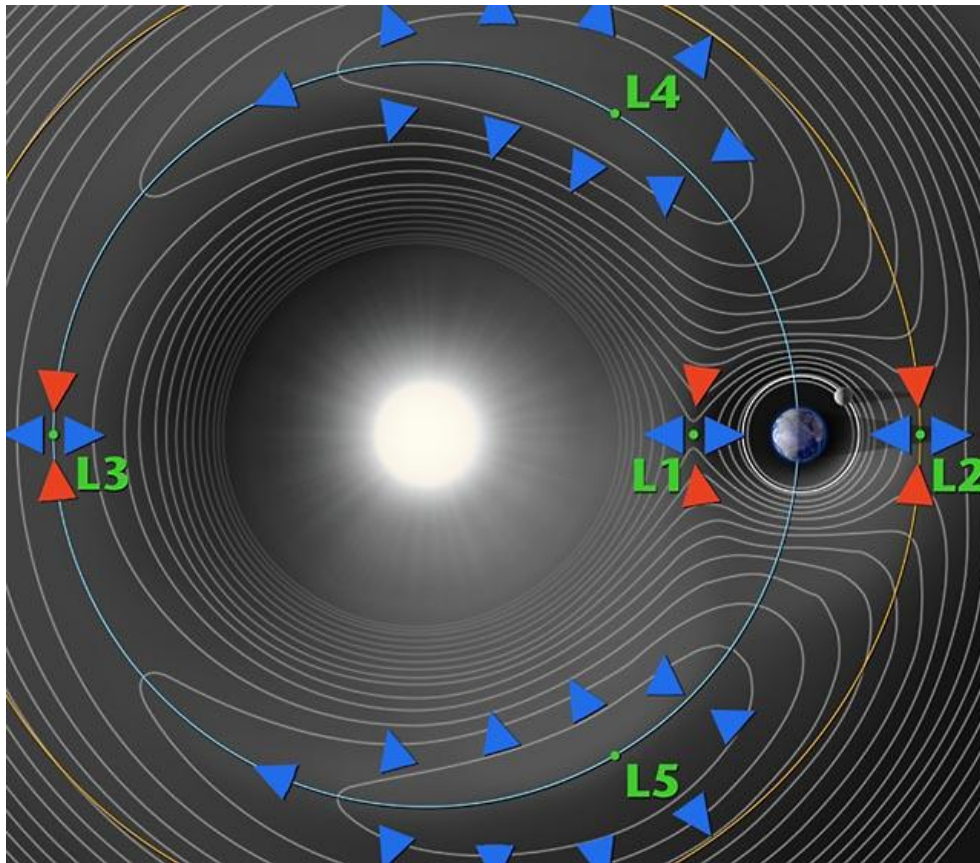


Diagram of Lagrange Points L1 through L5 and Gravitational Potential  
Red arrow is enhanced attraction, Blue arrow is enhanced repulsion.<sup>191</sup>

<sup>188</sup> [http://map.gsfc.nasa.gov/mission/observatory\\_l2.html](http://map.gsfc.nasa.gov/mission/observatory_l2.html)

<sup>189</sup> [http://en.wikipedia.org/wiki/Lagrangian\\_point](http://en.wikipedia.org/wiki/Lagrangian_point)

<sup>190</sup> [http://en.wikipedia.org/wiki/List\\_of\\_objects\\_at\\_Lagrangian\\_points](http://en.wikipedia.org/wiki/List_of_objects_at_Lagrangian_points)

<sup>191</sup> [http://en.wikipedia.org/wiki/Lagrangian\\_point](http://en.wikipedia.org/wiki/Lagrangian_point)

### **Light Index of Refraction, Speed of light, etc.**

Index of Refraction  $n = \text{Speed of light in medium} / \text{Speed of light in Vacuum} = v/c$

When light enters a medium with greater  $n$ , the speed  $v$  is slower, the wavelength  $\lambda$  is shorter, but the frequency  $f$  or  $\nu$  remains the same. In fact,  $\lambda = \lambda_0 / n$  where  $\lambda_0 = \text{wavelength in vacuum}$ .

When light passes from a medium 1 with index of refraction  $n_1$  across an interface into a medium with index of refraction  $n_2$ , Snell's law is observed regarding the angle with respect to the Normal (going to higher index causes bending toward the normal thus a smaller angle with respect to Normal):

$$\frac{\sin \theta_1}{\sin \theta_2} = \frac{v_1}{v_2} = \frac{n_2}{n_1}$$

### **Lunar Reconnaissance Orbiter—Lyman-Alpha Mapping Project (LAMP)**

Launched June 18, 2009. "The Lyman-Alpha Mapping Project (LAMP) will search for surface ice and frost in the polar regions [of the moon] and provide images of permanently shadowed regions illuminated only by starlight and the glow of interplanetary hydrogen emission, the Lyman-Alpha line. Permanently shadowed regions on the moon's surface, such as the bottoms of some of the deep craters at the lunar poles, are very cold and might hold water ice."<sup>192</sup>

### **Mars Science Laboratory MSL and Curiosity**

"With its rover named Curiosity, Mars Science Laboratory mission is part of NASA's Mars Exploration Program, a long-term effort of robotic exploration of the red planet... MSL will study Mars' habitability"<sup>193</sup> Launched Nov. 26, 2011.<sup>194</sup> Curiosity is in Gale crater, a 150km diameter crater containing a central mound 5.5 km tall of layered sediments named "Mt. Sharp" that Curiosity is driving towards." [SEW] It landed at Bradbury Landing and traveled to Pahrump Hills outcrop, which is part of the basal layer of Mount Sharp. This rover follows Sojourner (launch 1997), Spirit (launch 2003) and Opportunity (launch 2003).

### **Mercury Surface, Space Environment, Geochemistry, and Ranging (MESSENGER)—Gamma-Ray Spectrometer (GRS)**

Launch August 3, 2004. "Scientists can use gamma rays to determine the elements on other planets. The Mercury Surface, Space Environment, Geochemistry, and Ranging (MESSENGER) Gamma-Ray Spectrometer (GRS) can measure gamma rays emitted by the nuclei of atoms on planet Mercury's surface that are struck by cosmic rays."<sup>195</sup>

---

<sup>192</sup> [http://www.nasa.gov/mission\\_pages/LRO/spacecraft/index.html](http://www.nasa.gov/mission_pages/LRO/spacecraft/index.html)

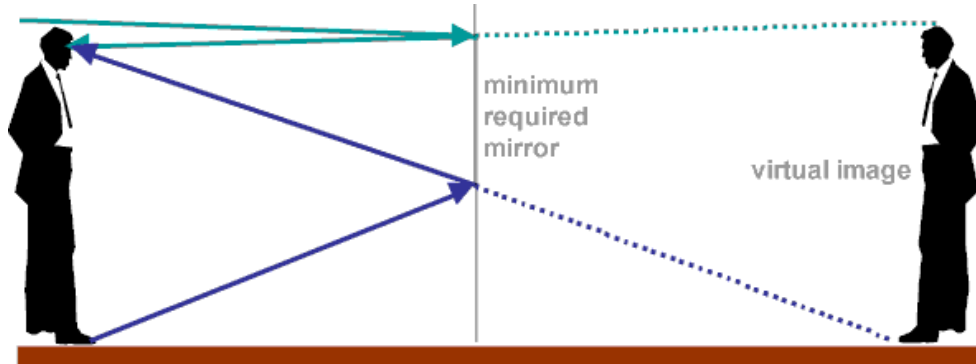
<sup>193</sup> <http://mars.jpl.nasa.gov/msl/mission/overview/>

<sup>194</sup> [http://mars.jpl.nasa.gov/msl/news/pdfs/MSL\\_Fact\\_Sheet.pdf](http://mars.jpl.nasa.gov/msl/news/pdfs/MSL_Fact_Sheet.pdf)

<sup>195</sup> [http://missionscience.nasa.gov/ems/12\\_gammarays.html](http://missionscience.nasa.gov/ems/12_gammarays.html)

### Mirror, Image Behavior Reflected in Plane Mirror

The image of an object of height  $H$  that is viewed as a reflected image in a plane mirror requires the mirror to be  $H/2$  in linear dimensions for its height to be fully seen. If one backs away from the mirror, the amount of the mirror occupied by the subject remains the same. This prompts the frequent statement that “the size of the image equals the size of the object; that is, the magnification of a plane mirror equals one.” What this statement neglects is that the angular dimension subtended by both the mirror and the reflected object decrease with increasing distance to the mirror. Thus, although the object fills the same portion of the mirror, its perceived angular size decreases with increasing distance. In this sense, it gets smaller with distance.<sup>196</sup>



### Moon's Orbit about Earth<sup>197</sup>

Moon is on elliptical orbit w one focus at Earth-Moon barycenter (~4600 km from Earth center). Moon equatorial radius = 1736 km.

Semi-major axis [maximal distance from moon center to ellipse center] = 384,403 km<sup>198</sup>

Average (mean) center to center (CTC) Earth-Moon distance ~384,400 km (about 60  $R_E$  = 6378 km equatorial)<sup>199</sup> or 385,000 km<sup>200</sup>

Apogee CTC 406,696 km, perigee CTC ~363,104 km<sup>201</sup>

Period is c. 28 d.

### NASA Science Missions and NASA's Science Mission Directorate (SMD)

- NASA Science Missions are listed chronologically here.<sup>202</sup> Sortable on 4 header fields (Division, Name, Date, Phase) and probably comprehensive. Past and Present Missions listed go back to 1960.
- NASA's Science Plan 2007 to 2017 is given here.<sup>203</sup> Includes planned mission like James Webb Space Telescope JWST, GOES-R, MMS, SMAP, LISA, etc.
- NASA Missions are listed alphabetically by spacecraft mission name here<sup>204</sup> (a less comprehensive list)

<sup>196</sup> [http://dev.physicslab.org/Document.aspx?doctype=3&filename=GeometricOptics\\_PlaneMirrors.xml](http://dev.physicslab.org/Document.aspx?doctype=3&filename=GeometricOptics_PlaneMirrors.xml)

<sup>197</sup> <http://nssdc.gsfc.nasa.gov/planetary/factsheet/moonfact.html>

<sup>198</sup> <http://www.universetoday.com/103206/what-is-the-distance-to-the-moon/>

<sup>199</sup> [http://en.wikipedia.org/wiki/Lunar\\_distance\\_%28astronomy%29](http://en.wikipedia.org/wiki/Lunar_distance_%28astronomy%29)

<sup>200</sup> <http://eclipse.gsfc.nasa.gov/SEhelp/ApolloLaser.html> ,

<http://www.jpl.nasa.gov/news/news.php?feature=605>

<sup>201</sup> <http://www.universetoday.com/103206/what-is-the-distance-to-the-moon/>

<sup>202</sup> <http://science.nasa.gov/missions/>

<sup>203</sup> [http://science.nasa.gov/media/medialibrary/2010/03/31/Science\\_Plan\\_07.pdf](http://science.nasa.gov/media/medialibrary/2010/03/31/Science_Plan_07.pdf)

<sup>204</sup> <http://www.nasa.gov/missions/index.html>

## Orbital Types and Properties

The Earth Observatory lists these major types of orbits<sup>205</sup> (comments from other sources also added). Distance are either height above surface or center to center (CTC), will try to avoid ambiguity.

- **High Earth orbits HEO** (weather, communications including search and rescue beacons, and solar monitoring satellites) are at 36,000 km or greater [about 3 times further from Earth than a MEO]. **Geostationary weather satellites** such as GOES are at ~36,000 km (35,786 km = 22,236 mi) from Earth's equatorial surface. The orbital radius from Earth's center  $R_E = 6,378$  km is added to yield CTC distance = 42,164 kilometres (26,199 mi).<sup>206</sup> The **Lagrange orbital points L1, L2, L4 and L5** are all high Earth orbits (see above). Satellites launched as HEO are initially placed in a very highly elliptical **Transfer Orbit** "with an appropriate very high apogee (35,780 km) so that the spacecraft can later be pushed into a circular GEO."<sup>207</sup> "A **geosynchronous satellite** is a satellite in geosynchronous orbit, with an orbital period the same as the Earth's rotation period. Such a satellite returns to the same position in the sky after each sidereal day, and over the course of a day traces out a path in the sky that is typically some form of analemma."<sup>208</sup>

The path loss is much greater than for MEO or LEO. It is easier however to keep a **Very Small Aperture Terminal VSAT** (two-way satellite ground station) permanently aimed at a GEO. "A **geostationary satellite** would be one that remains constantly at the same longitude all the time and also remains exactly in the equatorial plane at 0 degrees latitude. Such a perfectly geostationary orbit is, in fact, almost impossible to achieve in the real world because of Earth's orbital mechanics... Most **geosynchronous satellites** [nadir fixed in relation to Earth longitude but varying in Earth latitude] have some inclination build up and go up and down a small bit from the equator each day and thus are not truly geostationary, especially in terms of north and south latitude excursions." [Pelton 2012]

- **Medium Earth orbits MEO** (occasionally called **Middle Earth orbits**, navigation and specialty satellites, designed to monitor a particular region) are at 2,000 to 35,780 km [10,000 to 20,000 km: Pelton 2012] from Earth surface. Example: "The semi-synchronous orbit is a near-circular orbit (low eccentricity) 26,560 kilometers from the center of the Earth (about 20,200 kilometers above the surface) [thus in medium Earth orbit]. A satellite at this height takes 12 hours to complete an orbit. As the satellite moves, the Earth rotates underneath it. In 24-hours, the satellite crosses over the same two spots on the equator every day. This orbit is consistent and highly predictable. It is the orbit used by the Global Positioning System (GPS) satellites."<sup>209</sup>

A second common medium Earth orbit is the Molniya orbit, invented by the Russians. It works well for observing high latitudes. "A geostationary orbit is valuable for the constant view it provides, but satellites in a geostationary orbit are parked over the equator, so they don't work well for far northern or southern locations, which are always on the edge of view for a geostationary satellite. The Molniya orbit offers a useful alternative... The Molniya orbit combines high inclination (63.4°) with high eccentricity (0.722) to maximize viewing time over high latitudes. Each orbit lasts 12 hours, so the slow, high-altitude portion of the orbit repeats over the same location every day and night... As it moves away, its speed slows, so it spends more time at the top of its orbit farthest from the Earth. A satellite in a Molniya orbit takes 12 hours to complete its orbit, but it spends about two-thirds of that time over one hemisphere. Russian communications satellites and the Sirius radio satellites currently use this type of orbit... This type of orbit is useful for communications in the far north or south."<sup>210</sup>  
Examples: NAVSTAR Global Positioning System GPS.

- **Low Earth orbits LEO** (most scientific satellites, including NASA's Earth Observing System, and many weather satellites) are at 180 to 2,000 km [Pelton 2012: 500 to 1200 km, below the lowest Van Allen high radiation belts] above Earth surface. E.g., NASA Aqua satellite at 705 km above surface. Most are circular. Atmospheric drag is higher with low orbits, especially when the Sun is active. "The Tropical Rainfall Measuring Mission (TRMM) satellite was launched to monitor rainfall in the tropics. Therefore, it has a relatively low inclination (35 degrees), staying near the equator [and in low Earth orbit]..."

---

<sup>205</sup> <http://earthobservatory.nasa.gov/Features/OrbitsCatalog/>

<sup>206</sup> [http://en.wikipedia.org/wiki/Geostationary\\_orbit](http://en.wikipedia.org/wiki/Geostationary_orbit)

<sup>207</sup> Pelton 2012

<sup>208</sup> [http://en.wikipedia.org/wiki/Geosynchronous\\_satellite](http://en.wikipedia.org/wiki/Geosynchronous_satellite)

<sup>209</sup> <http://earthobservatory.nasa.gov/Features/OrbitsCatalog/>

<sup>210</sup> <http://earthobservatory.nasa.gov/Features/OrbitsCatalog/>

Many of the satellites in NASA's Earth Observing System EOS have a nearly **polar** [and low Earth] orbit. In this highly inclined orbit, the satellite moves around the Earth from pole to pole, taking about 99 minutes to complete an orbit. During one half of the orbit, the satellite views the daytime side of the Earth. At the pole, the satellite crosses over to the nighttime side of Earth... In a 24-hour period, polar orbiting satellites will view most of the Earth twice: once in daylight and once in darkness... Just as the geosynchronous satellites have a sweet spot over the equator that lets them stay over one [geographic] spot on Earth, the polar-orbiting satellites have a sweet spot that allows them to stay in one [local] time. This orbit is a **Sun-synchronous orbit**, which means that whenever and wherever the satellite crosses the equator, the **local solar time** on the ground is always the same. For the Terra satellite for example, it's always about 10:30 in the morning when the satellite crosses the equator in Brazil. When the satellite comes around the Earth in its next overpass about 99 minutes later, it crosses over the equator in Ecuador or Colombia [again] at about 10:30 local [mean solar] time... The Sun-synchronous orbit is necessary for science because it keeps the angle of sunlight on the surface of the Earth as consistent as possible, though the angle will change from season to season. This consistency means that scientists can compare images from the same season over several years without worrying too much about extreme changes in shadows and lighting, which can create illusions of change. Without a Sun-synchronous orbit, it would be very difficult to track [year to year] change over time. It would be impossible to collect the kind of consistent information required to study climate change... The path that a satellite has to travel to stay in a Sun-synchronous orbit is very narrow [tightly constrained]. If a satellite is at a height of 100 kilometers, it must have an orbital inclination of 96 degrees to maintain a Sun-synchronous orbit. [I.e., as it rises from the equator at the ascending node, this orbit is tilted a little to the NW.] Any deviation in height or inclination will take the satellite out of a Sun-synchronous orbit. Since the drag of the atmosphere and the tug of gravity from the Sun and Moon alter a satellite's orbit, it takes regular adjustments to maintain a satellite in a Sun-synchronous orbit." "The orbital plane of a sun-synchronous orbit must also precess (rotate) approximately one degree each day, eastward, to keep pace with the Earth's revolution around the sun."<sup>211</sup> "When the inclination is chosen just right (about 8 degrees off the polar orbit) the motion matches the motion of the Sun across the sky. The plane of the orbit executes one full rotation about the axis of the Earth in one year. They are typically orbiting about 800-1000 km above the Earth."<sup>212</sup> Examples include the Landsats, Radarsat, Hinode, TRACE, ERS-1, ERS-2. "Iridium, Globalstar and ICO global mobile satellite systems in the 1990" faced bankruptcies, and Orbcomm data relay systems had similar difficulties. [Pelton2012]

**Eccentricity:** Orbits can vary from 0 eccentricity (circular) to high eccentricity (such as **Tundra** and **Molniya orbits**). "The most exotic orbit of this kind [high eccentricity] is what is called the **Loopus Orbit**, which can serve different parts of the Northern Hemisphere with very long "hang times" to provide telecommunications or direct broadcast type services. There could also be an 'inverse Loopus' geared to serve the southern latitudes." [Pelton 2012]

**Inclination** is the angle of the orbital plane relative to Earth's equatorial plane, measured CCW at the ascending node while looking toward Earth. A N to S orbit has inclination 90°, a retrograde equatorial orbit has inclination 180°. Satellites with low inclination can utilize the Earth's rotation to boost it into orbit (especially when launched near the equator), whereas more energy is required to place a satellite in near polar orbit.<sup>213</sup>

Orbits in which the rotation is in the same direction as the Earth's rotation (and  $0^\circ \leq \text{inclination} < 90^\circ$ ) are called **prograde**, as opposed to orbits that are **retrograde** (in which  $90^\circ < \text{inclination} \leq 180^\circ$ ). Specifically, for a prograde orbit viewed from the NP, the direction of rotation is CCW. A retrograde orbit appears to rotate CW when seen from the NP. An equatorial orbit has inclination of 0° or 180°. A polar orbit has inclination of 90°. A sun-synchronous orbit has inclination 96-97 degrees and is retrograde.<sup>214</sup>

Satellites closer to Earth move faster (in both linear and angular velocities). A "constellation" of LEO satellites must include greater numbers than MEO or GEO satellites in order to ensure coverage of the Earth. However, flux density received diminishes with higher altitude as path loss increases. [Pelton 2012]

<sup>211</sup> [http://www.centennialofflight.net/essay/Dictionary/SUN\\_SYNCH\\_ORBIT/DI155.htm](http://www.centennialofflight.net/essay/Dictionary/SUN_SYNCH_ORBIT/DI155.htm)

<sup>212</sup> [http://imagine.gsfc.nasa.gov/ask\\_astro/satellites.html](http://imagine.gsfc.nasa.gov/ask_astro/satellites.html)

<sup>213</sup> [http://www.au.af.mil/au/awc/space/primer/orbital\\_mechanics.pdf](http://www.au.af.mil/au/awc/space/primer/orbital_mechanics.pdf)

<sup>214</sup> <https://www.youtube.com/watch?v=4K5FyNbV0nA>

**Equatorial Circular Orbit (ECO):** These are circular orbit in the equatorial plane but deployed in MEO. [Pelton 2012]

**Quazi-Zenith or “Figure 8” Orbit:** “This is essentially a GEO that is inclined some 45 degrees. Three satellites in this orbit provide excellent high-look angles to countries located at 45 degrees latitude. This orbit is being used by Japan for mobile satellite communications and to provide supplemental space navigation services.” [Pelton 2012]

### **Remote Sensing**

“the art, science, and technology of obtaining reliable information about physical objects and the environment, through the process of recording, measuring and interpreting imagery and digital representations of energy patterns derived from noncontact sensor systems” [per ASPRS = American Society of Photogrammetry and Remote Sensing]

### **Satellite Services as defined by the ITU [International Telecommunication Union]:**

- **Fixed Satellite Services (FSS)** “[ITU:] A radio-communication service between Earth stations at given positions, when one or more satellites are used; the given position may be a specified fixed point or any fixed point within specified areas; the fixed-satellite service may also include feeder links for other space radio-communication services.”
- Inter-Satellite Services (ISS)
- **Broadcast Satellite Services (BSS):** “[ITU:] “A radio-communication service in which signals transmitted or retransmitted by space stations are intended for direct reception by the general public. In the broadcasting satellite service, the term ‘direct reception’ shall encompass both individual reception and community reception.”
- Broadcast Satellite Services for Radio (BSSR): “This involves a new radio frequency allocation that is used for audio broadcasting services. Today Sirius XM Radio (representing the merger of XM Radio and Sirius Radio) plus Worldspace both provide this type of satellite service. These systems provide audio-only broadcast satellite service either to automobile-based radios or handsets capable of direct reception from high-powered satellites. (This service is also called Satellite Digital Audio Radio Services (SDARS).”
- Radio Determination Satellite Services (RDSS)
- Radio Navigation Satellite Services (RNSS)
- **Mobile Satellite Services (MSS):** “[ITU:] A radio-communication service (a) between mobile Earth stations and one or more space stations, or between space stations used by this service; or (b) between mobile Earth stations by means of one or more space stations. This service may also include feeder links necessary for its operation.”
- Aeronautical Mobile Satellite Services (AMSS)
- Maritime Mobile Satellite Services (MMSS)
- Maritime Radio Navigation Satellite Services (MRNSS)
- Land Mobile Satellite Services (LMSS)
- Space Operations Satellite Services (SOSS)
- Space Research Satellite Services (SRSS)
- Earth Exploration Satellite Services (EESS)
- Amateur Satellite Services (ASS)
- Radio Astronomy Satellite Services (RASS)
- Standard Frequency Satellite Services (SFSS)
- Time Signal Satellite Services (TSSS) [all quoted from Pelton 2012, which quotes ITU]

### **Spitzer Space Telescope (Infrared)**

Represents the fourth and final element in NASA's Great Observatory program—the thermal infrared. “The Spitzer Space Telescope (formerly SIRTF = the Space Infrared Telescope Facility) was launched into space August 25, 2003. During its cryogenic mission, Spitzer obtained images and spectra by detecting the infrared energy, or heat, radiated by objects in space between wavelengths of 3 and 180 microns... Most of this infrared radiation is blocked by the Earth's atmosphere and cannot be observed from the ground. Consisting of a 0.85-meter telescope and three cryogenically-cooled science instruments, when it was launched Spitzer was the largest infrared telescope in space.”

### Swift Satellite—Gamma Ray “Burst Alert Telescope (BAT)”

November 2004 launched. “NASA's Swift satellite recorded the gamma-ray blast caused by a black hole being born 12.8 billion light years away... This object is among the most distant objects ever detected”<sup>215</sup> “Swift's three instruments work together to glean as much information about each [gamma ray] burst as possible. Swift's multi-wavelength observations of GRBs and afterglow are completely simultaneous. The X-ray Telescope (XRT) and Ultraviolet/Optical Telescope (UVOT) have co-aligned fields-of-view, both within the Burst Alert Telescope (BAT) field-of-view, so that any source can be observed in all three wavebands... When a GRB occurs, the BAT will be the first of Swift's instruments to detect it. Within about 10 seconds of the burst trigger, the BAT produces a burst localization, which is transmitted to ground observers. In addition, the BAT's position is fed to the Swift spacecraft so a slew can be performed, bringing the GRB into the XRT and UVOT's fields-of-view.”<sup>216</sup>

### Terrain System, Terrain Facet, and Terrain Element (e.g., bluff, stream, surface, channel, gully)

These are component of terrain at increasingly smaller scale and increasing detail.

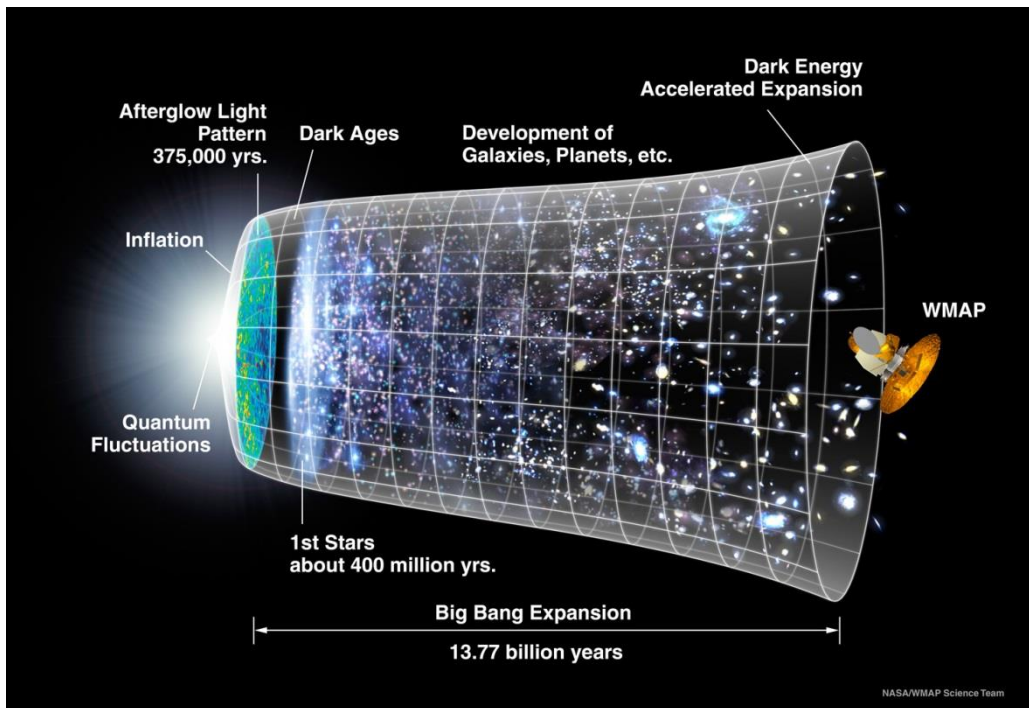
Terrain System—e.g., hilly country with valleys

Terrain Facet—e.g., terrace, hill, valley

Terrain Element—bluff, stream, surface, channel, gully<sup>217</sup>

### Wilkinson Microwave Anisotropy Probe (WMAP)

“is a NASA Explorer mission that launched June 2001 to make fundamental measurements of cosmology—the study of the properties of our universe as a whole. WMAP has been stunningly successful, producing our new Standard Model of Cosmology. WMAP's data stream has ended. Full analysis of the data is now complete. Publications have been submitted as of 12/20/2012.”<sup>218</sup>



Model of Cosmic History after the Big Bang Including Inflation and Expansion

<sup>215</sup> [http://missionscience.nasa.gov/ems/12\\_gammarays.html](http://missionscience.nasa.gov/ems/12_gammarays.html)

<sup>216</sup> [http://www.nasa.gov/mission\\_pages/swift/spacecraft/index.html](http://www.nasa.gov/mission_pages/swift/spacecraft/index.html)

<sup>217</sup> *Hot Deserts: Engineering, Geology and Geomorphology : Engineering Group ...*, ed. M. J. Walker, 2012

<sup>218</sup> <http://map.gsfc.nasa.gov/> including Timeline of the Universe image (above)